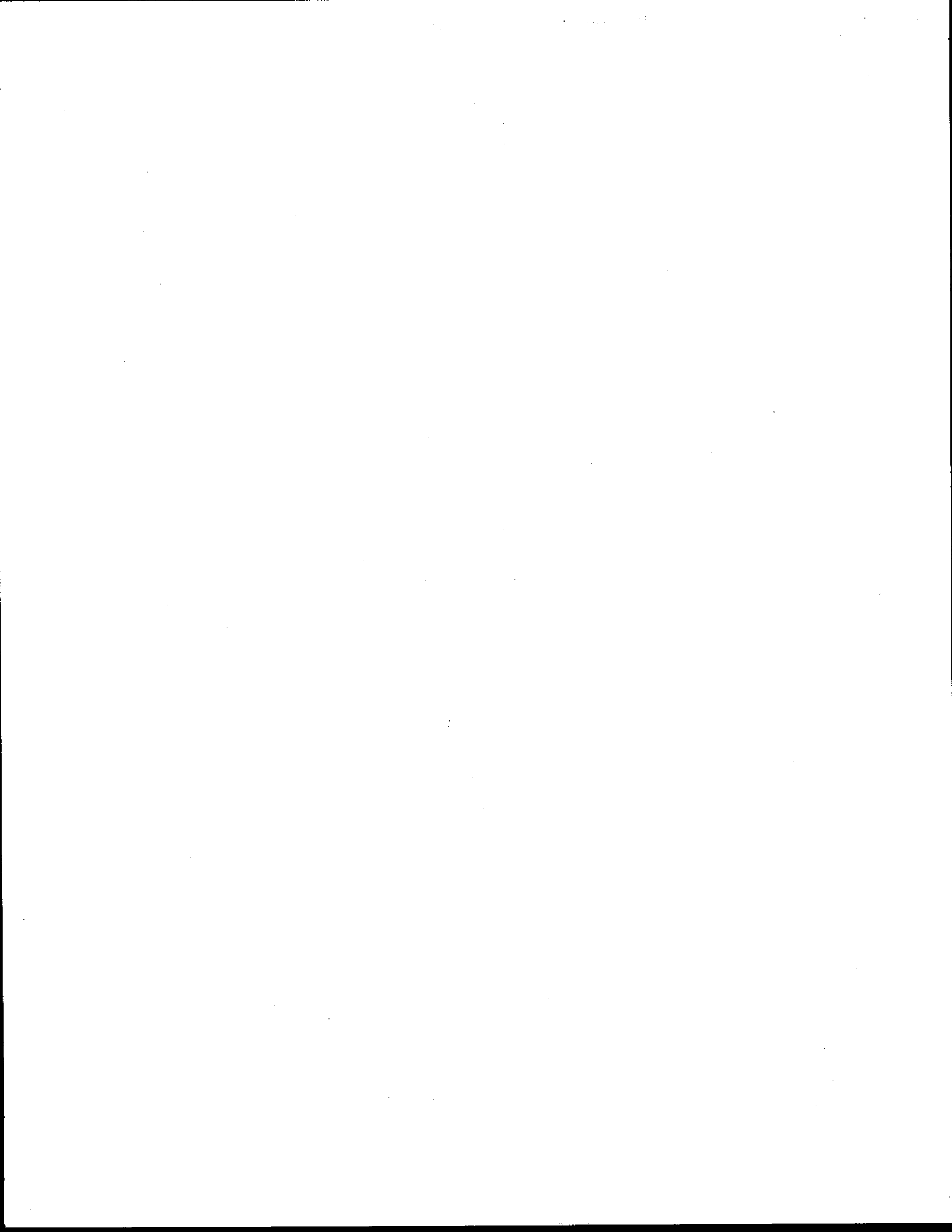

PASSIVE PROTECTION AT 50 MILES PER HOUR



**U.S. DEPARTMENT OF TRANSPORTATION
National Highway Traffic Safety Administration**

JUNE 1972



PASSIVE PROTECTION AT 50 MILES PER HOUR



**A Paper Presented Before The Second
International Conference On Passive
Restraints, May 22-25, 1972 By:**

**ROBERT L. CARTER
Associate Administrator
Motor Vehicle Programs
National Highway Traffic Safety Administration**



Illustrations

FIGURE 1	– Distribution of Fatalities with Impact Speed	1
FIGURE 2	– Distribution of Casualties with Equivalent Test Speed (Frontal Collisions)	1
FIGURE 3	– Comparison of Fatality Distribution Data (Frontal Collisions)	1
FIGURE 4	– Cumulative % Fatalities Injuries within Equivalent Test Speed Range	2
FIGURE 5	– Square Wave Acceleration Pulse	4
FIGURE 6	– Required Stopping Distances, Using a Square Wave Acceleration Pulse	4
FIGURE 7	– Effects of Deviations from Square Wave Acceleration Pulse on Stopping Distance from 60 MPH	4
FIGURE 8	– Comparison of Occupant Compartment Acceleration from a 38 MPH Crash	5
FIGURE 9	– Crash Response of Ford Sedan in Head-On Flat Faced Barrier Crash	5
FIGURE 10	– 59.2 MPH Pole Barrier Crash Motion of Ford Sedan	5
FIGURE 11	– 1966 Ford Sedan Impacting Pole Barrier Head-On at 59.2 MPH	6
FIGURE 12	– Design G as Function of Weight for Desired Load Limiting Structure	6
FIGURE 13	– Sketch of Mod. 2A(2) Design	7
FIGURE 14	– Mod. 2A(2) Design Modifications	8
FIGURE 15	– Mod. 2A(2), 15° Oblique Pole Impact	8
FIGURE 16	– Pole Impact – Unmodified Ford	9
FIGURE 17	– Passenger Compartment Motion – Oblique Pole Barrier Crash – Mod. 2A(2) and Unmodified Ford sedan	9
FIGURE 18	– Passenger Compartment Deceleration – Displacement Data – Oblique Pole Barrier Crash – Mod. 2A(2) and Unmodified Ford Sedan	9
FIGURE 19	– Passenger Compartment Acceleration – Displacement Data – Pole Barrier Crash – Mod. 1B(2)R and Unmodified Ford Sedan	9
FIGURE 20	– Passenger Compartment Penetration Pole Barrier Crash – Mod. 1B(2)R and Unmodified Ford Sedan	10
FIGURE 21	– Mod. 2D(1) Test Vehicle	11
FIGURE 22	– Passenger Compartment Interior of Ford Sedan Following Impact with Another Ford and with Mod. 2D(1)	11
FIGURE 23	– Occurrence of Death or Serious Injury as a Function of Vehicle Weight	11
FIGURE 24	– Weight Mix Car – Car Acceleration Response – Ford – vs – Opel	12
FIGURE 25	– Ford vs Opel Head-On Crash Test – Closure Speed 87.6 MPH	12
FIGURE 26	– Weight Mix Car-Car Acceleration Response – Ford vs Modified Opel	13
FIGURE 27	– Ford vs Modified Open Head-On Crash Test – Closure Speed 55.7 MPH	13
FIGURE 28	– Six Degree of Freedom Spring – Mass Model	13
FIGURE 29	– Fixed Force Structure – Matched 40G Acceleration Crash Response	14
FIGURE 30	– Velocity Sensitive Structure – Matched V_{des} and G_{des} Crash Response	14
FIGURE 31	– Matched Acceleration Structures Impacting Rigid Barrier	15
FIGURE 32	– Matched Acceleration Structures Impacting Head-On	15

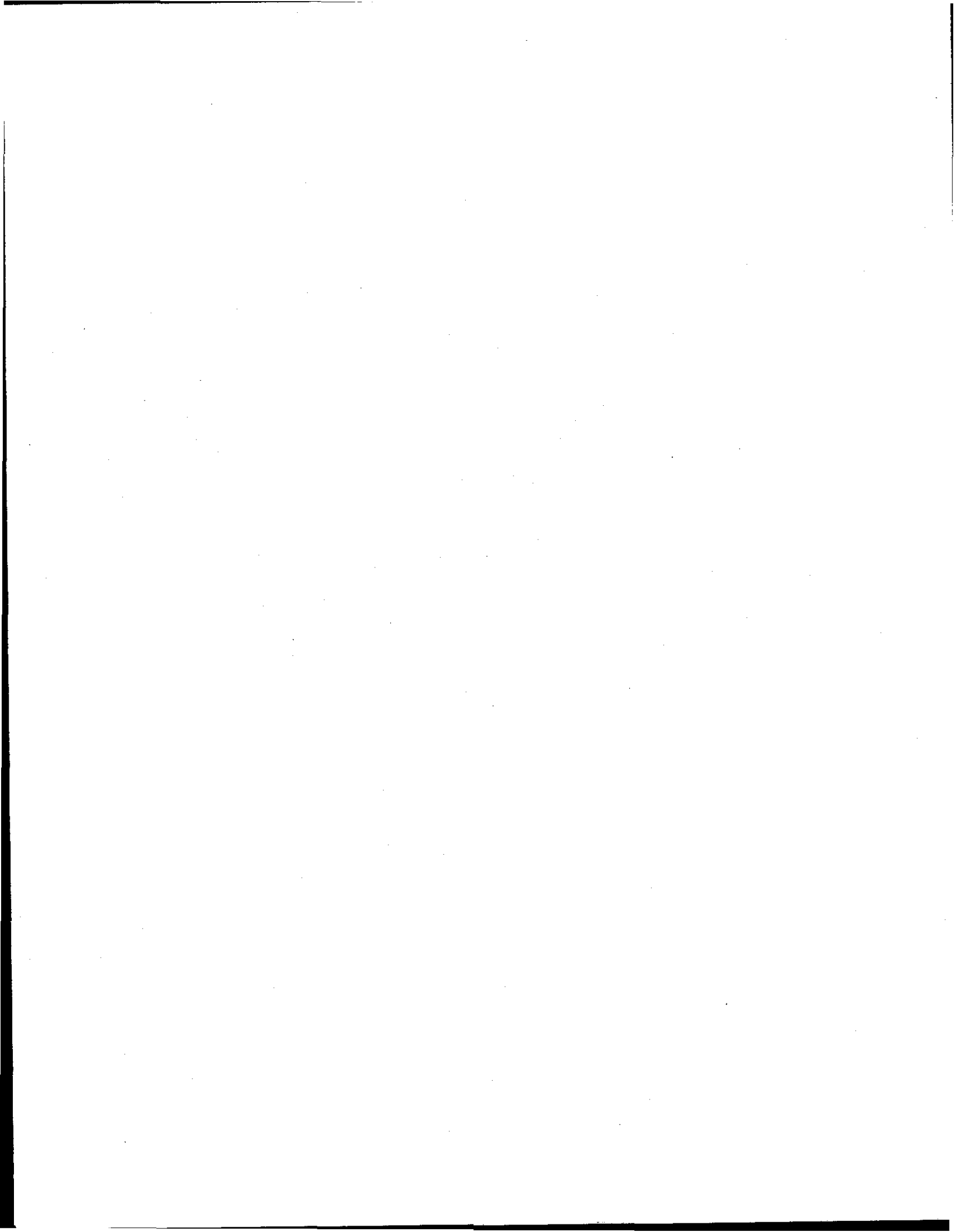


FIGURE 33 – Distance Between Bumper and Firewall as a Function of Weight	15
FIGURE 34 – Required V_{DESIGN} for Velocity Sensitive Energy Absorbers As a Function of Vehicle Weight for Crush Compatibility	16
FIGURE 35 – Design Maximum Accelerations for Velocity Sensitive Systems	16
FIGURE 36 – Design Acceleration Response for Fixed Force Systems	16
FIGURE 37 – Modified Velocity Sensitive and Fixed Force Structures in Rigid Barrier Crashes	17
FIGURE 38 – Modified Velocity Sensitive and Fixed Force Structures in Head-On Car-to-Car Crashes	17
FIGURE 39 – Side Structure Response Characteristics	17
FIGURE 40 – Side Impact Responses with Velocity Sensitive and Fixed Force Impacting Frontal Structures	18
FIGURE 41 – Compartment Deceleration as a Function of Front-End Deflection for the Modified Standard-Size Vehicle	21
FIGURE 42 – Velocity Histories for the Modified Standard-Size Vehicle at 20, 30, 40, and 50 MPH Barrier Impacts	21
FIGURE 43 – A Comparison of the Velocity Histories of a Conventional Standard- Size Vehicle with the Modified Standard-Size Vehicle in a 30 MPH Barrier Impact	21
FIGURE 44 – The Assumed Interior Geometry of the Modified Standard-Size Vehicle	22
FIGURE 45 – The Assumed Force-Deflection Characteristics of the Knee Restraint	23
FIGURE 46 – Load Efficiency Versus System Activation Time for the Standard- Size Vehicle	23
FIGURE 47 – Sensing Time as a Function of Barrier Impact Speed for the Modified Standard-Size Vehicle	24
FIGURE 48 – Air Bag Model Configuration	24
FIGURE 49 – Femur Force Versus Pelvis X-Component Acceleration for Sierra and Alderson Dummies	24
FIGURE 50 – Torso Acceleration History for a Simulated 30 MPH Impact with a Conventional Standard-Size Vehicle	25
FIGURE 51 – Torso Acceleration as a Function of Torso Penetration for a Simulated 50 MPH Impact with a Modified Standard-Size Vehicle	25
FIGURE 52 – Torso Acceleration as a Function of Torso Penetration for a Simulated 50 MPH Impact with a Modified Standard-Size Vehicle	25
FIGURE 53 – Aspirator Deployment During Inflation	26
FIGURE 54 – The Assumed Interior Geometry of the Driver Position of the Modified Standard-Size Vehicle	27
FIGURE 55 – Steering Column Model	27
FIGURE 56 – A Comparison of Steering Column Model Results with Experimental Data	27
FIGURE 57 – The Assumed Force-Deflection Characteristics of the Human Thorax	28
FIGURE 58 – The Results of Simulated 10 MPH Impacts with the 50th and 95th Percentile Male and 5th Percentile Female Thorax	28
FIGURE 59 – Static Force-Deflection Characteristic of the Assumed Steering Column for the Modified Standard-Size Vehicle	28
FIGURE 60 – Static Force-Deflection Characteristic of the Assumed Bag and Steering Column Combination for the Modified Standard-Size Vehicle	29
FIGURE 61 – The Resulting Kinematics of a 50th Percentile Male Driver from a Two-Dimensional Simulation of a 50 MPH Barrier Impact with a Modified Standard-Size Vehicle	29

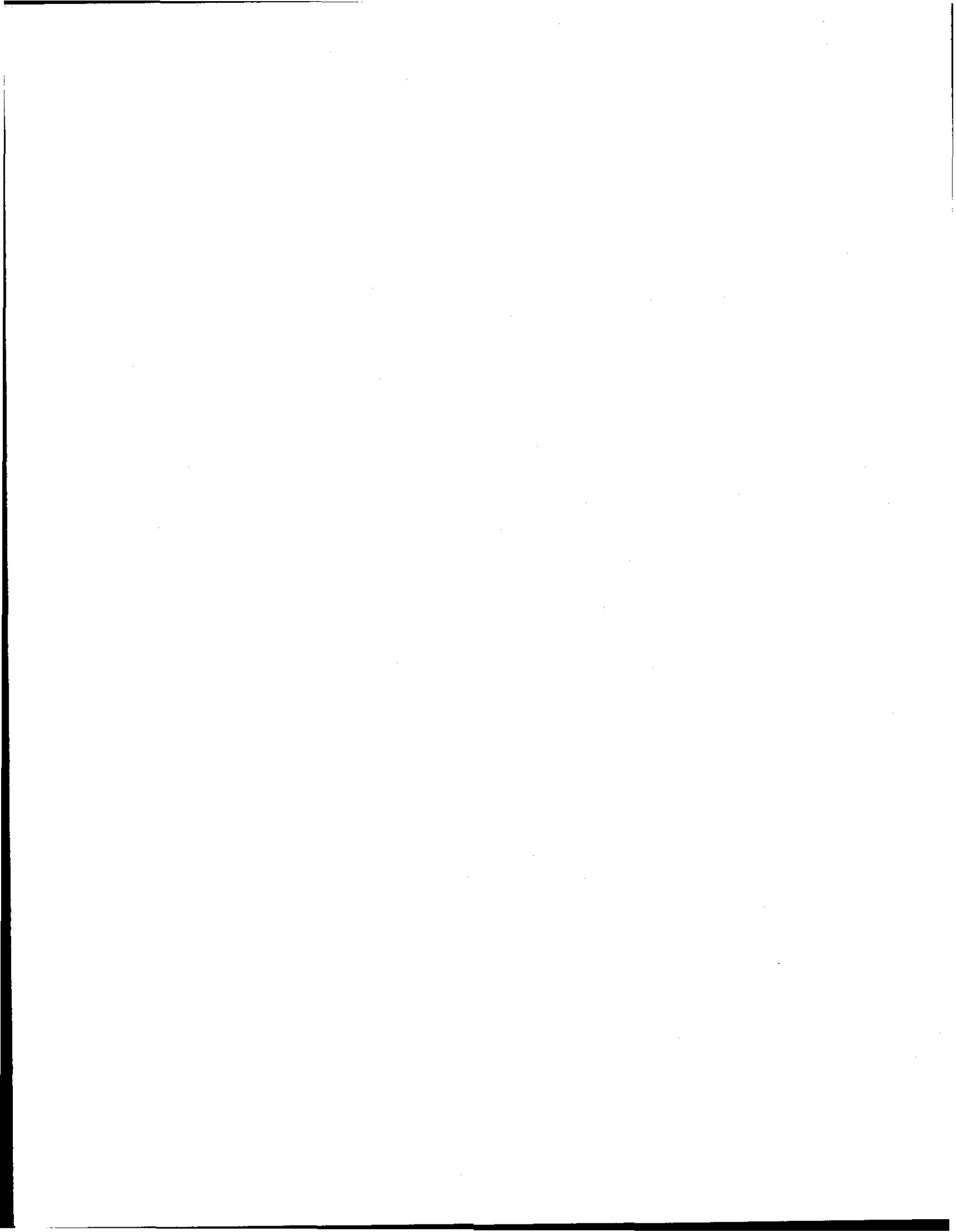
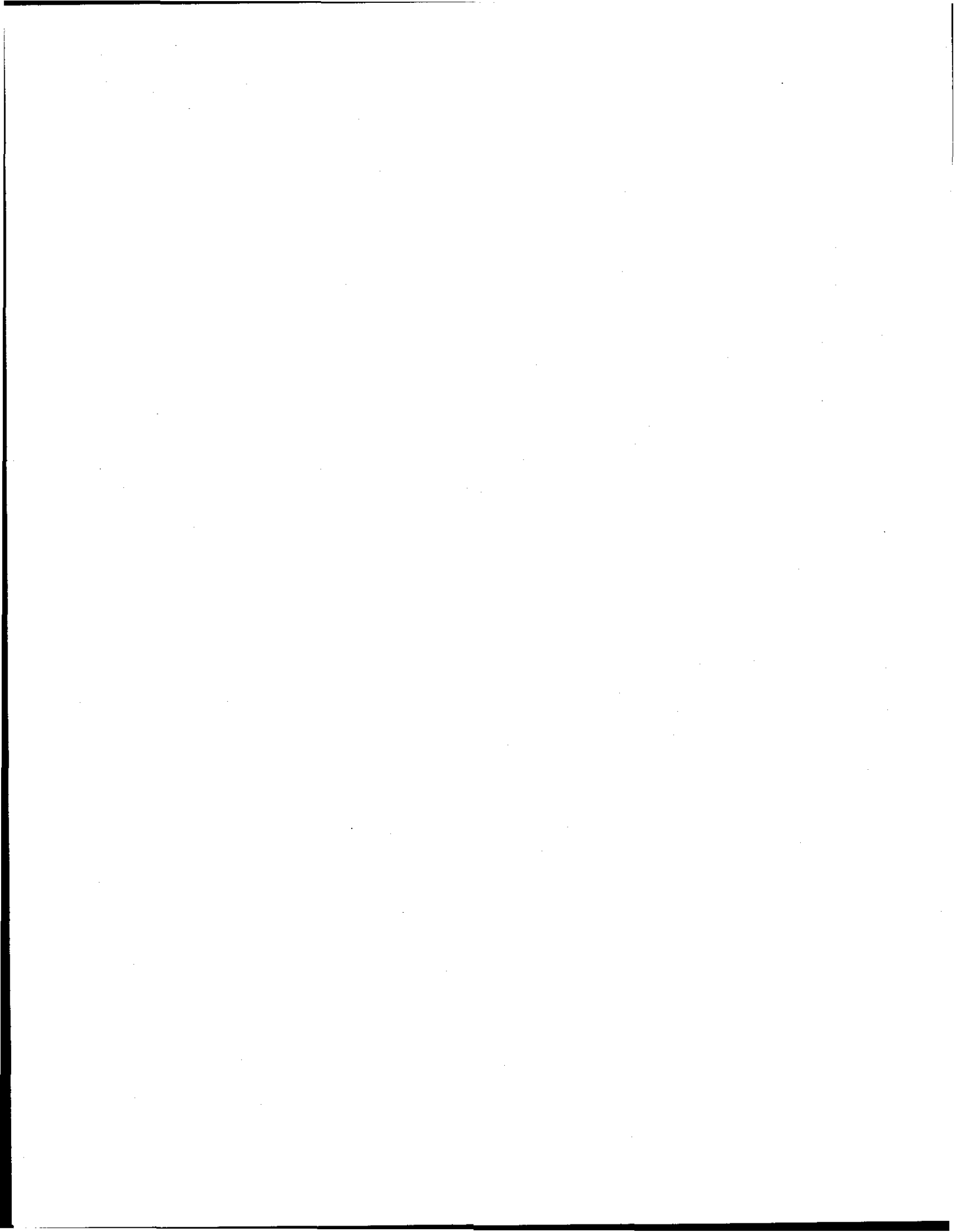
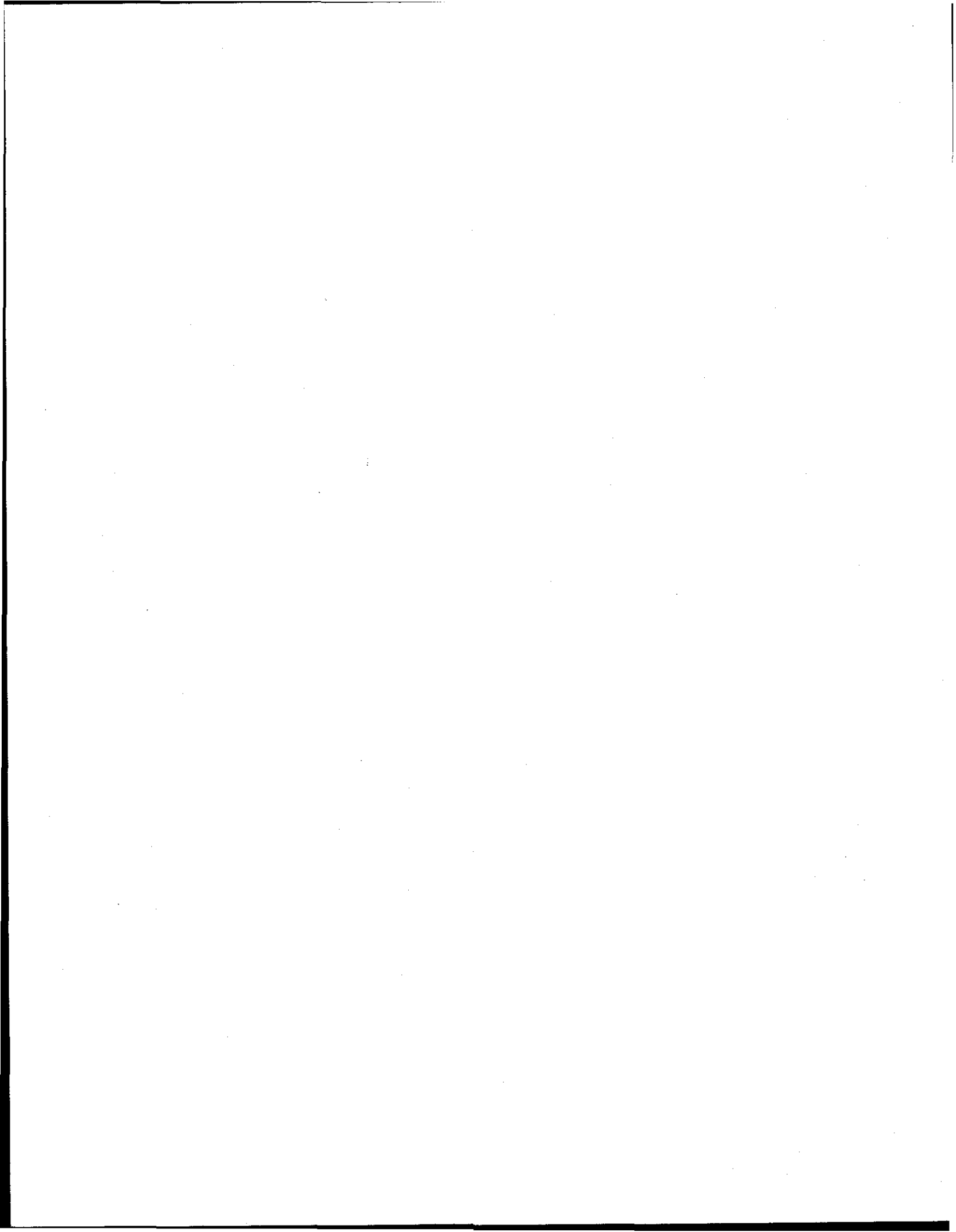


FIGURE 62 – The Calculated Head and Chest Resultant Accelerations of a 50th-Percentile Male Driver in a 50 MPH Barrier Impact with a Modified Standard-Size Vehicle – Two-Dimensional Simulation	29
FIGURE 63 – Force-Deflection Characteristics of an Alternate Steering Column Design for 50 MPH Protection	30
FIGURE 64 – Compartment Deceleration as a Function of Front-End Deflection for the Modified Sub-Compact Vehicle	30
FIGURE 65 – Velocity Histories for the Modified Sub-Compact Vehicle in 20, 30, 40, and 50 MPH Barrier Impacts	30
FIGURE 66 – The Assumed Interior Geometry of the Modified Sub-Compact Vehicle	31
FIGURE 67 – Load Efficiency Versus System Activation Time for the Sub-Compact Vehicle	31
FIGURE 68 – Sensing Time as a Function of Barrier Impact Speed for the Modified Sub-Compact Vehicle	31
FIGURE 69 – The Resulting Kinematics of a 50th-Percentile Male Driver from a Two-Dimensional Simulation of a 50 MPH Barrier Impact with a Modified Sub-Compact Vehicle	31
FIGURE 70 – The Calculated Head and Chest Resultant Accelerations of a 50th-Percentile Male Driver in a 50 MPH Barrier Impact with a Modified Sub-Compact Vehicle – Two-Dimensional Simulation	32
FIGURE 71 – Estimates of Possible Consumer Costs Resulting from Installation of Energy Management Improvements and a Passive Restraint System	33
FIGURE 72 – Comparison of Annual Estimated Benefits with Consumer Cost for 50 MPH Passive Protection	35
	36



Abstract

This paper examines the engineering and economic feasibility of inflatable restraint systems and structural modifications required to achieve passive protection for occupants in passenger car frontal collisions at 50 mph equivalent barrier speed. Vehicle structural modifications, already proven in prototype tests, are examined for compatibility in car-to-car crashes. The special aspects of inflatable restraint systems capable of 50 mph protection are also discussed, taking into account the improvements in system behavior made possible by structural modifications. Costs and benefits are also projected. It is concluded that cost effective 50 mph protection can be achieved.



Preface

The material presented in this report was developed by members of the Engineering Staff of the National Highway Traffic Safety Administration in the Department of Transportation.

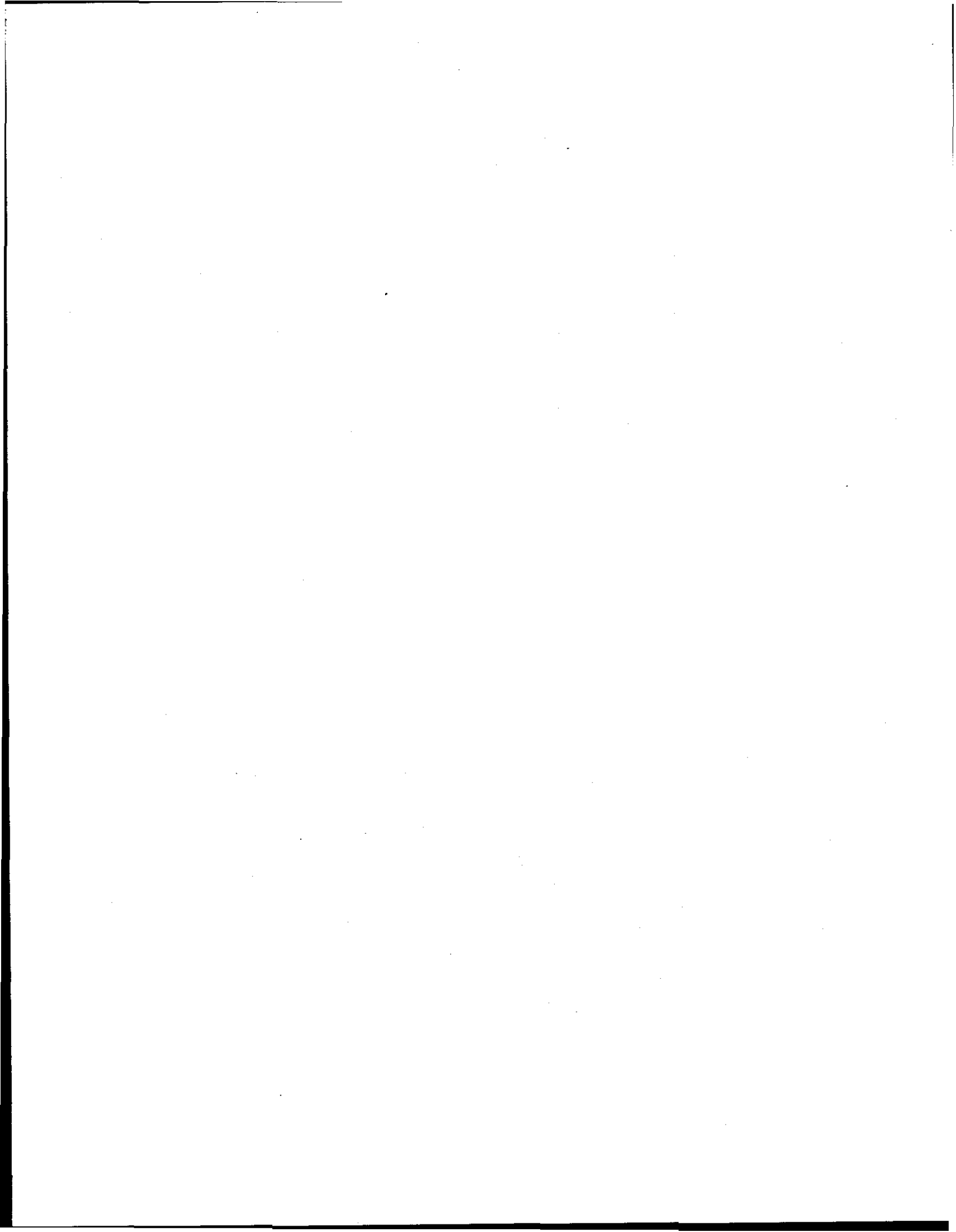
The Energy Management Section was developed by Mr. J.E. Hofferberth, with the assistance of Messrs. W.C. Brubaker, S. Daniel, R.J. Dennison and J.E. Tomassoni.

The Section on Passive Restraints was developed by Mr. C.E. Strother, with the assistance of Mr. W.A. Boehly and Dr. C.Y. Warner.

Safety Benefits were determined by Mr. C.H. Cooke and Vehicle System Costs were estimated by Mr. C. Westphal.

General direction and coordination was provided by Mr. R.M. Crone.

The Energy Management System designs and developments described in the report were carried out by Cornell Aeronautical Laboratory, Inc. (CAL), for the National Highway Traffic Safety Administration, under contract to the Department of Transportation. In a number of cases, material presented in the Energy Management Section was taken directly from CAL reports.



Introduction

The National Highway Traffic Safety Administration has identified crash survivability as one of its highest priority goals. This priority is based on several primary considerations. The 55,000 annual death toll on the highways requires that action be taken as soon as possible. Further, it has been generally agreed that passive restraints, together with improved structural crashworthiness, have a significant potential for saving lives and preventing serious injuries when motor vehicle crashes occur.

Motor vehicles are involved in numerous types of collisions with other vehicles and fixed objects, each representing a complex problem for analysis and determination of possible system improvements. While each collision mode and risk of serious injury must be investigated for possible benefits, the frontal collision mode clearly must be given highest priority. It is estimated from 1970 statistics that 17,650 occupants are killed and 990,000 are injured in passenger cars in frontal collisions annually. Figure 1 shows the impact speeds at which these fatalities occur in the form of the percent distribution of fatalities versus impact speeds for passenger car collisions involving one or more vehicles and for all frontal collisions.

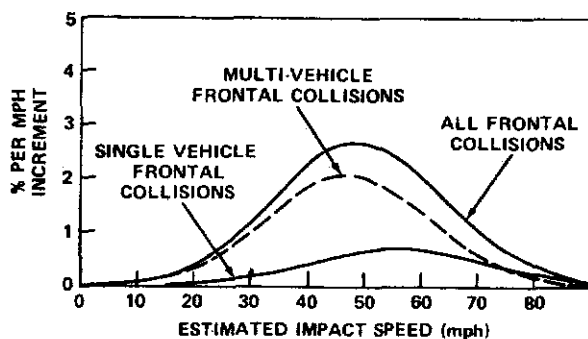


FIGURE 1 - Distribution of Fatalities with Impact Speed

Figure 2 presents the percent distribution of deaths and injuries for all passenger cars versus dynamically equivalent frontal barrier test speeds. NHTSA studies¹ have correlated the severe test impacts into a fixed base, flat rigid barrier with a broad variety of real collision interactions, taking into account the mitigating factors of momentum transfer and shared energy absorption, and also considering the probability of occurrence of each type of collision. It is noted from Figure 2 that the equivalent

barrier test speed distribution for deaths has a mean at 33 mph as compared to mean values for deaths of 47 mph for the multivehicular frontal collisions and 56 mph for the less frequent single vehicle frontal collisions as seen in Figure 1. Figure 3 illustrates a comparison of the equivalent barrier test speed results with independent studies, submitted to the NHTSA Docket No. 69-7 by General Motors Corporation,²

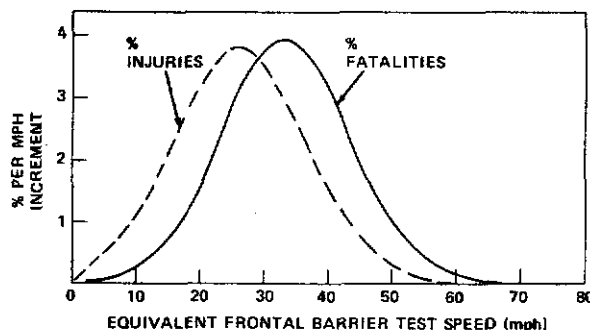


FIGURE 2 - Distribution of Casualties with Equivalent Test Speed (Frontal Collisions)

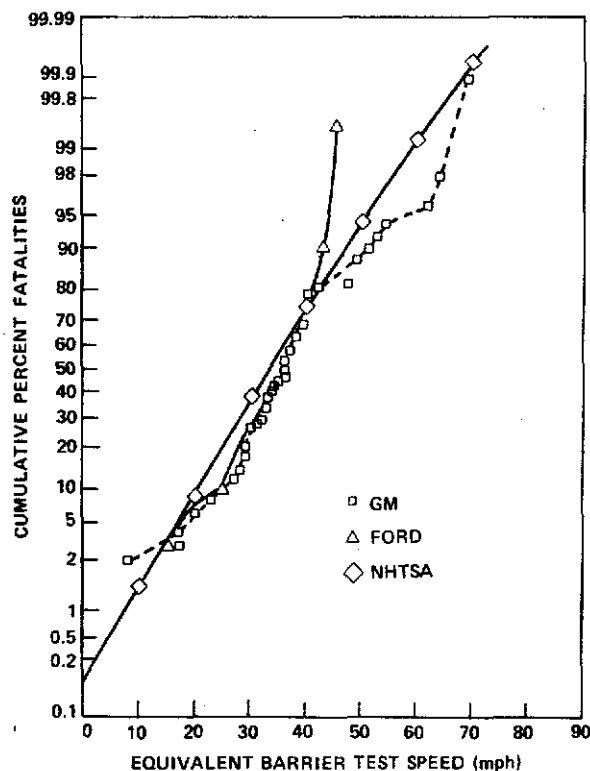
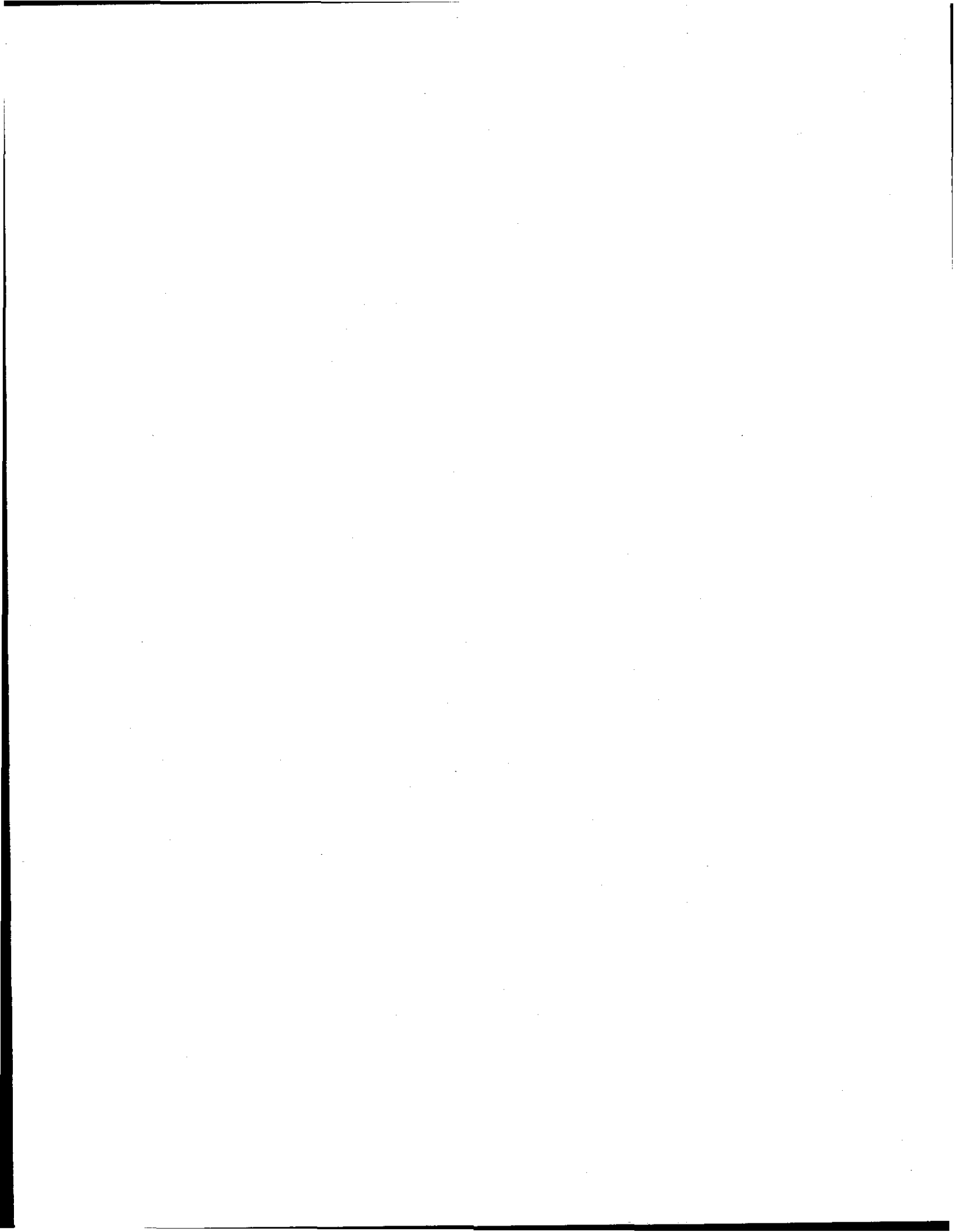


FIGURE 3 - Comparison of Fatality Distribution Data (Frontal Collisions)



and by the Ford Motor Company,³ plotted on a cumulative probability basis. Although each curve was developed independently, the NHTSA estimate is considered to compare reasonably well with the Ford and GM results.

A distribution of injuries on a cumulative probability basis with respect to equivalent barrier frontal speed was estimated and plotted in Figure 4, together with a curve showing the cumulative fatalities. It is seen that the equivalent test speeds associated with frontal collision injuries are approximately 7 mph lower than those for frontal fatalities. From these results, it can be seen that about 38% of the deaths and 64% of the injuries fall below an equivalent barrier speed of 30 mph, while 94% and 98%, respectively, fall below 50 mph equivalent barrier speed. It is further noted that nearly 55% of the fatalities and 34% of the injuries occur between equivalent barrier speeds of 30 and 50 mph.

The following sections discuss the results of studies of improved vehicle structures and passive restraint systems to examine the feasibility of crash-worthy designs for 50 mph equivalent barrier frontal speed crashes. The results of preliminary analyses of the safety benefits that may be derived from 50 mph crash protection systems, together with an estimate

of the incremental cost to the consumer, are also presented.

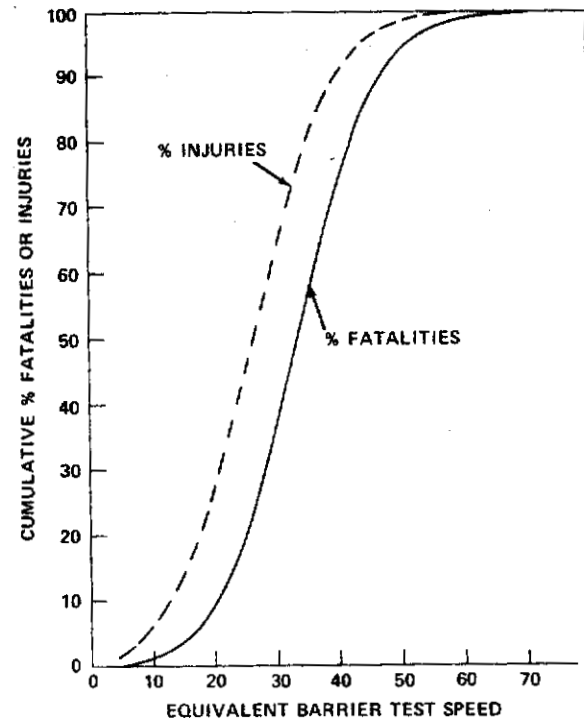
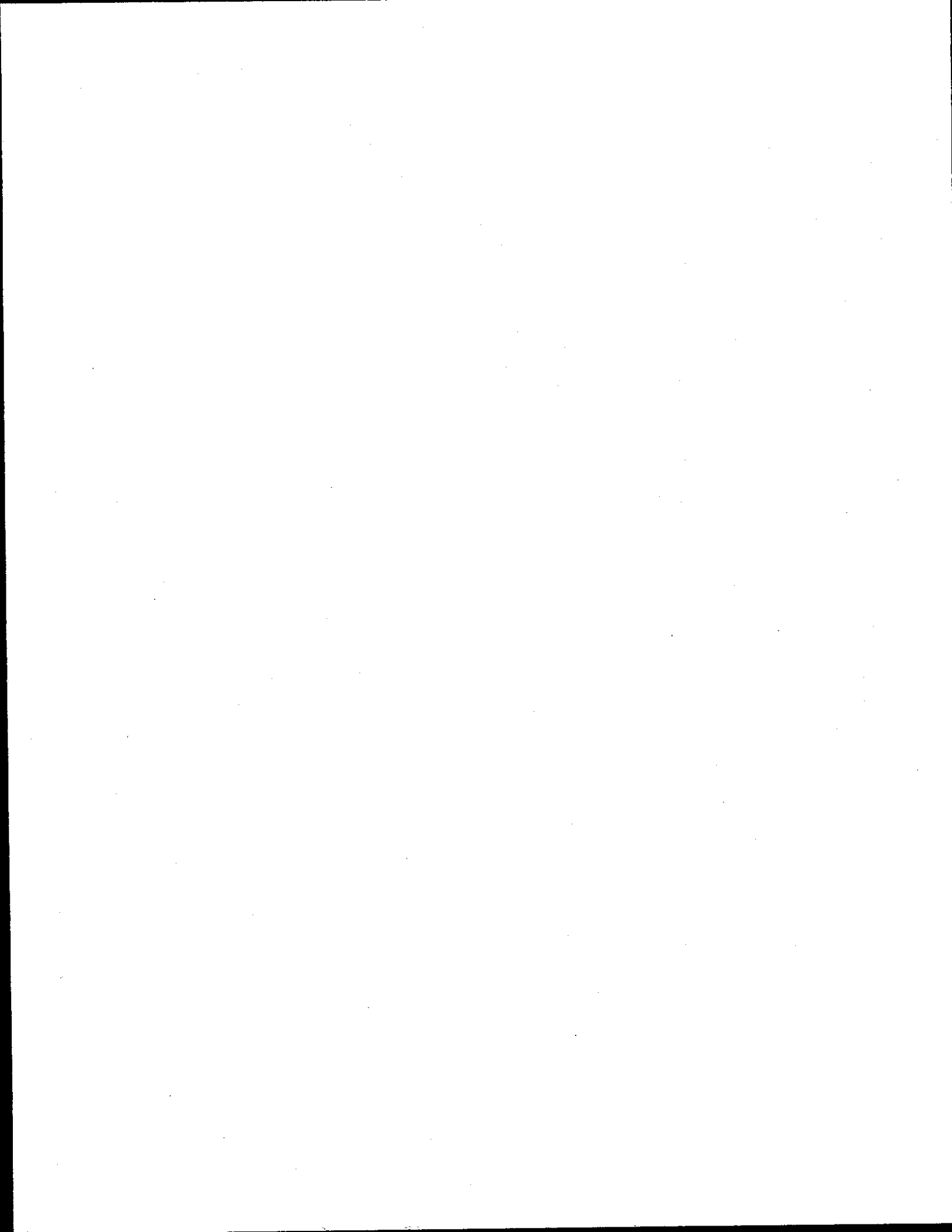


FIGURE 4 - Cumulative % Fatalities Injuries within Equivalent Test Speed Range



Crash Energy Management

An automobile crash is an impact between the vehicle and another object. During the impact, large forces are generated between the vehicle and the object. These forces abruptly accelerate, or change the speed and direction of travel of both the vehicle and the object until motion stops, or until the vehicle is moving in the same direction or away from the object.

In the case of two vehicles colliding, there is almost always some residual motion after the crash is over. Either they lock together and move in the same direction as one body, or they separate from each other and continue moving in different directions. In the case of a vehicle striking a rigid stationary object, such as a large tree, the object moves very little. If the vehicle strikes the object squarely, the vehicle will come to a complete stop or rebound away from the object at relatively low speed. An off-center impact may cause the vehicle to glance off, or spin past, the object and continue to travel with some speed in another direction. In every case, however, an abrupt change in speed or direction of travel occurs. This, by definition, is an acceleration. The magnitude and direction of the crash acceleration is the first of two important factors that determine occupant crash survivability.

The vehicle acceleration environment is extremely important because it affects the occupant acceleration environment. People are injured when exposed to excessive accelerations. Acceleration tolerance varies with the physical condition of the person, with the direction of the acceleration relative to the person's body, the dynamic characteristics of the acceleration pulse, and in the way the forces causing the acceleration are applied to the person's body. In car crashes, acceleration forces are applied to the crash victim through the restraint system or, if the occupant is not restrained, by impact against the interior structure of the vehicle. The characteristics of the restraint system have a major influence on the magnitude of acceleration which can be tolerated without injury. To prevent injury, crash accelerations must be controlled so as not to exceed a tolerable level for the restraint system that is being used.

To control the acceleration environment, it is necessary to control the forces generated between the vehicle and the object striking, or being struck by the vehicle. Accelerations and forces are related according

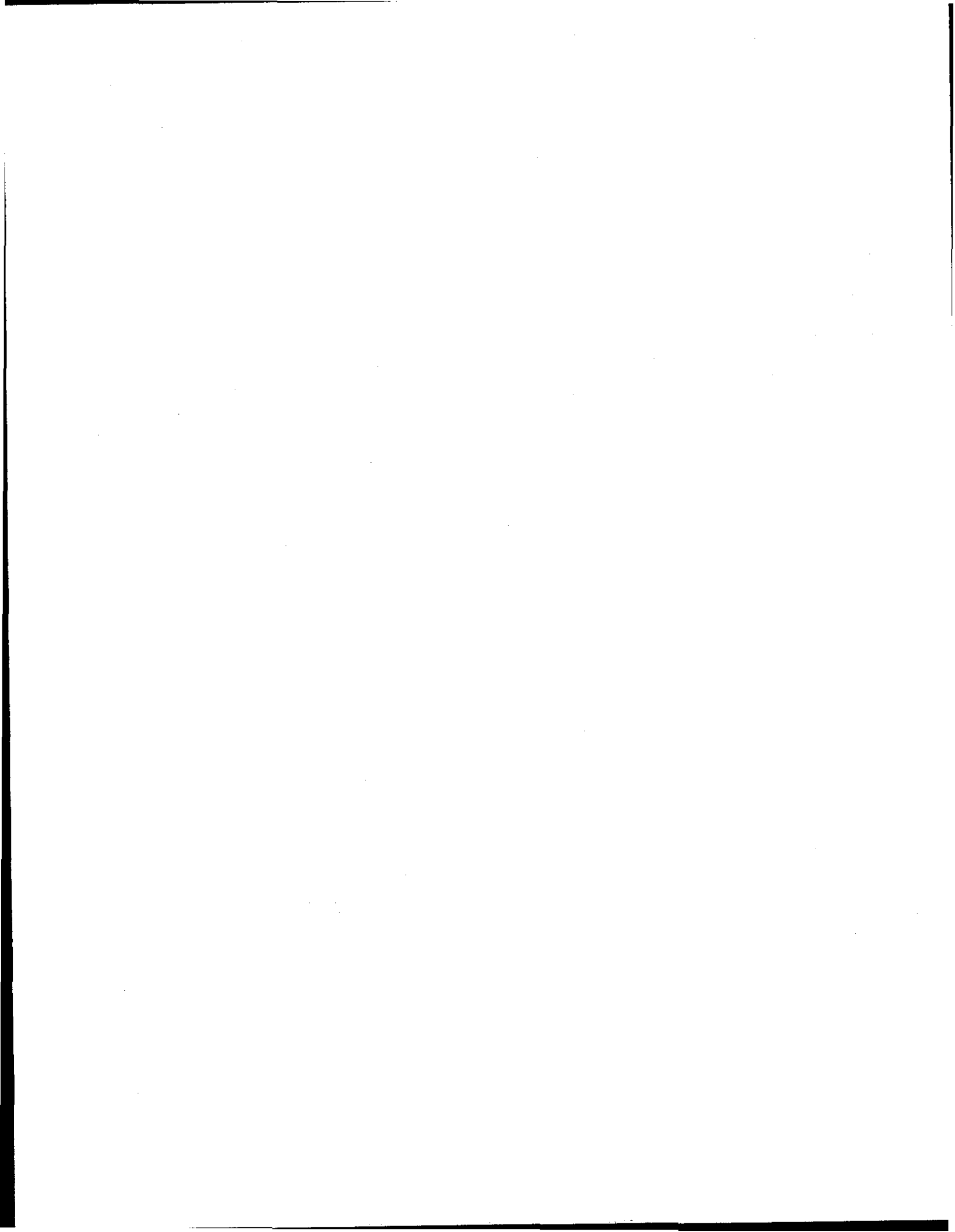
to Newton's Second Law, which in simplified form states that acceleration is directly proportional to force where the constant of proportionality is the mass ($F = MA$). By reducing crash forces, the acceleration can be reduced by a like amount. However, reductions in crash forces and accelerations reduce the ability of the vehicle structure to prevent crushing or penetration of the occupant compartment during the crash. Preventing excessive collapse or penetration of the occupant's physical environment is the second important factor determining the survivability of a crash.

The result is an apparent paradox where crash forces and accelerations must be low to preserve a tolerable acceleration environment for the restraint system being used, and yet high enough to protect the physical environment of the crash victims. A restraint system that allows higher accelerations to be tolerated without injury is of obvious merit since it allows the use of higher crash forces and accelerations to protect the occupant compartment.

To achieve crash survivability in a 50 mph barrier equivalent collision, a compromise must be reached between the requirement to prevent crushing of the occupant compartment, and assuring that the crash accelerations do not exceed levels for which the occupant restraint system provides adequate protection. The feasibility of achieving this compromise is examined starting with a review of experimental work to achieve adequate structural crashworthiness for high speed collisions against rigid barriers. This is followed by an analysis of the special requirements for structural compatibility in car-to-car crashes, a study of restraint system responses in the high speed crash dynamic environment, and an investigation of the projected benefits and costs associated with 50 mph crash survivability.

STRUCTURAL CRASH RESPONSE IN FRONTAL RIGID BARRIER COLLISIONS

Historically, structural crashworthiness research has relied heavily on rigid barrier crash tests. These conditions were chosen because they are repeatable, and because they simplify the task of studying the characteristics of the car being tested independent of the complex interactions that occur during impact with a moving and/or deformable object⁴. It is taken



as the starting point for discussion of structural crash response for the same reasons.

In a frontal crash against a rigid barrier, the objective is to stop the vehicle without exceeding the occupant acceleration tolerance limit before the firewall of the car (the front end of the occupant compartment) crashes against the barrier and before an object that might cause serious injury, such as the engine, is pushed into the occupant compartment.

The stopping distance available is the distance between the front bumper and the firewall less the length of the engine. For most cars, this is 2 to 3 feet. In some cases, it is possible to gain more distance by incorporating structural properties that will deflect the engine downward under the occupant compartment during the crash. There is additional space inside the compartment that can be used for stopping distance for the occupants. This space, however, is reserved to allow proper operation of a restraint system. The objective here is to stop the occupant compartment itself within acceptable acceleration limits while preserving the necessary space within the compartment to allow the restraint system to function effectively.

The most efficient use of distance to stop an object within a specified acceleration limit is a constant or "square wave" acceleration. This consists of an instantaneous increase from zero to the maximum tolerable acceleration, constant velocity decay at the maximum acceleration level until the motion stops, at which time the acceleration drops immediately to zero as illustrated in Figure 5. The required stopping distances, using a square wave acceleration pulse, for various initial speeds and acceleration limits, are plotted in Figure 6. It is seen, for example, that 3 feet of distance is required to stop a vehicle from an initial speed of 60 mph using a square wave 40g acceleration pulse. The effects of deviations from the square wave acceleration pulse on the distance required to stop from 60 mph are

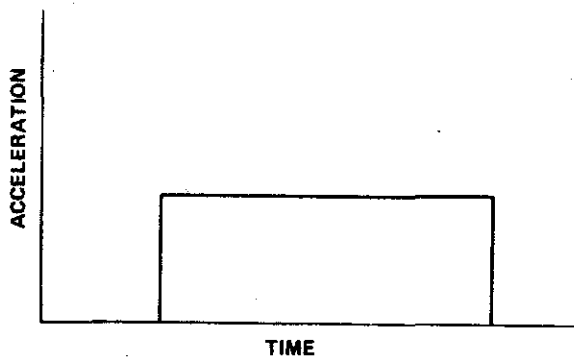


FIGURE 5 - Square Wave Acceleration Pulse

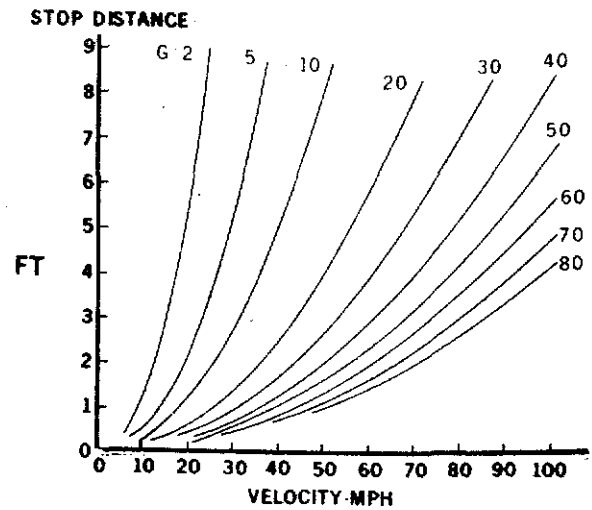


FIGURE 6 - Required Stopping Distances, Using a Square Wave Acceleration Pulse

illustrated in Figure 7. The required stopping distance increases rapidly, particularly when lower accelerations occur early in the acceleration pulse.

Although a square wave pulse is neither achievable with realistic structures, nor desirable based on current restraint system technology, it is necessary to more nearly approach square wave crash response, relative to conventional vehicles, in order to achieve 50 mph crash survivability, as is illustrated by the following crash test results.

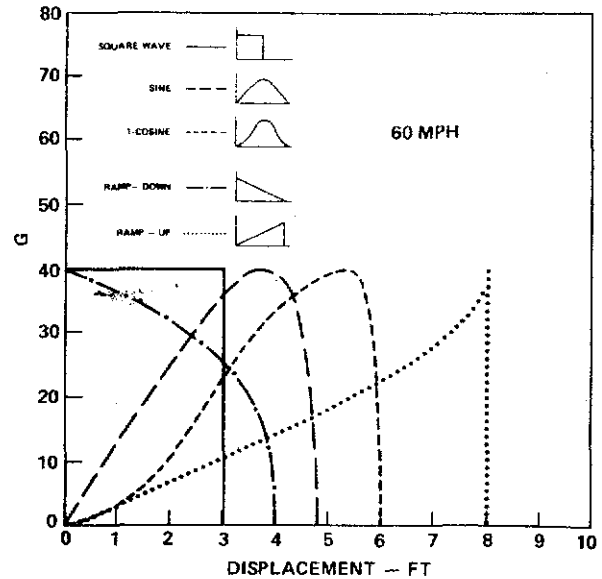
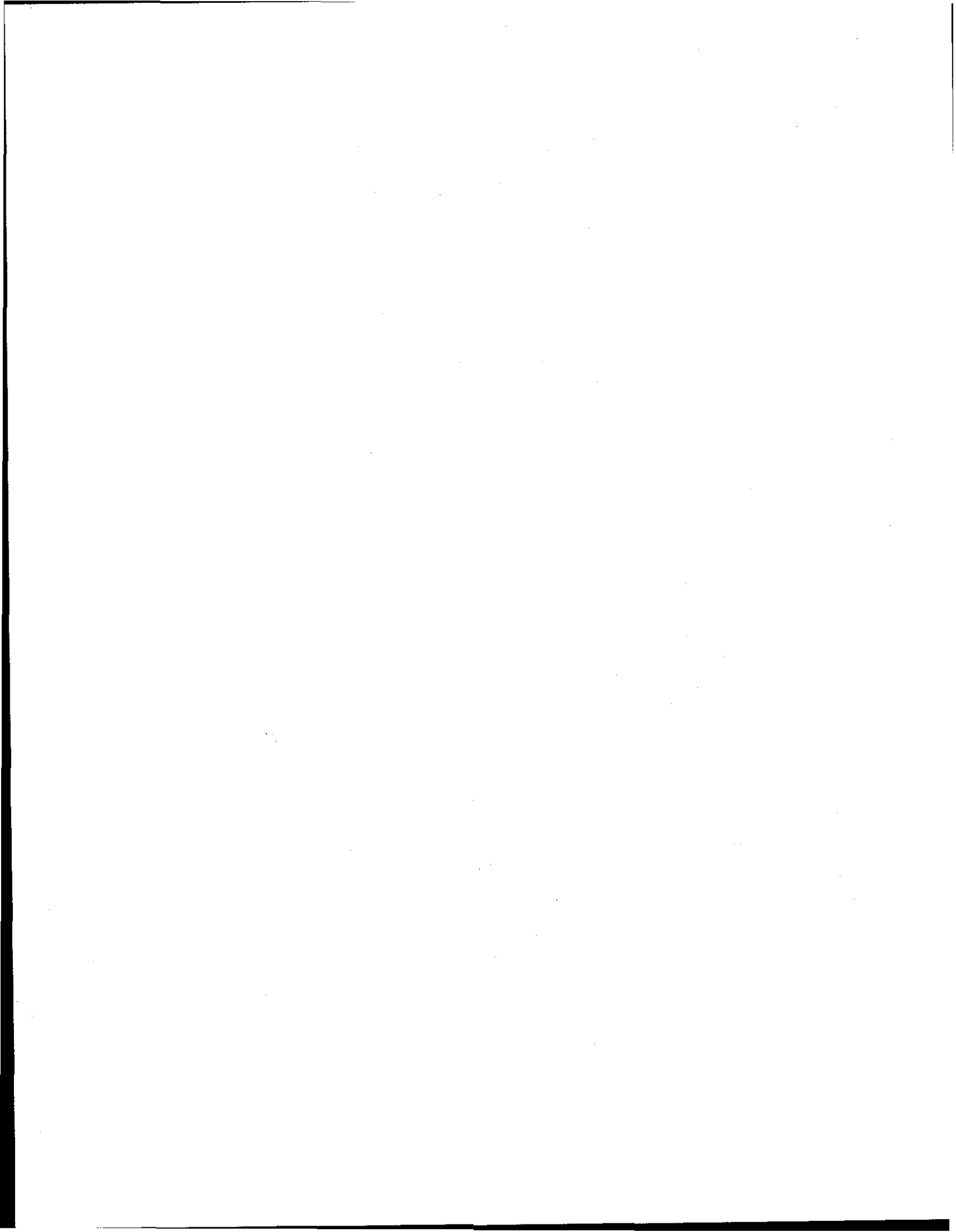


FIGURE 7 - Effects of Deviations from Square Wave Acceleration Pulse on Stopping Distance from 60 MPH

The occupant compartment accelerations resulting from a 38 mph head-on crash of a 1966 Ford sedan against a 12 3/4 inch diameter rigid pole are compared



with a 15° oblique pole crash and a 20° oblique flat faced barrier crash in Figure 8. The tests were performed by the Cornell Aeronautical Laboratory.⁵

The crash pulses are very similar during the first 25 inches of crush. The head-on pole crash develops higher peak accelerations between 25 and 35 inches of crush, as the engine is pressed into the fire wall. In the oblique crashes, the engine tends to move sideways, and the peak accelerations are somewhat delayed. Nevertheless, the acceleration responses in these varied crash tests are quite similar.

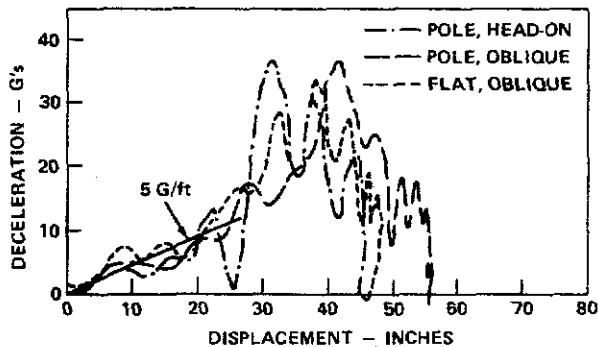


FIGURE 8 - Comparison of Occupant Compartment Acceleration from a 38 mph Crash

The pole barrier is used because it is considered to better reflect the varied crashes to be expected on the highway than the head-on flat faced barrier test traditionally used for automobile crash testing. The results of a 38 mph 90° frontal test⁵ of a 1966 Ford sedan against a flat barrier is compared with the head-on pole barrier test in Figure 9. The peak accelerations for the flat barrier crash test are higher than that of the pole test. Note that the static crush distance is considerably less; 29.6 inches compared to 46.6 inches. The test conditions of these two cases were nearly identical. The variation in response is caused primarily by the symmetrical, highly effective

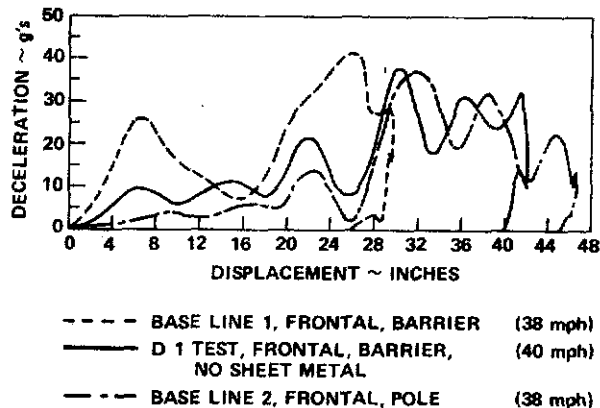


FIGURE 9 - Crash Response of Ford Sedan in Head-On Flat Faced Barrier Crash

loading of the body sheet metal in the 90° flat barrier crash. This is illustrated in Figure 9 where results of a similar test with most of the front body sheet metal removed is compared with the normal flat and pole barrier test results. Although the accelerations are a little higher early in the crash, the response closely resembles the pole impact results. It is apparent that head-on impact against a flat barrier represents a special case, and crash response changes rapidly as the crash conditions change. The pole barrier test, although a severe crash condition, better reflects real world crash conditions.

The results of a 1966 Ford sedan impacting a pole barrier head-on at 59.2 mph⁹ are presented in Figure 10. The pole penetrated six feet into the front of the car causing major intrusion of the front seat driver and passenger area. The test vehicle is shown before and after the crash in Figure 11. It is clear from the resulting compartment devastation, that six feet of crush is unacceptable. To preserve a tolerable physical

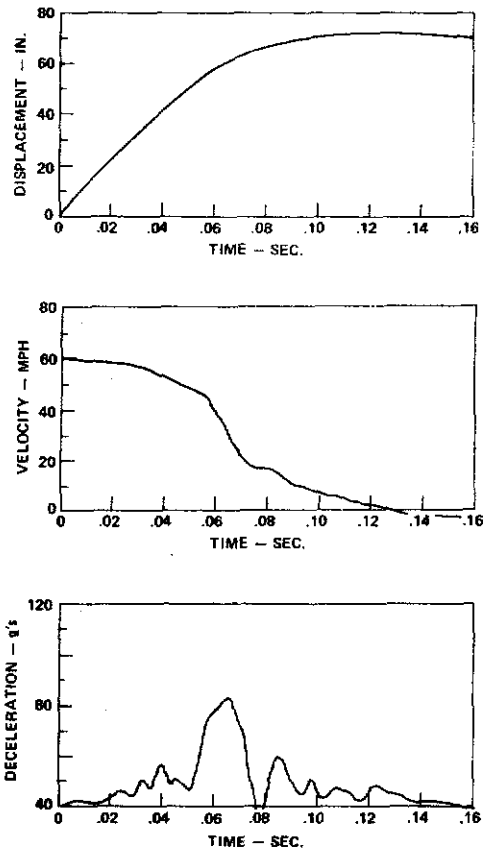
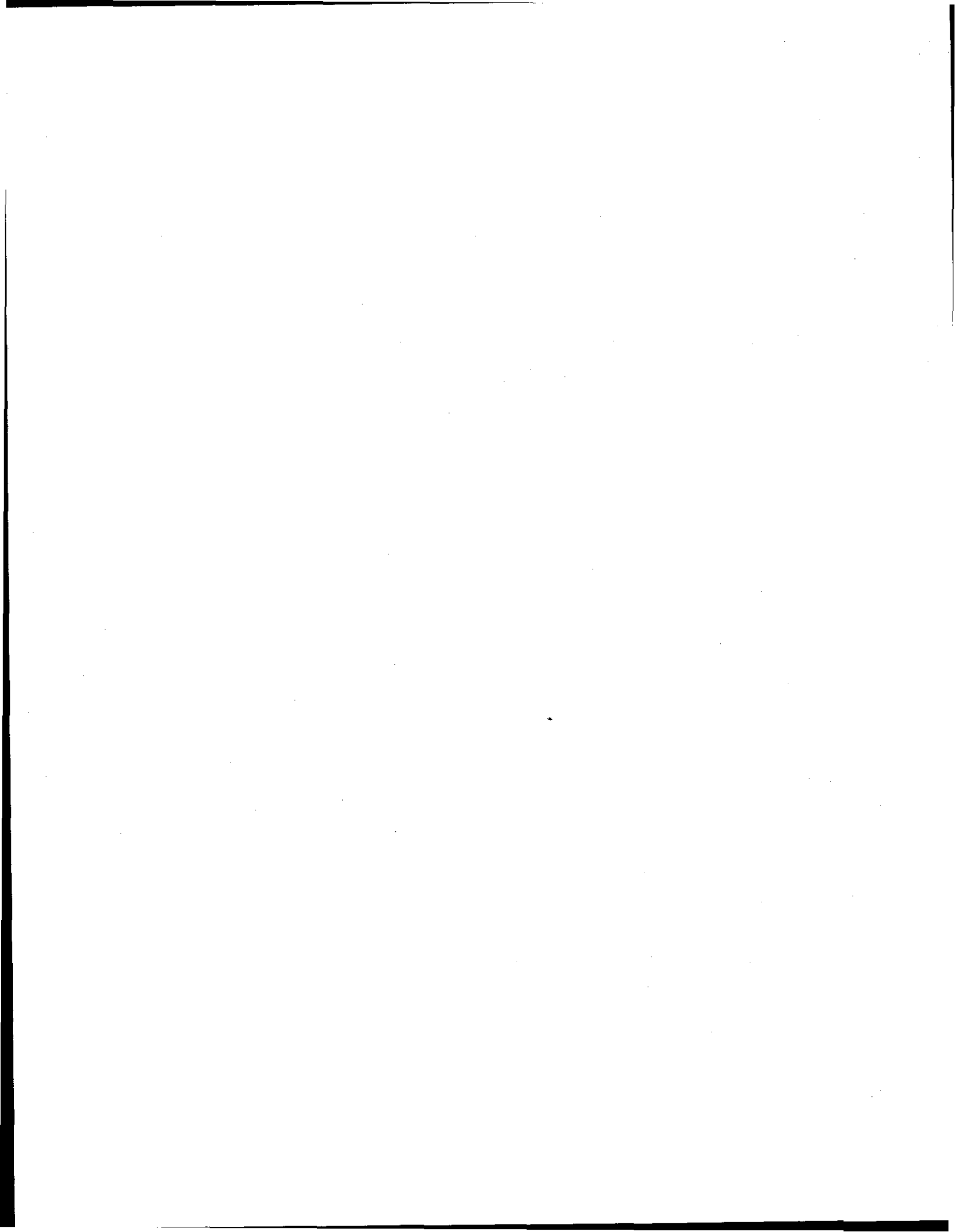
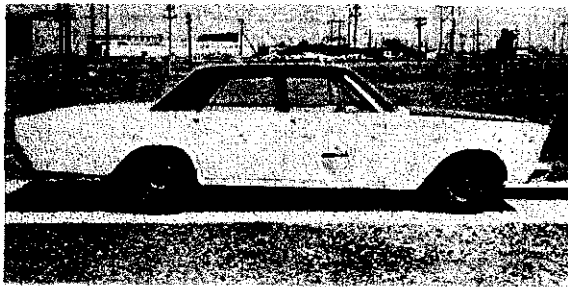
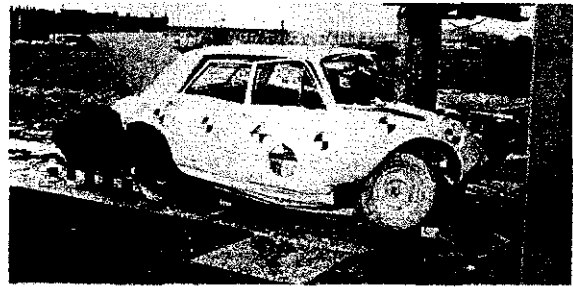


FIGURE 10 - 59.2 MPH Pole Barrier Crash Motion of Ford Sedan

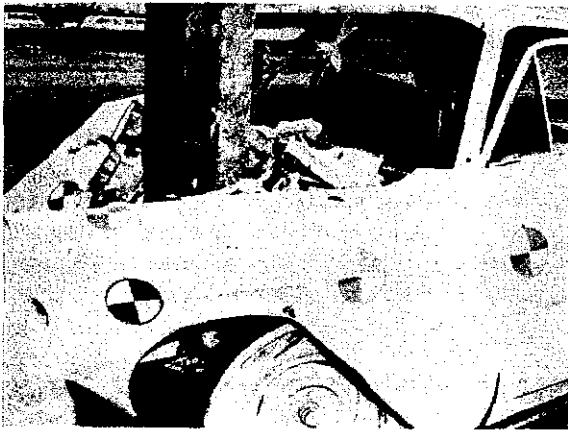




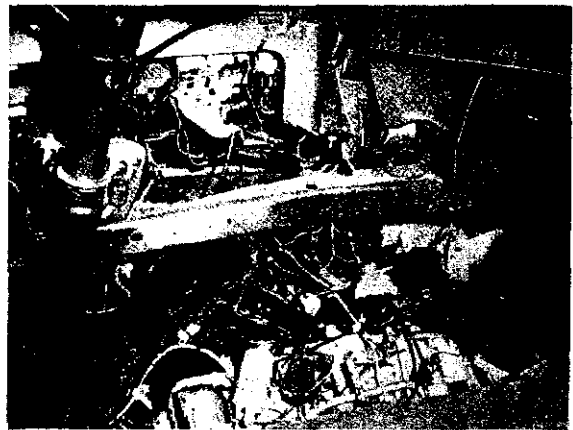
a



b



c



d

FIGURE 11 - 1966 Ford Sedan Impacting Pole Barrier Head-On at 59.2 MPH

environment for the crash victim in crashes of this severity, the car must either be made longer to increase the available crush distance, or the structure must be modified to generate higher accelerations early in the crash pulse to more efficiently use the available crush distance.

Several development projects have been undertaken to investigate the feasibility and practicability of improving structural crashworthiness. A few basic objectives and goals were established to guide the effort, the most important of which were:

- 1) In a rigid barrier impact, the structure should produce more nearly a square wave acceleration pulse of $120000/W$ expressed in g, where W is the weight of the vehicle. The crash acceleration response would, therefore, be inversely proportional to vehicle weight, and the crush force of all vehicles would be approximately equal. For example, a 2000-pound vehicle would be accelerated at about 60 g's in a crash. This is a fairly high acceleration level, but one that is considered to be tolerable with advanced restraint systems. Larger vehicles would accelerate at correspondingly lower levels in accord-

ance to their weight, as shown in Figure 12. Since each car develops the same crush force in the ideal case, each car would experience the same amount of crush in a car-to-car crash, even when the cars are of different size and weight. This provides the occupants of smaller cars a

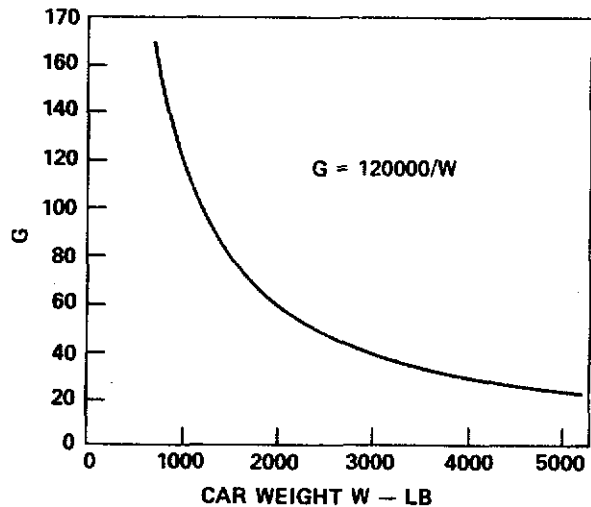
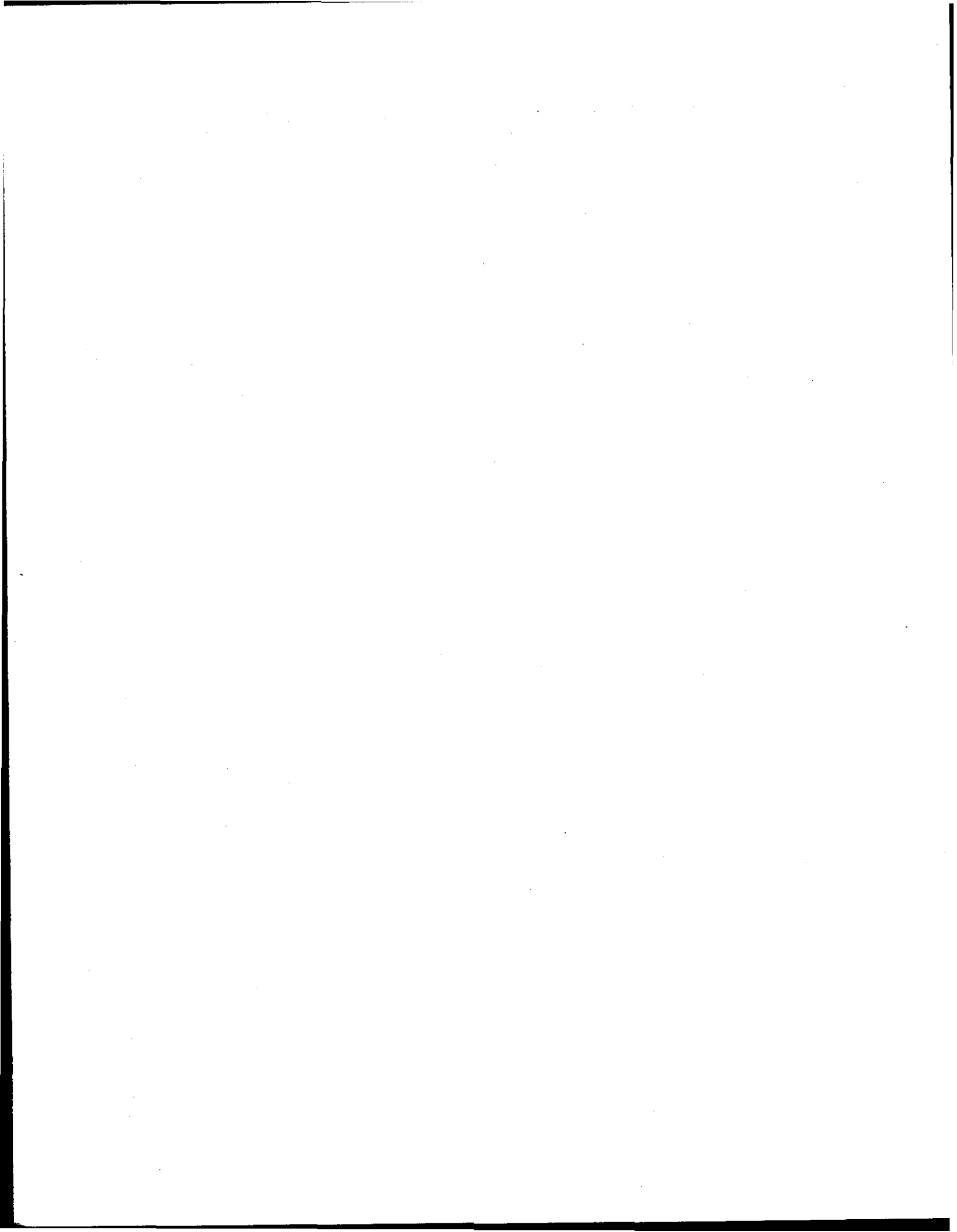


FIGURE 12 - Design G as Function of Weight for Desired Load Limiting Structure



much better chance of survival when they strike, or are struck by larger cars, since in conventional vehicles, the smaller car tends to crush more than the larger car, as will be seen below. In effect, the greater size (longer crush distance) of the heavier car is used to compensate somewhat for the inherent weight disadvantage of the smaller car. This technique for achieving compatible crash energy management characteristics for cars of various size and weight is further discussed below.

- 2) The size and functional characteristics of the vehicle should remain unchanged. The overall length of the vehicle should not be increased, the size of the occupant compartment and the usable trunk volume should not be decreased, the bumpers should not be extended beyond their current locations, the appearance of the vehicle should not be changed appreciably, etc.
- 3) Vehicle weight increases should be minimized.
- 4) Structural configurations should be compatible with efficient automobile mass production techniques.
- 5) Materials common to the automobile industry should be used to the greatest possible extent.
- 6) Other steps should be taken as necessary to minimize the cost of improving structural crashworthiness.

Under these broad guidelines, the development of increasing levels of structural crashworthiness was initiated as a means of studying feasibility and practicability. Some of the highlights of this program to date are reviewed in the following section.

FORWARD STRUCTURE MODIFICATION CONCEPTS

A 1966 Ford sedan was modified to more efficiently use the distance between the front bumper and the front of the engine, plus the distance between the back of the engine and the firewall, to dissipate crash energy and stop the vehicle. A critical requirement placed on the design was that the structure should not be sensitive to variations in crash conditions; i.e., it should respond at about the same acceleration levels in all types of frontal crashes (head-on and oblique, pole and flat barrier, etc.). Figure 13 shows the general configuration of the bumper and bumper support structural concept that was selected. Other modifications were made as required to assure the integrity and desired collision response of other parts of the structure⁶. A photo-

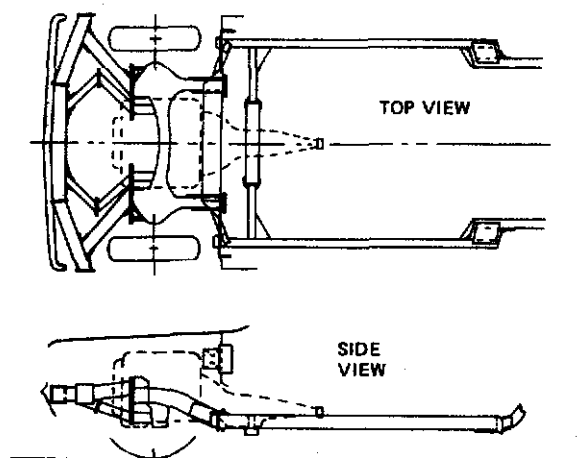


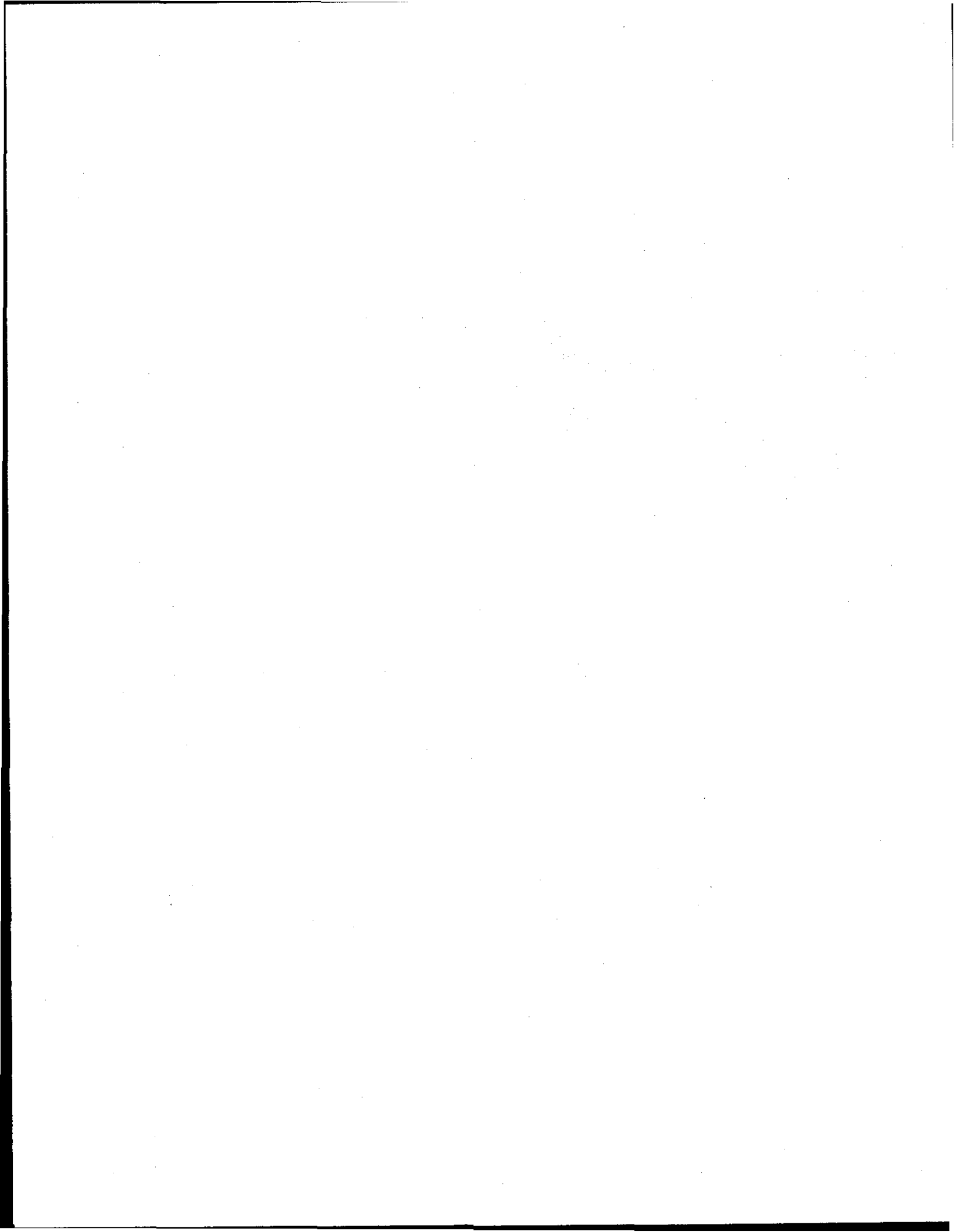
FIGURE 13 -- Sketch of Mod. 2A(2) Design

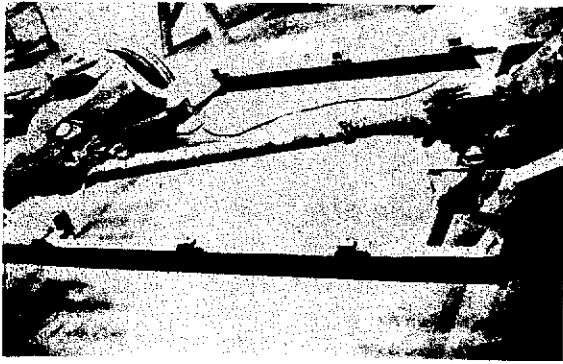
graph of the modified vehicle is shown in Figure 14. It should be noted that all body sheet metal and the front bumper are properly positioned on the vehicle. The size and external appearance of the vehicle was unchanged.

The test vehicle, designated Mod 2A(2), was crashed into a pole barrier at a speed of 35.3 mph.⁶ The test was a 15 degree oblique frontal impact with the point of impact occurring on the front bumper 15½ inches to the left of center. A 50th percentile anthropometric dummy was seated in the right front seat and restrained by a standard lap belt in combination with an air bag restraint system. Figure 15 shows the car before and after the test. The results are compared with the 38 mph head-on, and the 43 mph oblique pole barrier tests which were conducted with unmodified 1966 Ford sedans in Figure 16. The acceleration, velocity and crush responses for the modified vehicle are compared with the unmodified car oblique pole test results in Figures 17 and 18.

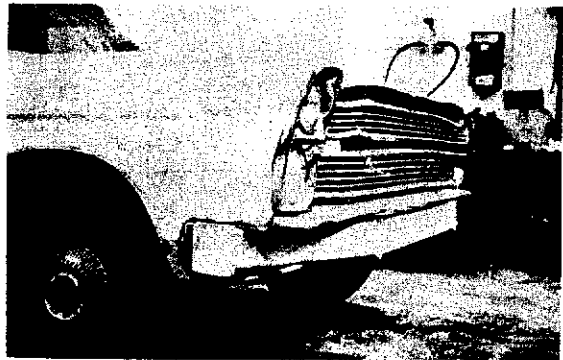
Although direct comparison with the unmodified vehicle tests are complicated by the difference in the crash test speeds, it is clear that significant accelerations are developed early in the crash sequence, and the amount of crush is greatly reduced. It is interesting that the peak acceleration of the modified vehicle is not higher than for the unmodified vehicles, but is simply developed earlier as the front bumper structure collapses, rather than later when the engine is forced into the firewall.

Modified Ford sedan structures that incorporate a mechanism to deflect the engine under the occupant compartment in high speed crashes have also been tested.⁷ In one such test, a modified vehicle, designated Mod 1B(2)R, impacted the rigid pole barrier at

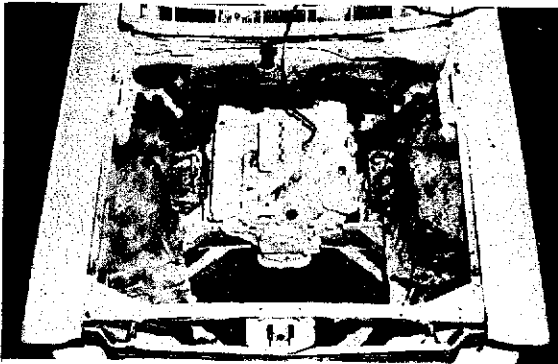




a



b

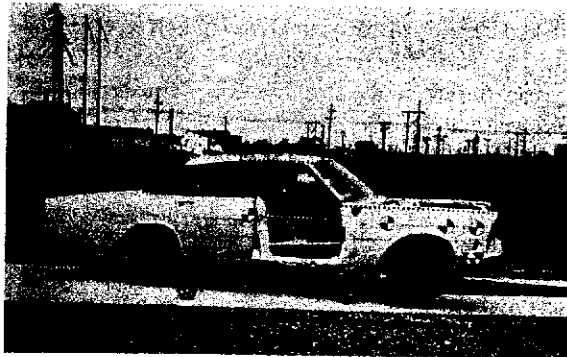


c

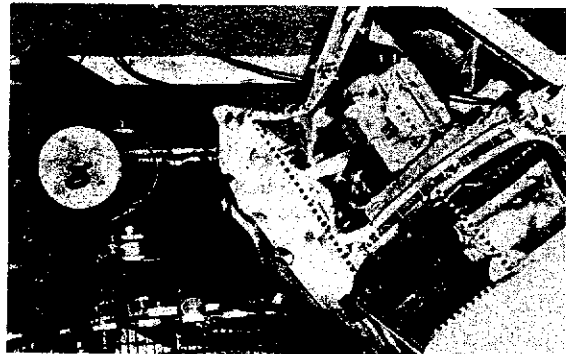


d

FIGURE 14 – Mod.2A(2) Design Modifications



a



b

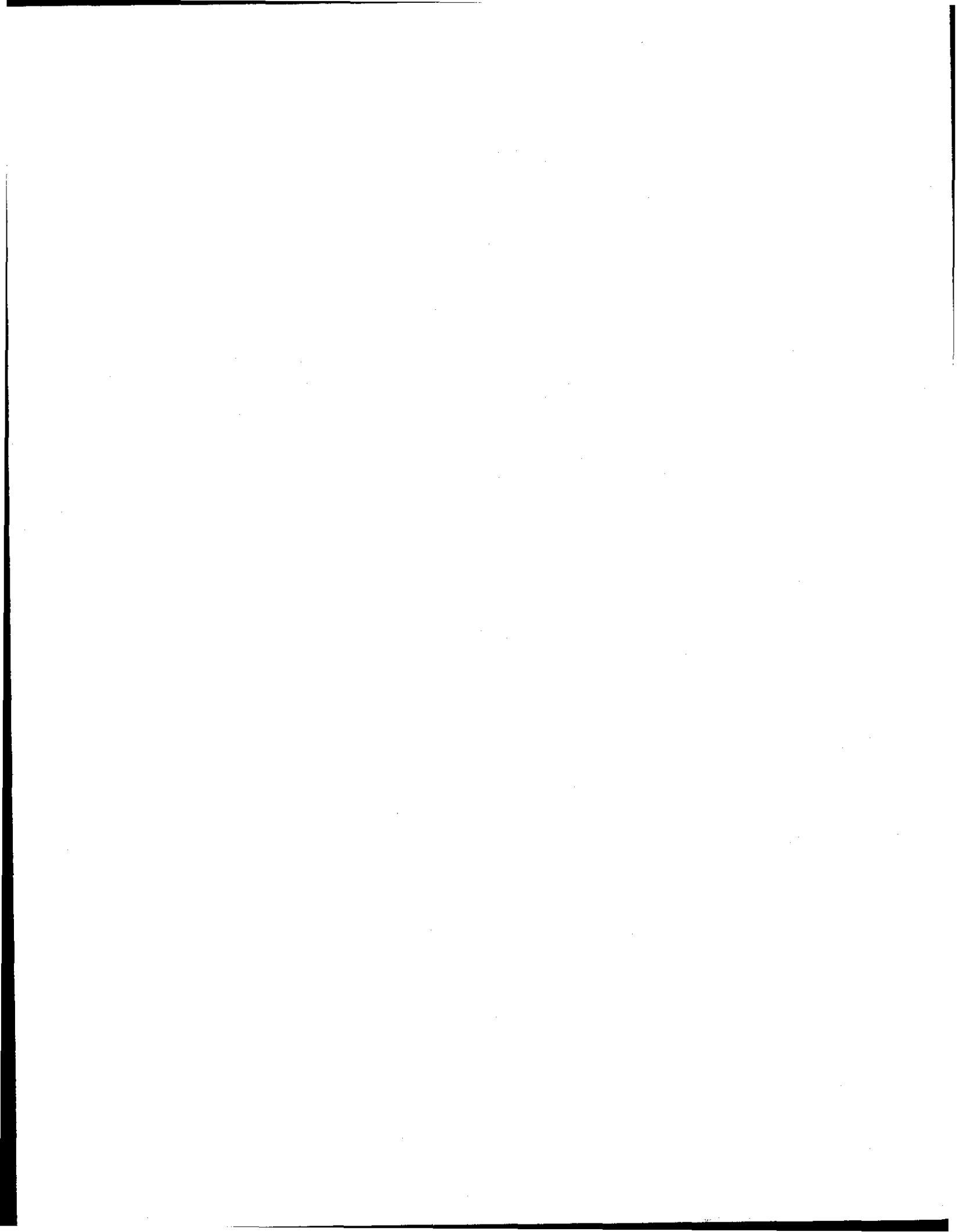


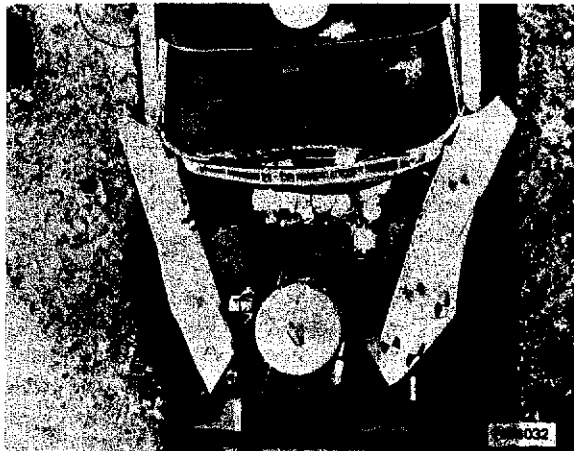
c



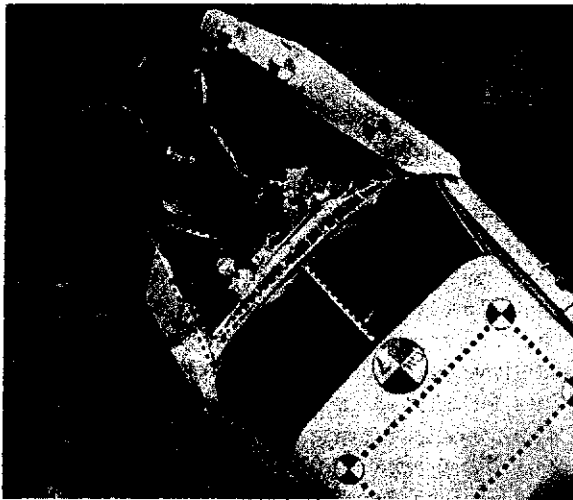
d

FIGURE 15 – Mod.2A(2), 15° Oblique Pole Impact





HEAD-ON



OBLIQUE

FIGURE 16 - Pole Impact - Unmodified Ford

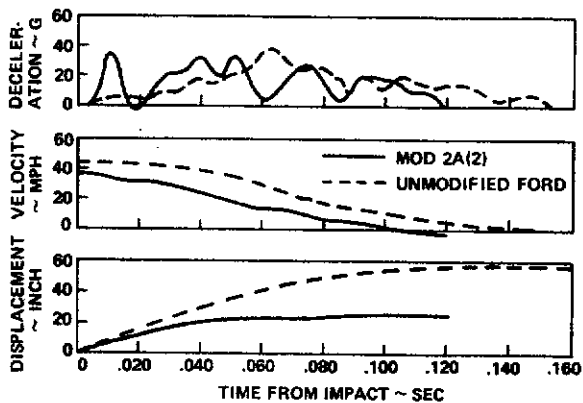


FIGURE 17 - Passenger Compartment Motion - Oblique Pole Barrier Crash - Mod 2A(2) and Unmodified Ford Sedan

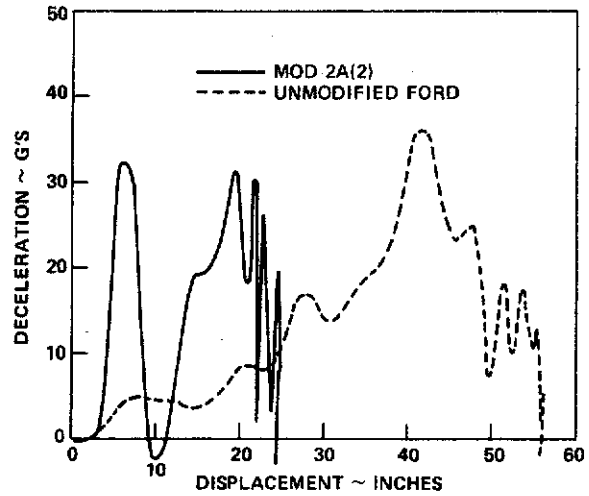


FIGURE 18 - Passenger Compartment Deceleration-Displacement Data - Oblique Pole Barrier Crash - Mod 2A(2) and Unmodified Ford Sedan

a speed of 63 mph. The acceleration-displacement response of the Mod 1B(2)R vehicle is compared with that of an unmodified Ford sedan in a similar crash test at a speed of 59 mph in Figure 19.

The Mod 1B(2)R vehicle generated higher accelerations early in the crash pulse, and avoided excessive intrusion of the occupant compartment by successfully deflecting the engine downward. In contrast, the unmodified Ford generated very low accelerations early in the crash pulse, a very high 85 g peak acceleration near the end of the pulse, and allowed extensive collapse of the occupant compartment in the front seat area. The front seat areas of both test vehicles are shown in Figure 20. Although the Mod 1B(2)R vehicle impacted the pole barrier with 25% more initial kinetic energy than the unmodified Ford, the occupant compartment remained reasonably intact, and the maximum acceleration was 60 g's.

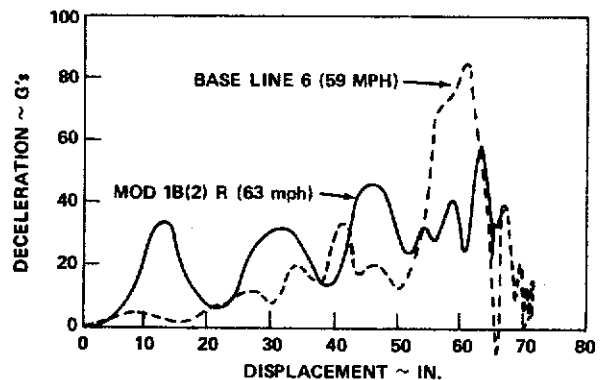
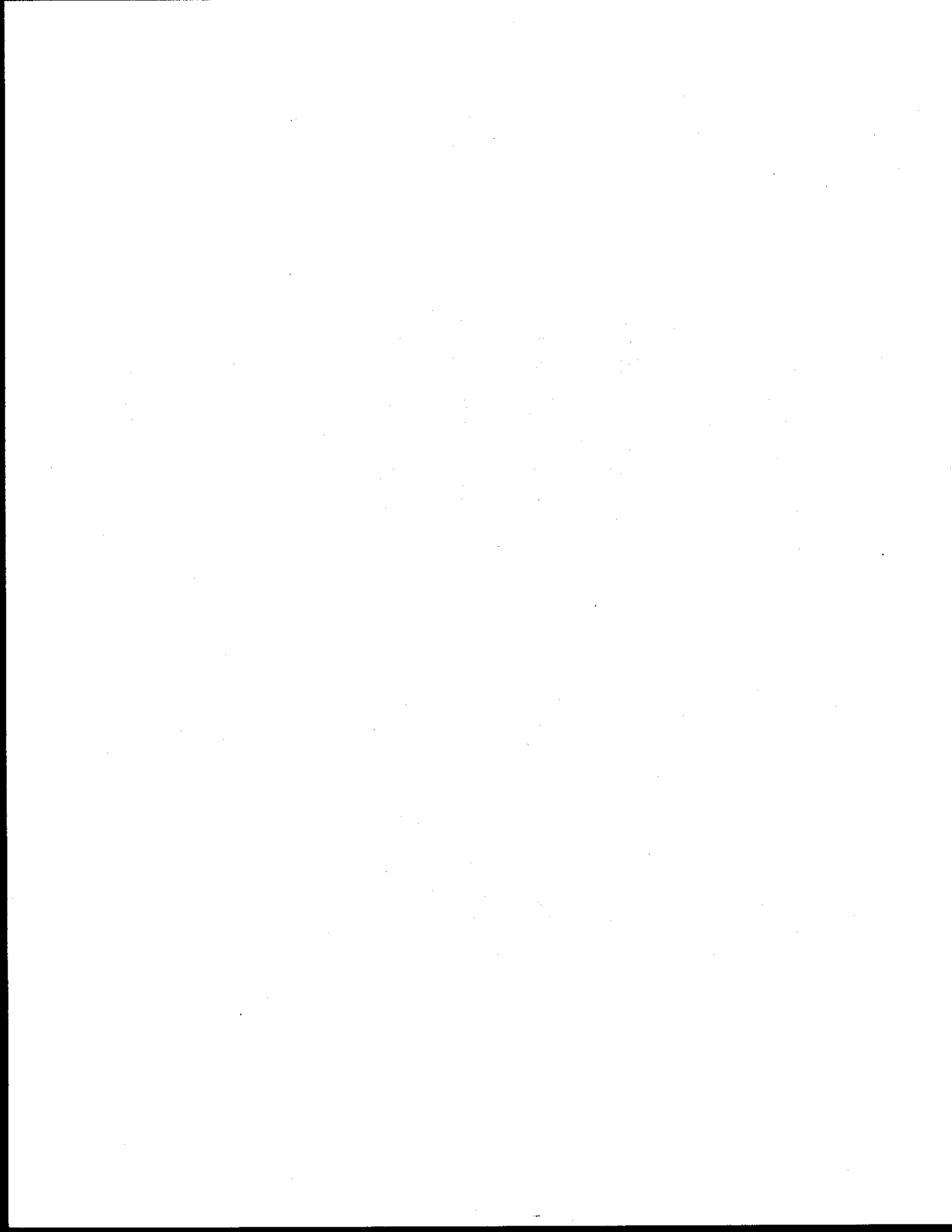
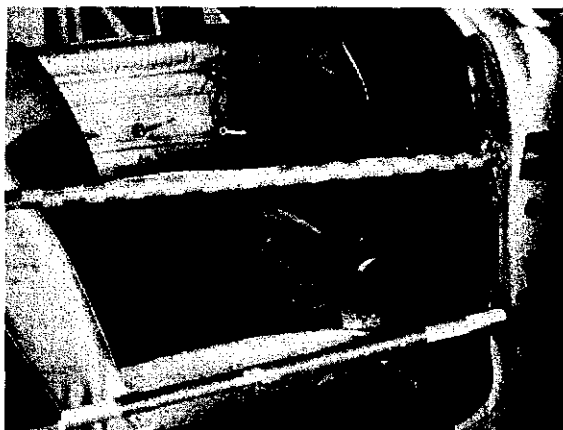
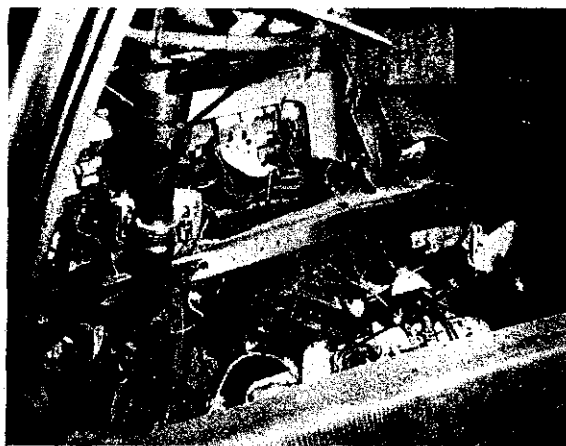


FIGURE 19 - Passenger Compartment Acceleration - Displacement Data - Pole Barrier Crash - Mod 1B(2)R And Unmodified Ford Sedan





MOD. 1B(2)R



UNMODIFIED FORD

FIGURE 20 - Passenger Compartment Penetration Pole Barrier Crash - Mod 1B(2)R and Unmodified Ford Sedan

These results illustrate the feasibility of building automobile structures with substantially improved crash energy management characteristics. The test results show that structural modifications can limit maximum acceleration while greatly increasing the acceleration rise rate during the early portion of the crash to provide an effective stiffness of 240,000 lbs/ft of crush, or 60 g's/ft for a 4000 lb vehicle. This compares with 20,000 lb/ft (5 g's/ft) for conventional automobiles, as shown in Figures 8 and 19.

It is thus possible to tailor the structural crash response characteristics to protect the occupant compartment and limit maximum acceleration. In like manner, structural response can be altered to improve compatibility between vehicles in car-to-car crashes, and to accommodate the specific requirements of whatever restraint system is selected for use in the vehicle.

CAR-TO-CAR CRASH RESPONSE

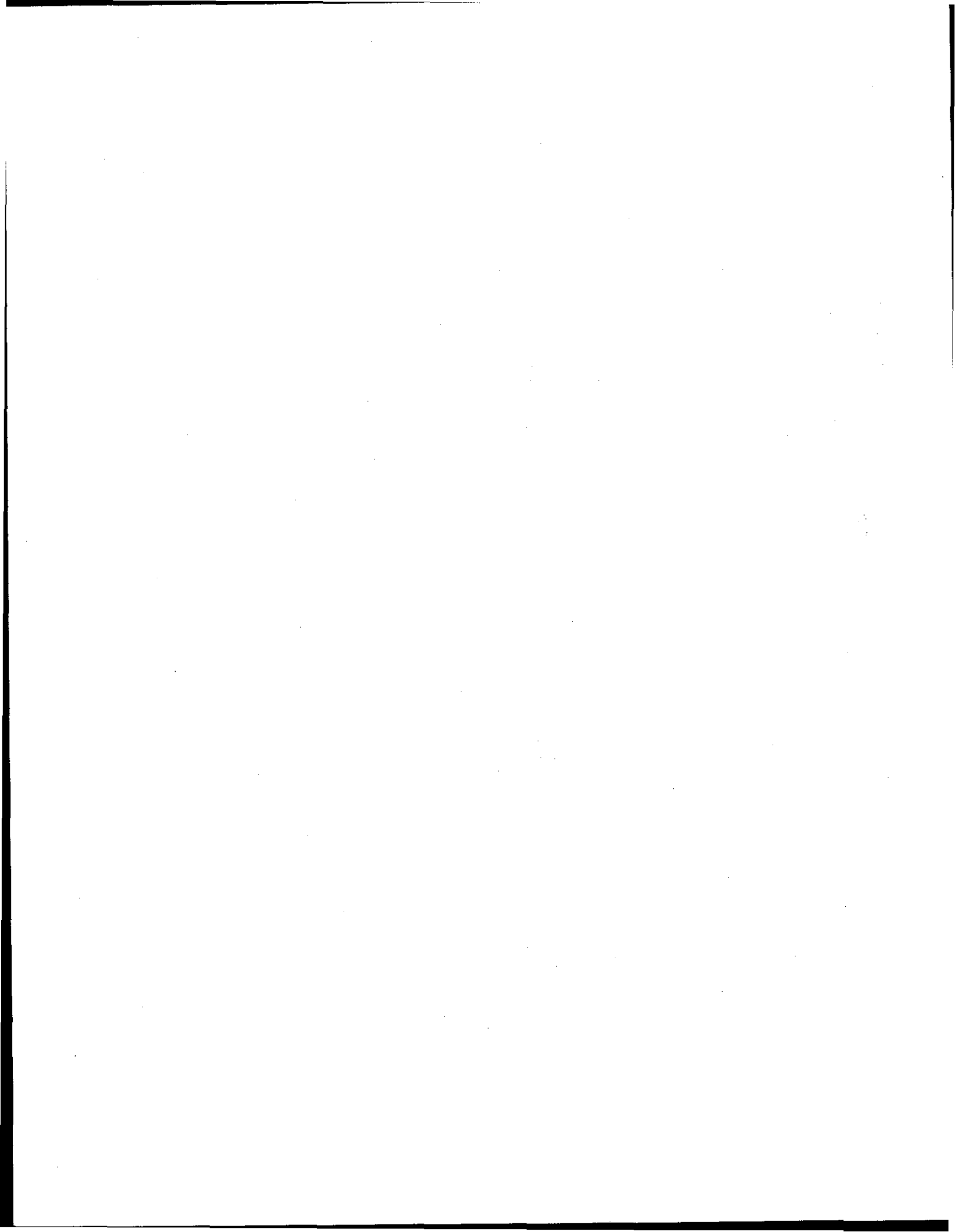
The requirements for survival of car-to-car crashes are the same as for barrier crashes; assure a tolerable acceleration environment and maintain adequate living space within the passenger compartment. To achieve this, however, careful attention must be directed to two important factors:

1. There must be an acceptable structural interface between the vehicles during the crash.
2. The crash response characteristics must be compatible between various size and weight vehicles, and in various crash situations.

The requirement for an acceptable structural interface between the cars during a crash is illustrated by comparing the results of two crash tests; the first test involved a head-on crash between two conventional 1968 Ford Sedans, the second test was a similar head-on impact between a conventional 1968 Ford Sedan and one modified for improved structural crashworthiness, including provisions that assure a good structural interface between the cars.

The two conventional Fords collided head-on, each car traveling 43.7 mph, a closing speed of 87.4 mph. One car weighed 3,850 lbs. and the other 3,910 lbs. Although the total crush of the two cars was nearly equal, 38 and 40 inches of crush, the intrusion into the front seat area of car No. 1 was greater. The frame members extending forward of the front wheel suspensions were virtually undamaged in this car, whereas these members were completely buckled in car No. 2. This indicates that the bumper and front structure of car No. 2 overrode car No. 1, and pushed the engine of car No. 1 deeper into the firewall, causing more intrusion in the front seat area.⁸

The second test between the conventional Ford and one modified for improved crashworthiness, designated Mod 2D1, was also a head-on crash at a closing speed of 88 mph. The test weights were 3,975 lbs. and 3,650, respectively. The structure of the modified Ford was considerably stronger than the unmodified car. Therefore, the unmodified car must absorb a larger share of the crash energy, which would normally be expected to result in more severe damage than would occur if both were conventional cars. However, the modified car was equipped with a wide forward face plate Figure 21, that prevented override and loaded the body sheet metal and other structure of the unmodified car more effectively. Because of the effective structural interface between the cars, damage to the unmodified car was no worse



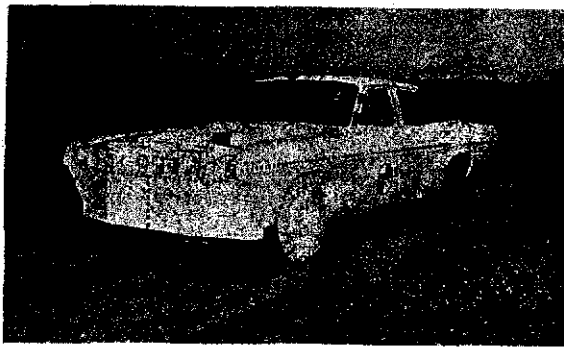


FIGURE 21 - Mod 2D(1) Test Vehicle

than in the previous test.⁹ The front seat passenger areas of car No. 1 in the previous test, and the unmodified car of the impact with the Mod 2D1 in the second test are compared in Figure 22.

The provision of a good structural interface is seen to improve the effective crashworthiness of a conventional structure by preventing override and more efficiently using body sheet metal and other related structures to react crash loads. This phenomenon was also apparent in comparing the crash response of conventional cars crashing head-on against a flat faced rigid barrier with other barrier impact situations. The crash response was appreciably better in the head-on flat barrier case, primarily because a better structural interface exists between the barrier and the car.

Crash response compatibility between cars of various size is a critical factor because small cars are handicapped in both size and weight during a crash with a larger vehicle. In today's cars, there is little effort to compensate for the smaller car's disadvantage. As a result, small car occupants are much more

likely to be seriously or fatally injured in a crash as are large car occupants¹⁰ as shown in Figure 23. This situation can be alleviated by using the greater length of heavier cars to help compensate for the weight and size disadvantage of the smaller ones.

The requirement for compatible crash response characteristics between cars of various sizes is illustrated by comparing the results of two crash tests; the first involved a head-on crash between a 1968 Ford Sedan and a 1968 Opel,¹¹ the second involved a similar 1968 Ford Sedan and a 1968 Opel modified for improved structural crashworthiness.¹²

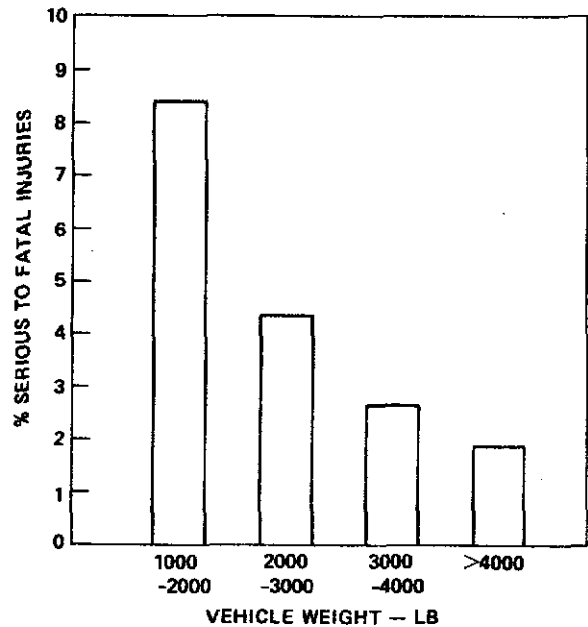
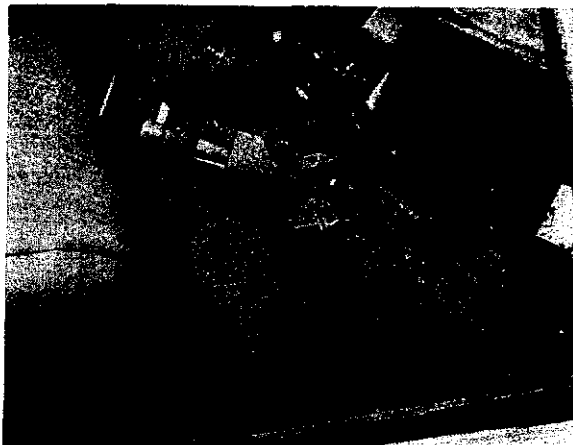
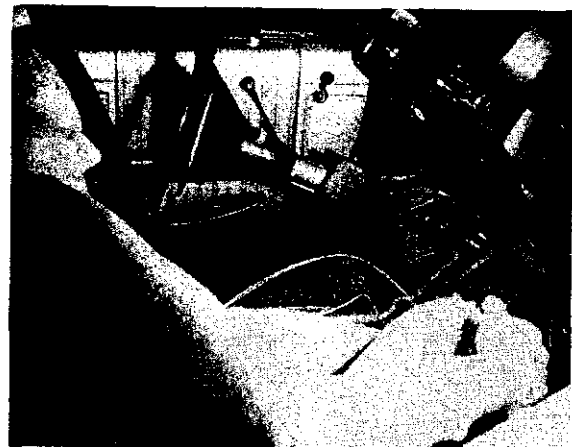


FIGURE 23 - Occurrence of Death or Serious Injury as a Function of Vehicle Weight

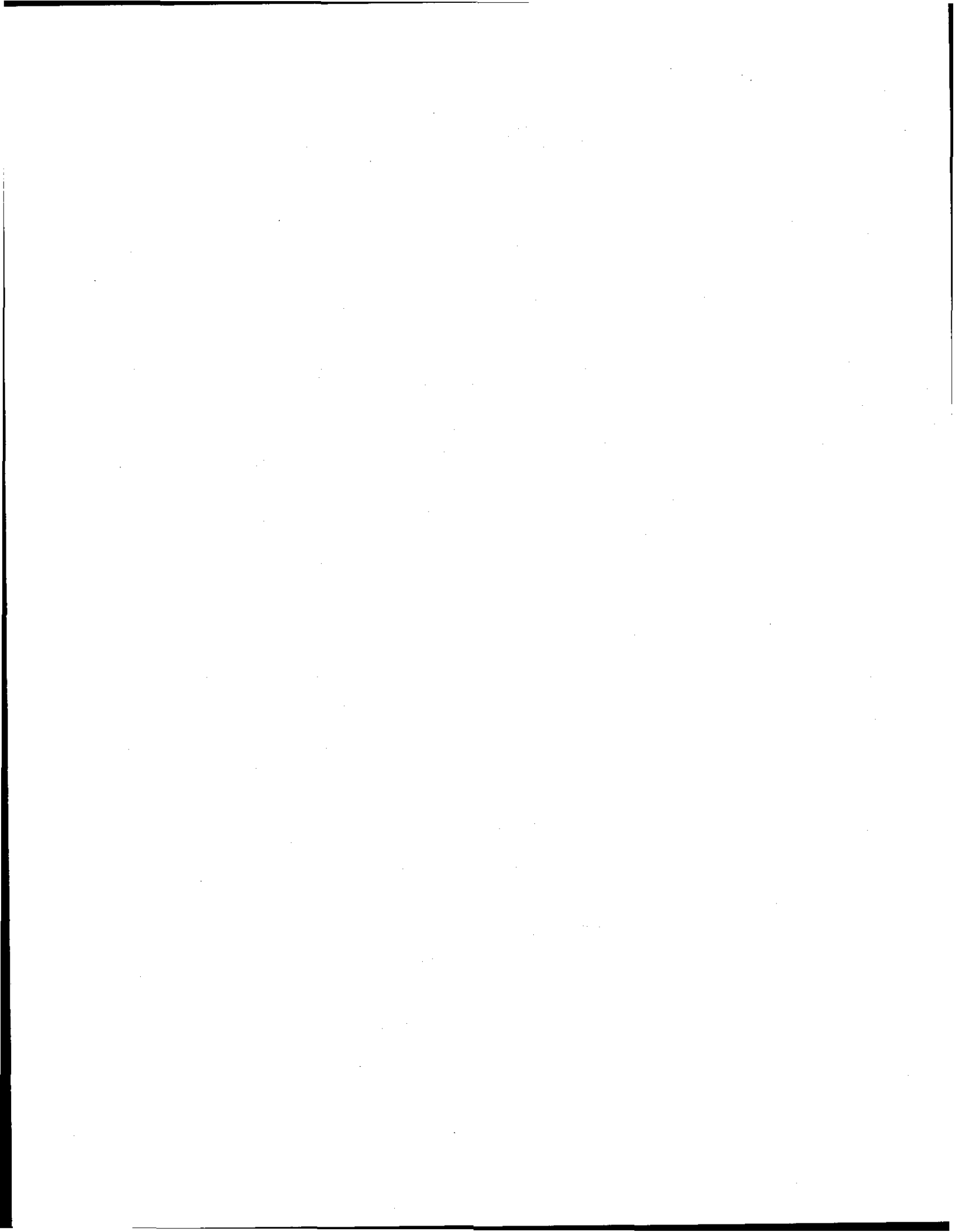


CAR 1 INTERIOR



UNMODIFIED CAR

FIGURE 22 - Passenger Compartment Interior of Ford Sedan Following Impact with Another Ford and with Mod 2D(1)



In the first test, the cars collided head-on at a closing speed of 87.6 mph. The Ford weighed 3960 lbs., and the Opel test weight was 1750 lbs. The acceleration responses of the two cars are compared in Figure 24. The acceleration level of the Opel is seen to be about twice as high as that for the Ford. This reflects the 2 to 1 weight disadvantage of the Opel. There is no way to compensate for this effect. When two cars collide, the ratio of their gross acceleration responses will always be inversely proportional to the ratio of their masses.

Although it is not possible to control the *ratio* of the gross accelerations, it is possible to control both the acceleration magnitude (consistent with mass ratio effects) and the relative amount of crush experienced by each car, by *designing the vehicle structures to collapse at the appropriate force levels.*

In the Ford-Opel test, the maximum acceleration in the Opel was about 60 g. This is within tolerable limits for cars using air bag restraints. However, the Opel incurred the major portion of the structural damage as seen in Figure 25. The post test crush of

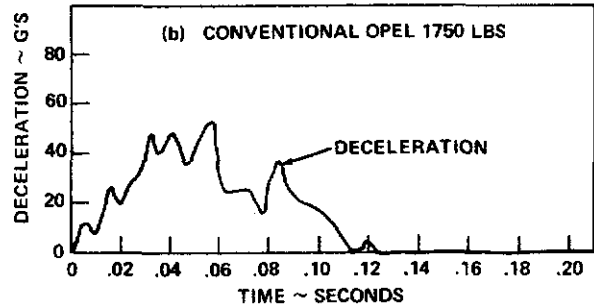
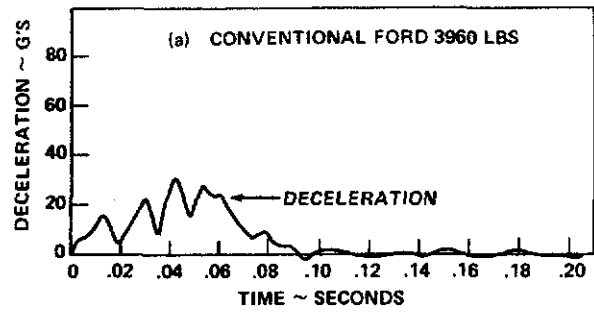


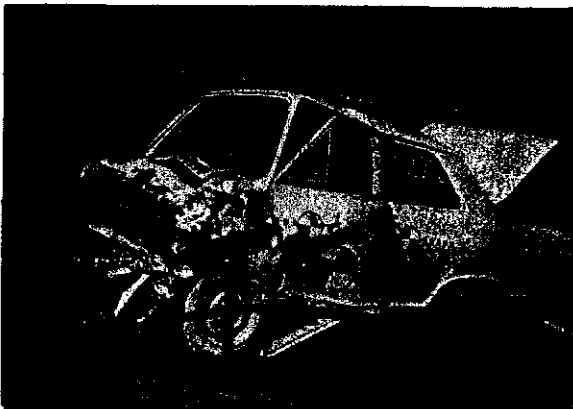
FIGURE 24 — Weight Mix Car-Car Acceleration Response — Ford-vs-Opel



FORD



POST-CRASH FORD INTERIOR

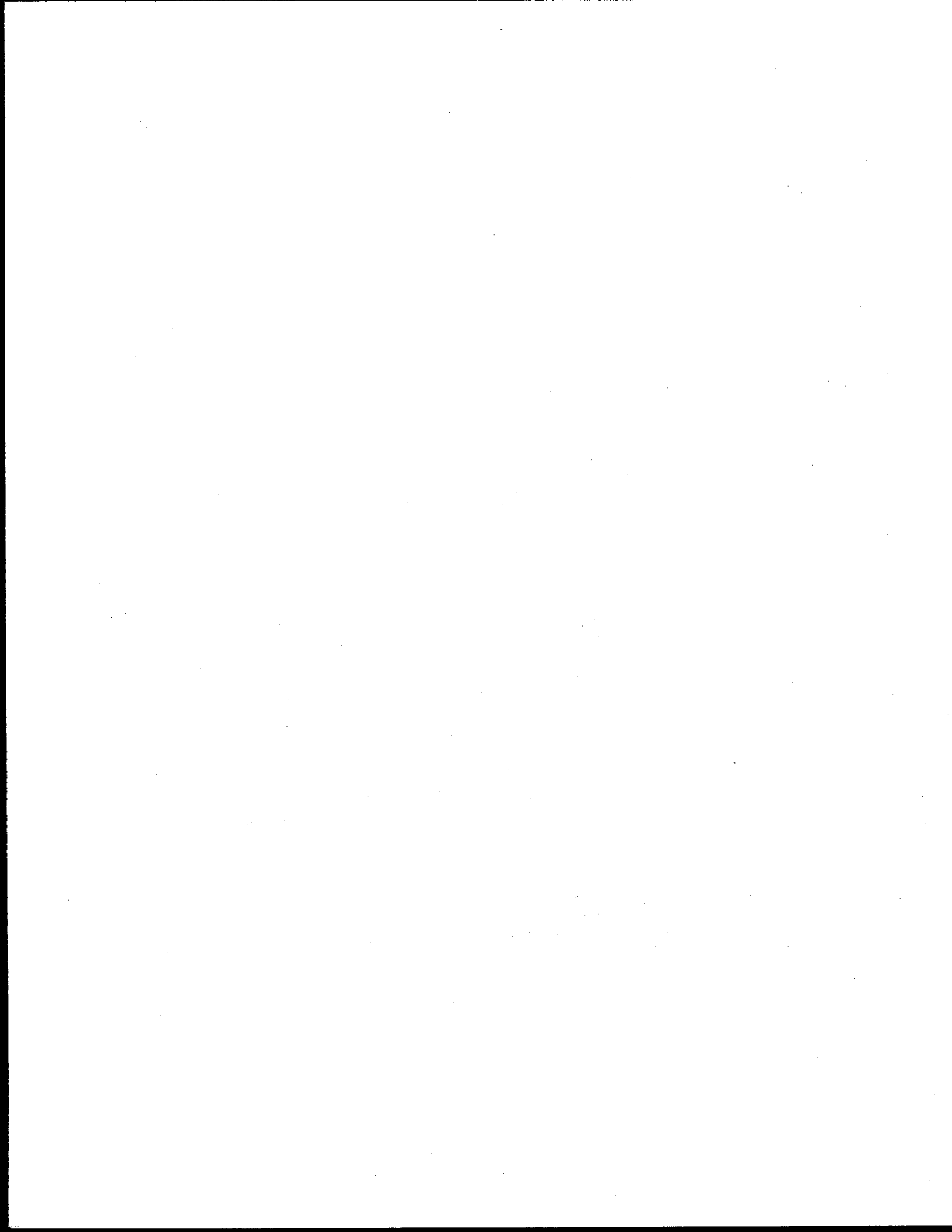


POST-CRASH OPEL



POST-CRASH OPEL INTERIOR

FIGURE 25 — Ford vs Opel Head-On Crash Test — Closure Speed 87.6 MPH



the Opel was 41 inches, compared to 23 inches for the Ford.

In the second test, the conventional Ford was traveling at 26.5 mph, and the modified Opel speed was 29.2 mph, for a closing speed of 55.7 mph. Car weights were 3840 lbs. and 1880 lbs. for the Ford and modified Opel respectively.

Although the lower speed precludes direct comparison with the first test, the basic relationships are evident. The acceleration responses of the cars are compared in Figure 26. The higher gross acceleration of the Opel is as expected. However, it is apparent from the post-test view of the cars shown in Figure 27 that the Opel incurred very little damage. The post-test crush of the Ford was 25 inches, compared with 2 inches for the Opel.

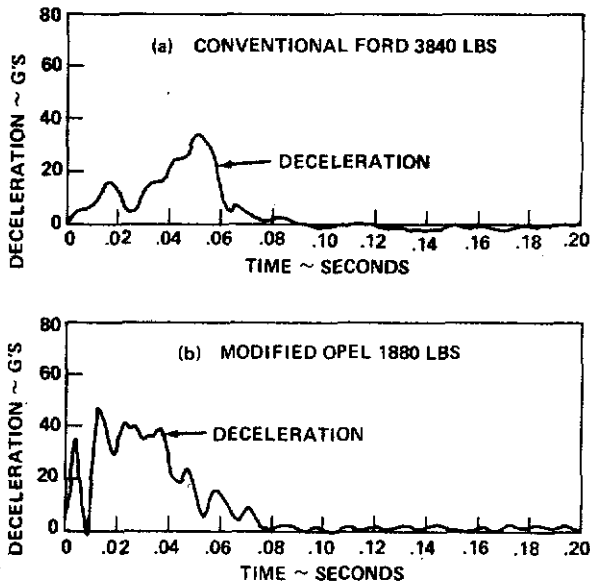


FIGURE 26 - Weight Mix Car-Car Acceleration Response - Ford vs Modified Opel

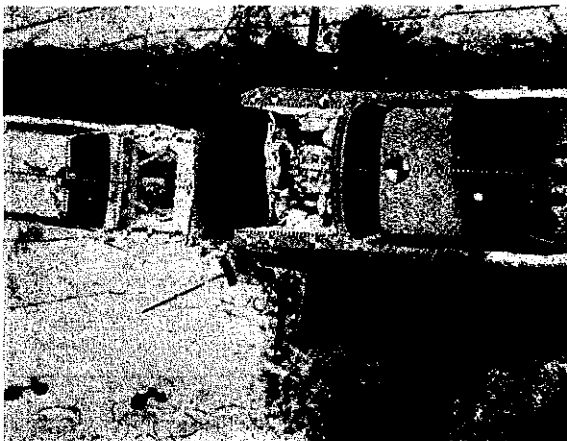


FIGURE 27 - Ford vs Modified Opel Head-On Crash Test - Closure Speed 55.7 MPH

The important point is that the relative collapse can be controlled, regardless of the weight ratio, by controlling the relative collapse strength of the cars. This allows the use of the greater size of heavy cars to compensate, in part at least, for the size and weight disadvantage of smaller vehicles.

There are several ways to accomplish this structural compatibility between cars of different size and weight. Two such approaches that are being extensively researched by the National Highway Traffic Safety Administration involve fixed force structures with carefully tailored collapse force characteristics similar to those discussed above, and velocity sensitive hydraulic force generators.

ANALYSIS OF MIXED VEHICLE CRUSH COMPATABILITY

A simplified analytical model was developed to study structural energy absorption characteristics in terms of crush and compartment peak g's resulting from a head-on collision of two unequal weight vehicles. The model is a lumped mass one-dimensional model containing six degrees of freedom - three for each vehicle. A schematic diagram of the model is presented in Figure 28.

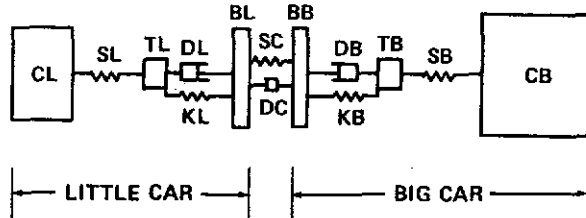
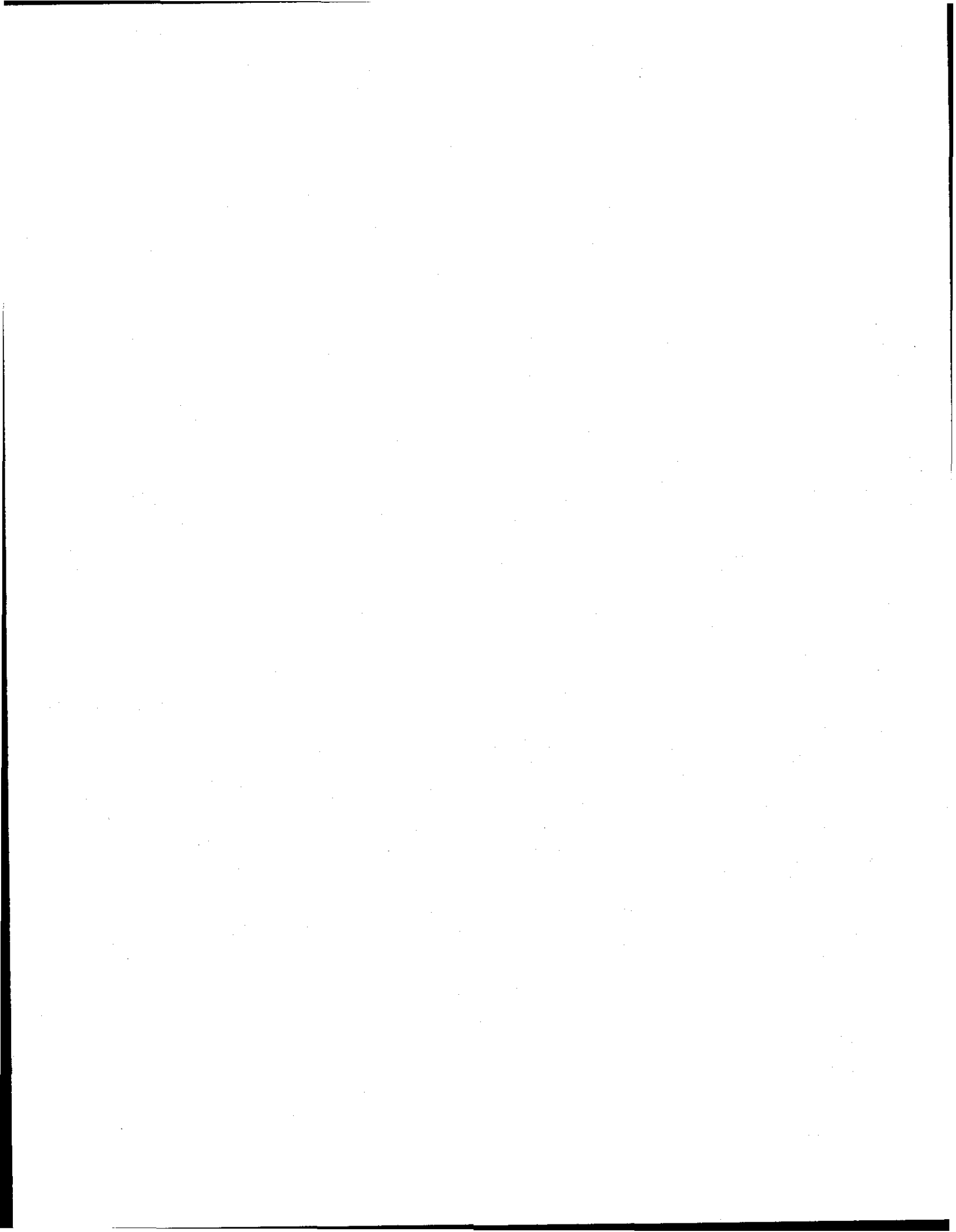


FIGURE 28 - Six Degree of Freedom Spring-Mass Model

Vehicle weights for the major portion of the study were 4,000 lbs. for the big car, and 2,000 lbs. for the small car. The vehicle mass consists of an effective bumper mass (BL for the little car and BB for the big car), effective compartment mass (CL and CB) and a small mass (TL and TB) which allows a series connection of the spring energy absorbers (SL and SB) with the velocity sensitive energy absorbers (DL and DB). A contact spring (SC) and damper DC are provided between the bumpers for system continuity.

The spring energy absorbers (SL and SB) represent inelastic load limiting structure with a prescribed ramp (spring-rate) to provide a desired deceleration deformation onset.

The equations used to define the velocity sensitive energy absorbers are those of a hydraulic cylinder system with a variable orifice area which provides a constant force under ideal barrier impact.



The CSMP program was written so that a variety of parametric studies could be made by merely changing input conditions or multiplying factors. For example, the spring constants K_L and K_B shown in Figure 28 are hydraulic system lockouts which are either activated or eliminated by a multiplying factor. A barrier simulation is achieved for each vehicle by restricting the bumper displacement under the control of a multiplying factor.

Side collision is simulated with the same model by adjusting the spring rates and the effective bumper mass of the struck car (simulating side frame and door structure) and setting the initial velocity of the struck car equal to zero.

Although the model is relatively simple, it provides a good basis for qualitative assessment of the effect of various structural energy absorption characteristics. It permits trends to be studied and possible trade-offs to be located quickly and inexpensively.

A study of intervehicular structural crash compatibility is presented. Structural responses are compared for three crash modes:

- (1) frontal collision of structures with matched acceleration properties,
- (2) velocity sensitive and fixed force structures designed for improved intervehicular compatibility in frontal crashes, and
- (3) implications of front structure modifications in front-to-side crashes.

In all cases, the crush force onset rate was restricted to 40,000 lbs. per foot of vehicle crush in the 2,000 lb. vehicle. This is necessary to allow adequate deployment time for the occupant restraint system. Although it may be possible to relax the 40,000 lb. per foot restriction, it was selected to assure a high level of confidence in achieving satisfactory restraint system performance.

A restriction of 60,000 lbs. per foot of vehicle crush is placed on the crush force onset rate for the 4,000 lb. vehicle with fixed force energy absorber. This provides reasonable compatibility with the 40,000 lbs. per foot limit on the 2,000 lb. vehicle without causing excessive crush of the larger vehicle in rigid barrier impacts. Further, it provides acceptable performance in front-to-side crashes, as discussed below.

The car-to-car crash response of the 4,000 lb. vehicle with velocity sensitive structure is not as sensitive to the force onset rate as the fixed force structure. However, some relief for the smaller vehicle is afforded by lowering the force onset rate, and a

60,000 lbs. per foot value is used for the velocity sensitive structure also.

MATCHED ACCELERATION RESPONSE

The matched acceleration response characteristics of the 2,000 lb. and 4,000 lb. vehicles are shown in Figure 29 for the fixed force structure. The design maximum acceleration is 40 g's for each vehicle, causing a 2 to 1 crush force ratio between the 4,000 lb. and the 2,000 lb. vehicles. The crush force of the fixed force structure increases as crush increases beyond the break point of 40 g. This was done to facilitate the analysis, and has little effect on the results.

For the velocity sensitive vehicle structures, the design maximum accelerations are a function of initial impact speed, as shown in Figure 30. The break points in the curves are referred to as V_{DES} and/or G_{DES} . The curve up to the break point is

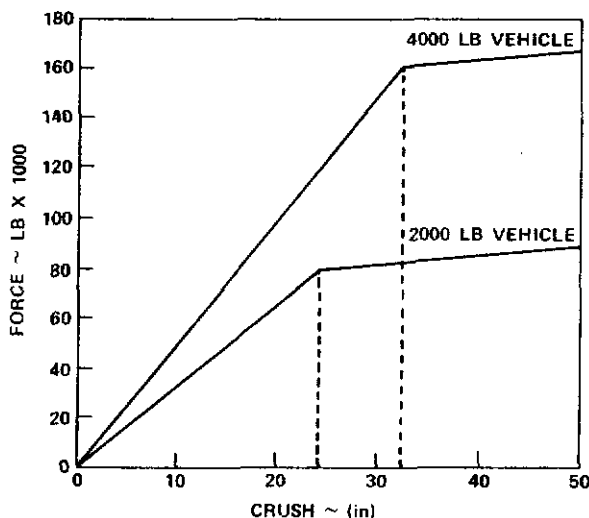


FIGURE 29 - Fixed Force Structure - Matched 40G Acceleration Crash Response

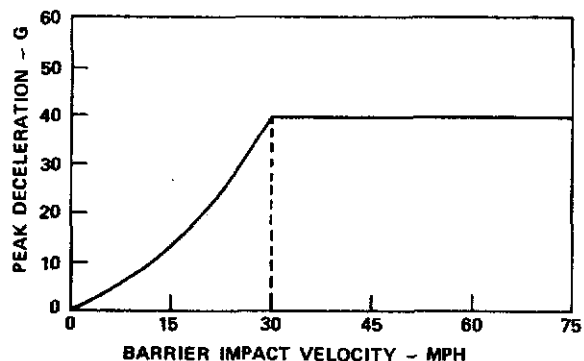


FIGURE 30 - Velocity Sensitive Structure - Matched V_{DES} and G_{DES} Crash Response



assumed proportional to the velocity squared. The term "velocity sensitive structure," as used in this discussion, refers to a structural force response that is essentially trapezoidal in nature, but has a limiting force which is velocity dependent.¹³ Specifically, the structural force is given by

$$F = \left[\frac{K(\Delta V)^2}{A_0^2 \left(1 - \frac{\Delta X}{L}\right)} \right]$$

where K = hydraulic system constant
 ΔV = piston velocity
 A_0 = initial orifice area
 ΔX = piston displacement
 L = total stroke

Data obtained using the matched acceleration response structures are presented in Figures 31 and 32. In figure 31, the crush depths and the peak accelerations in a rigid barrier crash for both the 4,000 lb. and the 2,000 lb. vehicle with fixed force and velocity sensitive structures are shown. The fixed force structures crush a little less, and generate slightly higher accelerations than the velocity sensitive structures at lower impact speeds.

The response of these structures in car-to-car crashes between the 4,000 lb. and the 2,000 lb. vehicles are shown in Figure 32. The "Impact Velocity" is the speed of each vehicle; the closure speed is twice the "Impact Speed." Once again the

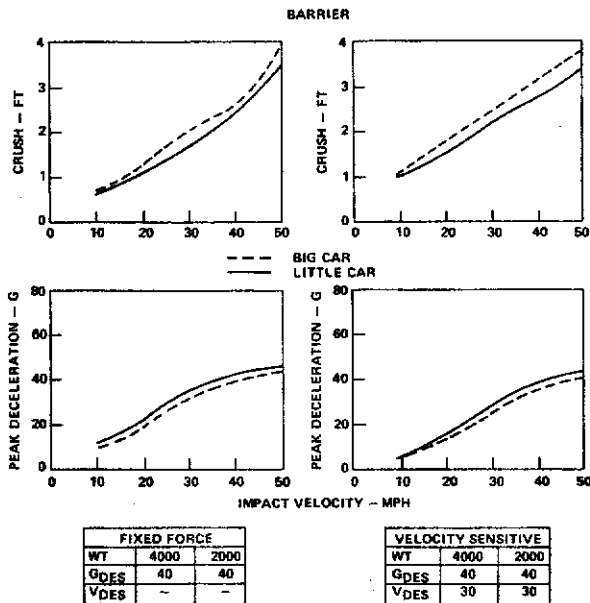


FIGURE 31 - Matched Acceleration Structures Impacting Rigid Barrier

fixed force structures are seen to crush a little less, and generate slightly higher accelerations than the velocity sensitive structures in lower speed impacts. The significant point, however, is that the crush of the 2,000 lb. vehicle with either structure is over 4½ feet in 50 mph barrier crashes.

Figure 33 shows the relationship between vehicle weight and distance between the front bumper and the firewall for a collection of 1970 automobiles. For 2,000 lb. vehicles, this distance is approximately 3½ feet. Thus, it is necessary to modify both the velocity sensitive and the fixed force structures to provide some relief for the 2,000 lb. compact in the 50 mph head-on crash with the 4,000 lb. vehicle.

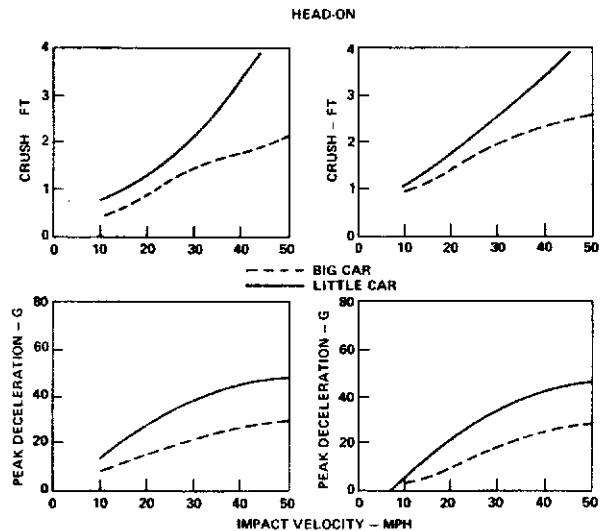


FIGURE 32 - Matched Acceleration Structures, Car-to-Car, Head-On

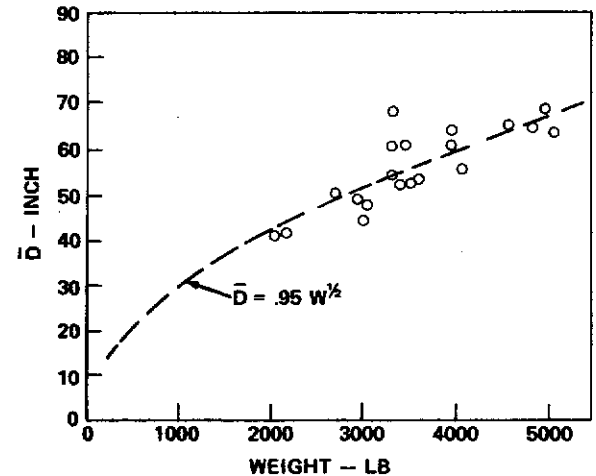
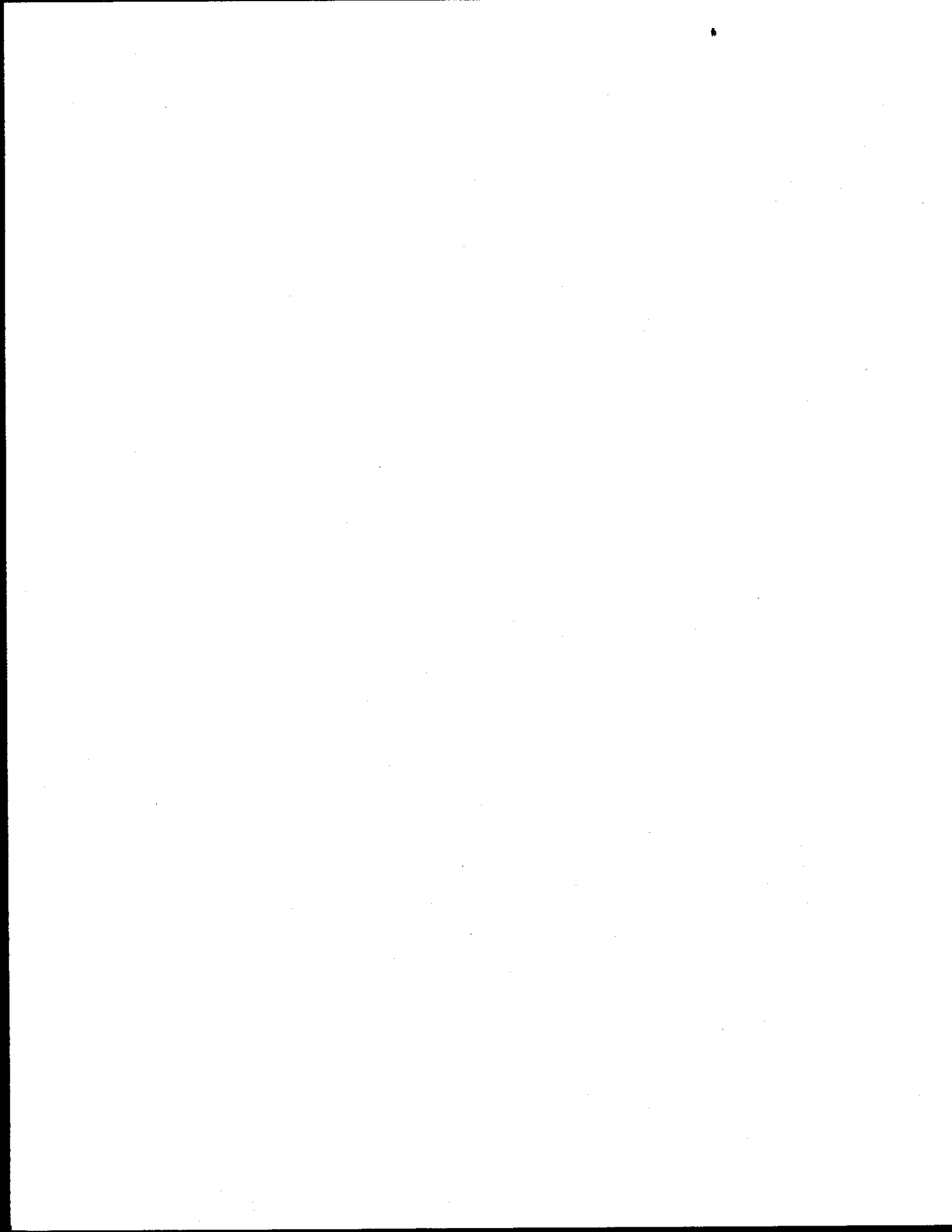


FIGURE 33 - Distance Between Bumper and Firewall as a Function of Weight - 1970 Automobiles



MATCHED CRUSH RESPONSE

The technique used to modify the velocity sensitive structure involves changing V_{des} as a function of vehicle weight to achieve near equal crush in a 50 mph head-on crash for all weight combinations. The required V_{des} as a function of vehicle weight is shown in Figure 34. The G_{des} is held constant at 40 g's. The resulting design maximum accelerations as a function of initial barrier impact speed for the 2,000 lb. and 4,000 lb. vehicles, are shown in Figure 35.

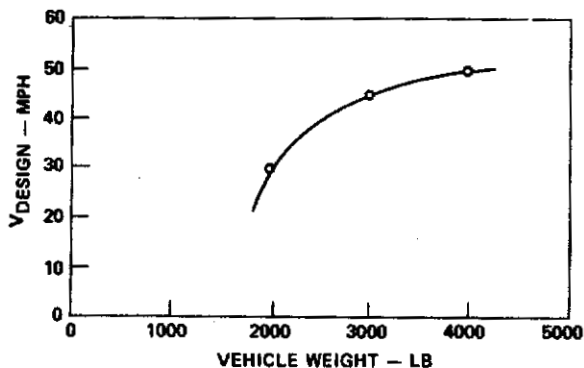


FIGURE 34 - Required V_{DESIGN} For Velocity Sensitive Energy Absorbers As a Function of Vehicle Weight For Crush Compatibility

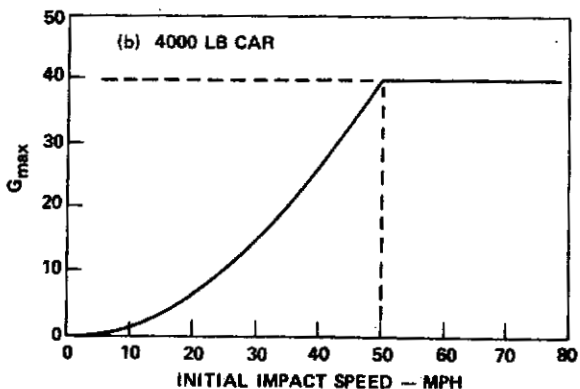
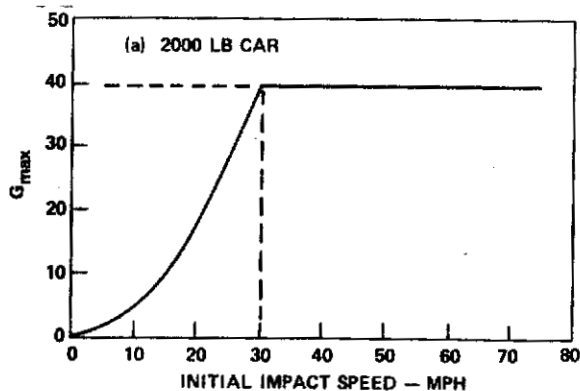


FIGURE 35 - Design Maximum Accelerations for Velocity Sensitive Systems

The fixed force structure is modified by scaling structural accelerations response to achieve nearly equal crush force on vehicles of all sizes. The design acceleration response of the 2,000 lb. and 4,000 lb. vehicles are shown in Figure 36.

The response of the modified velocity sensitive and fixed force structures in rigid barrier crashes are shown in Figure 37. The modified fixed force structures exhibit less crush depth, and slightly higher accelerations, than the modified velocity sensitive structures. The crush of the 2,000 lb. vehicle is less than 3½ feet in both cases.

Car-to-car crash response between 2,000 lb. and 4,000 lb. vehicles with the two modified structural configurations are shown in Figure 38. Once again, the modified fixed force structure crushes somewhat less at higher peak acceleration than the modified velocity sensitive structures. The 2,000 lb. and 4,000 lb. velocity sensitive vehicle structures are seen to have equal crush in the 50 mph impact. This is consistent with the design condition of equal crush in a 50 mph impact for all vehicle weight combinations.

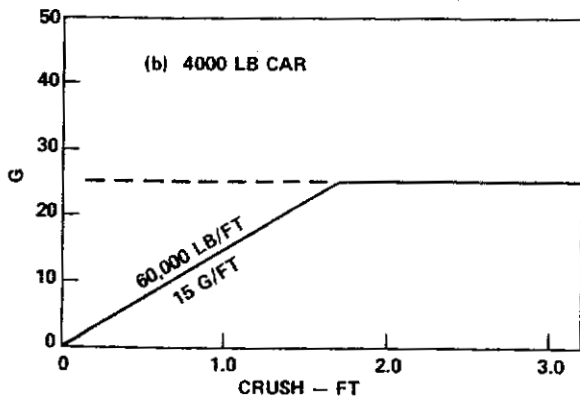
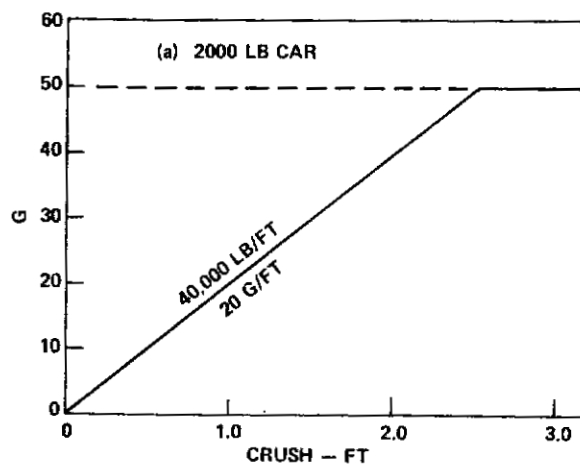
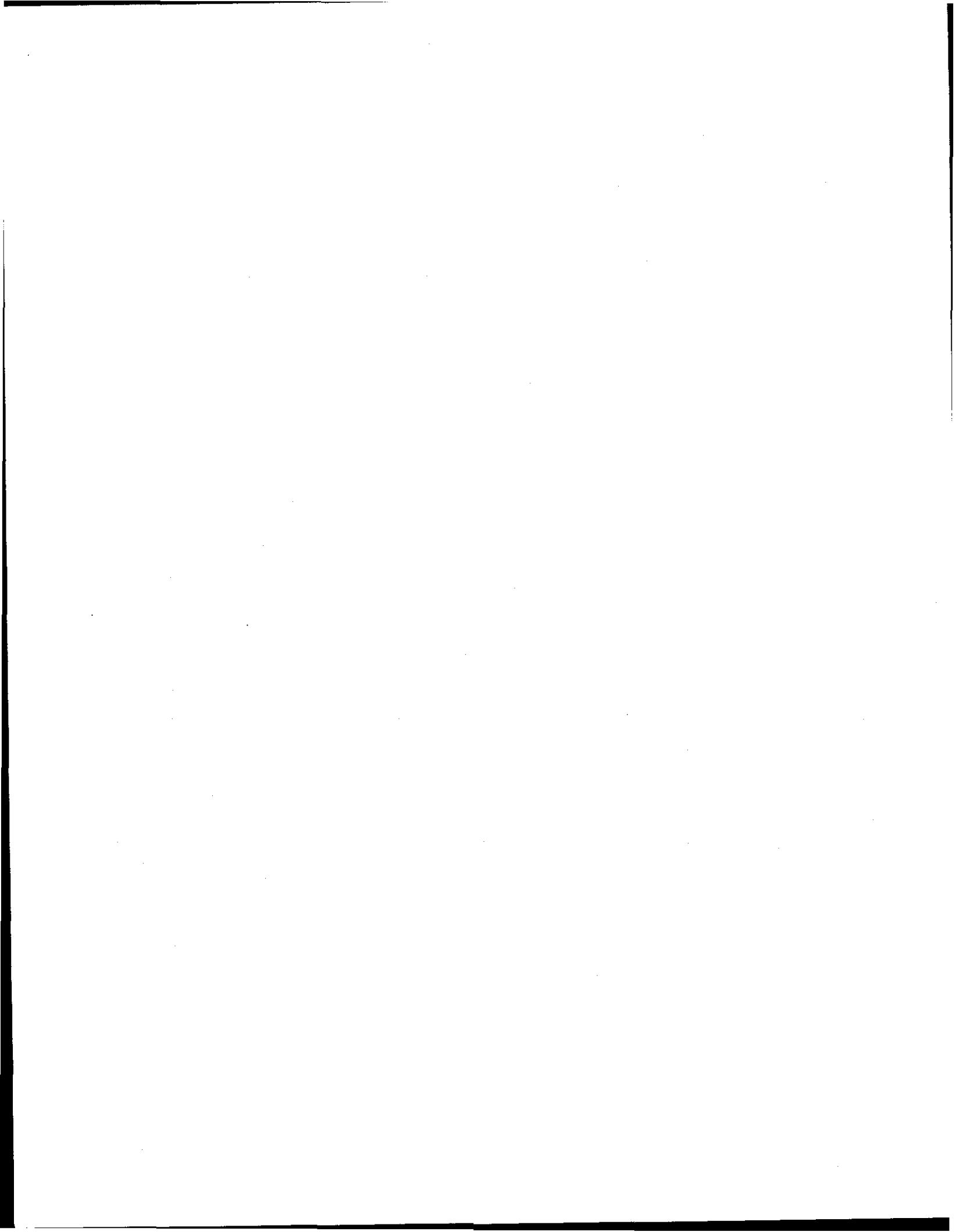


FIGURE 36 - Design Acceleration Response for Fixed Force Systems



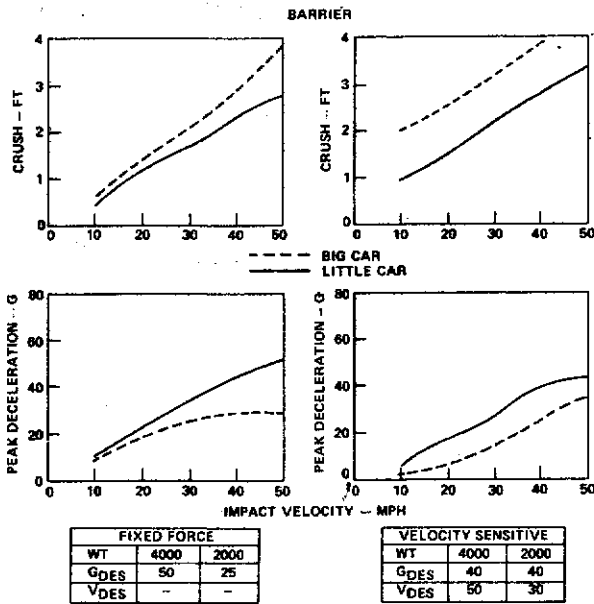


FIGURE 37 — Modified Velocity Sensitive and Fixed Force Structures in Rigid Barrier Crashes

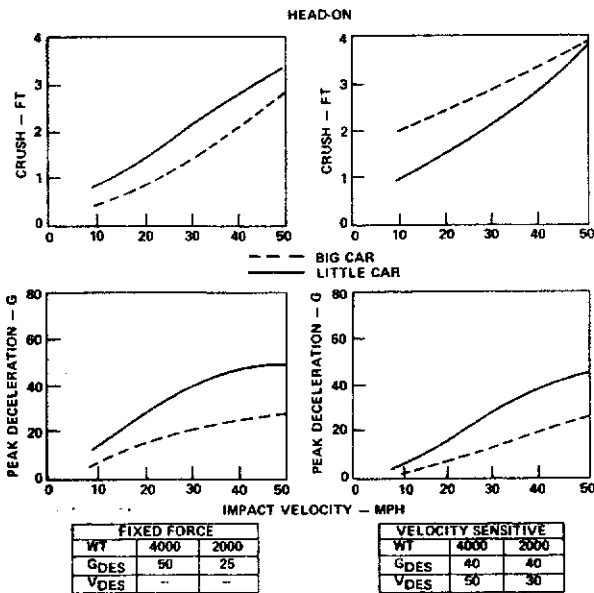


FIGURE 38 — Modified Velocity Sensitive and Fixed Force Structures in Head-On Car-to-Car Crashes

Although the 3.9 feet of crush for the 2,000 lb. velocity sensitive vehicle is still above the 3.5 foot design goal, there is little question that additional modifications of either V_{des} or G_{des} would correct the situation. The fixed force 2,000 lb. vehicle structure crushes 3.4 feet, within the design goal.

It is seen that by careful design, structural response can be adjusted to achieve improved crush compatibility for various size vehicles in head-on crashes using either velocity sensitive or fixed force

structures. The velocity sensitive structures tend to allow somewhat more crush and generate lower peak accelerations than the fixed force structures. This is an inherent characteristic of the velocity sensitive system at low speeds. At higher speeds, near 50 mph, this results primarily from the design parameters selected for this study, and does not represent a significant difference between the systems. The situation could easily be reversed by selecting slightly different parameters.

SIDE IMPACT RESPONSE

The characteristics assumed for the side structure of the struck vehicles are shown in Figure 39. The 160,000 pounds per foot rate of onset of side crush force was selected to reduce penetration by forcing the striking vehicle to absorb most of the crash energy. This onset rate is high relative to conventional automobiles, but it appears to be reasonable for side structures modified for improved crashworthiness.¹⁴

The crush and peak acceleration responses in front to side crashes of both fixed force and velocity sensitive front structures are shown in Figure 40 for various combination of 2,000 lb. and 4,000 lb. vehicles. In all cases, the velocity sensitive structures produced somewhat less penetration of the struck vehicle, and considerable more crush of the striking vehicle. Peak accelerations also tend to be somewhat lower with the velocity sensitive front structure.

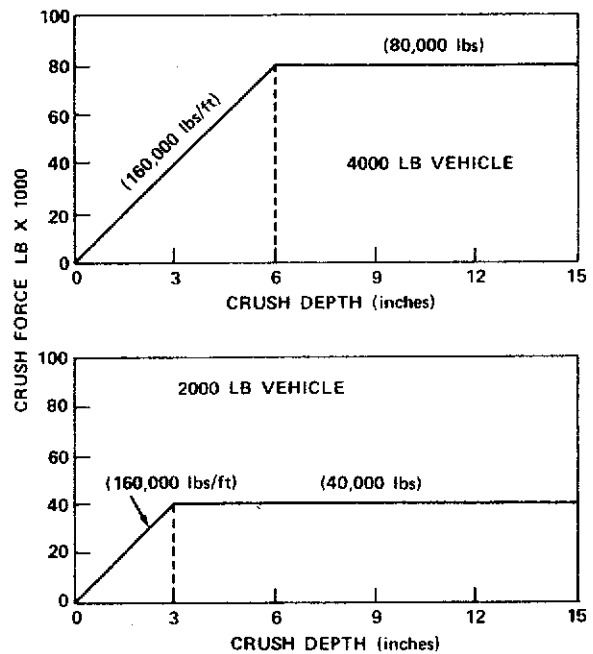


FIGURE 39 — Side Structure Response Characteristics



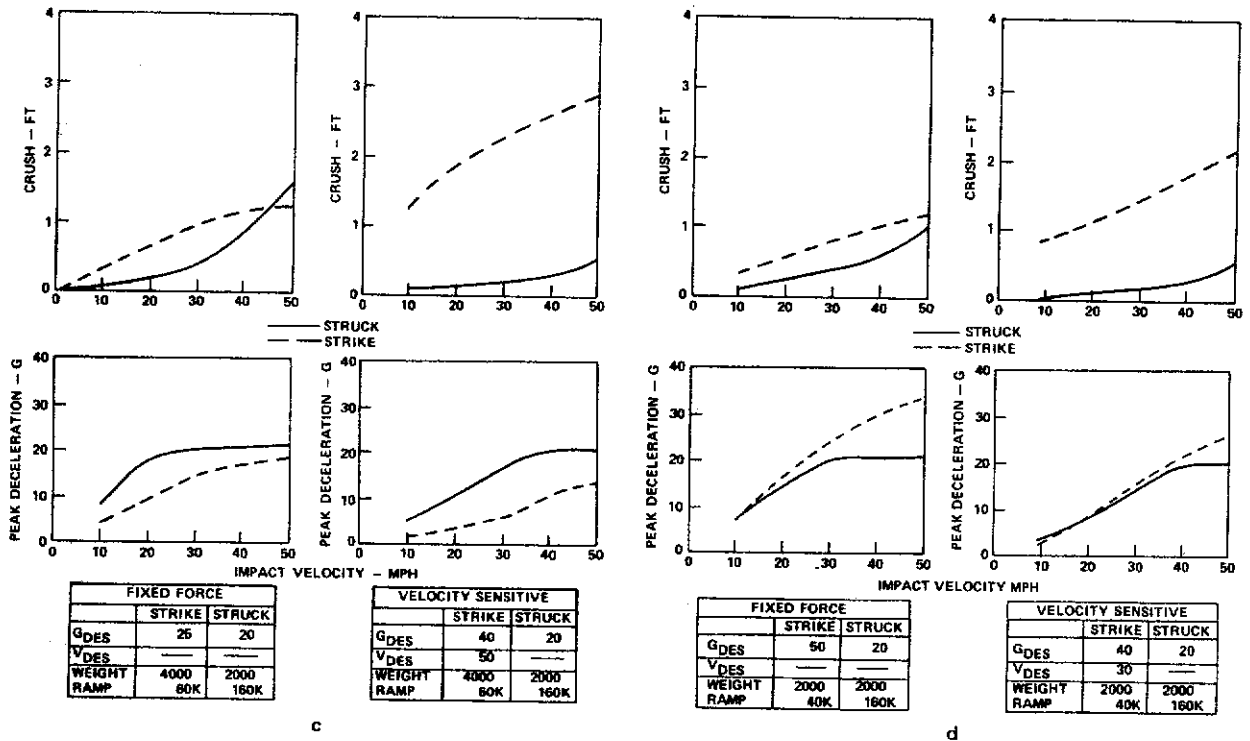
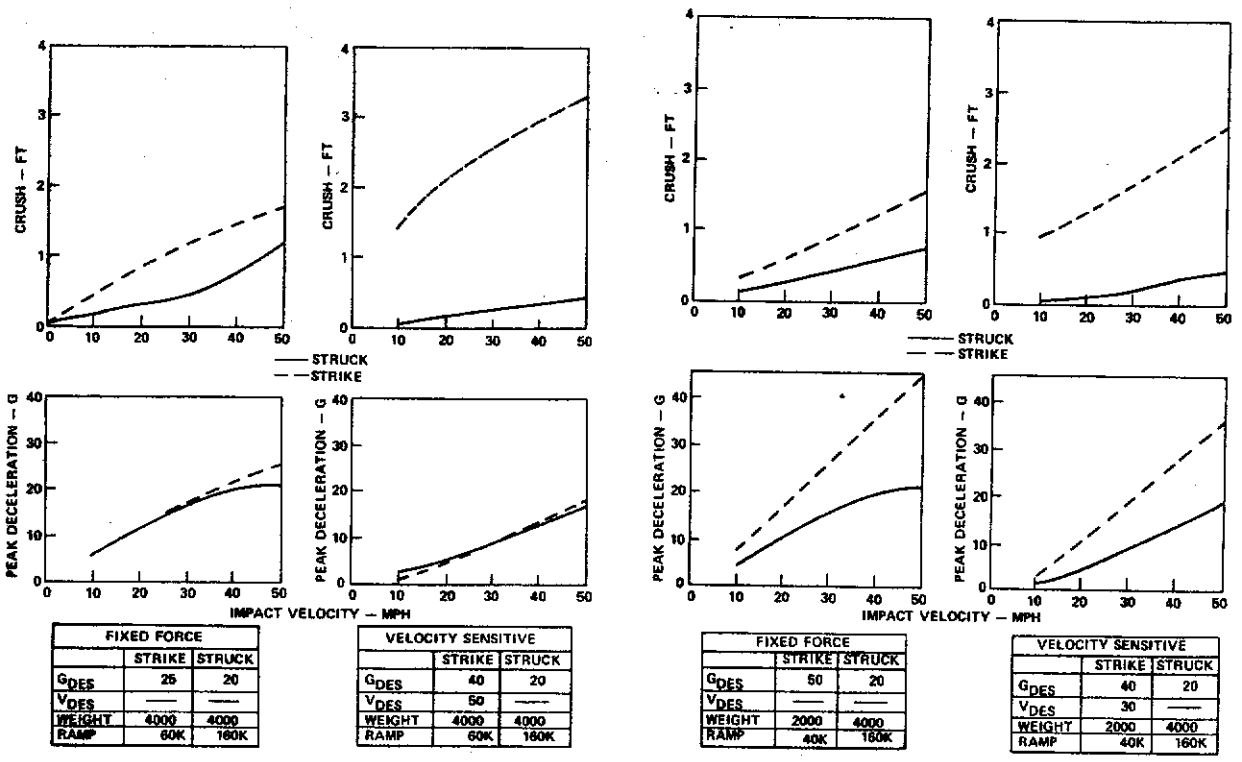
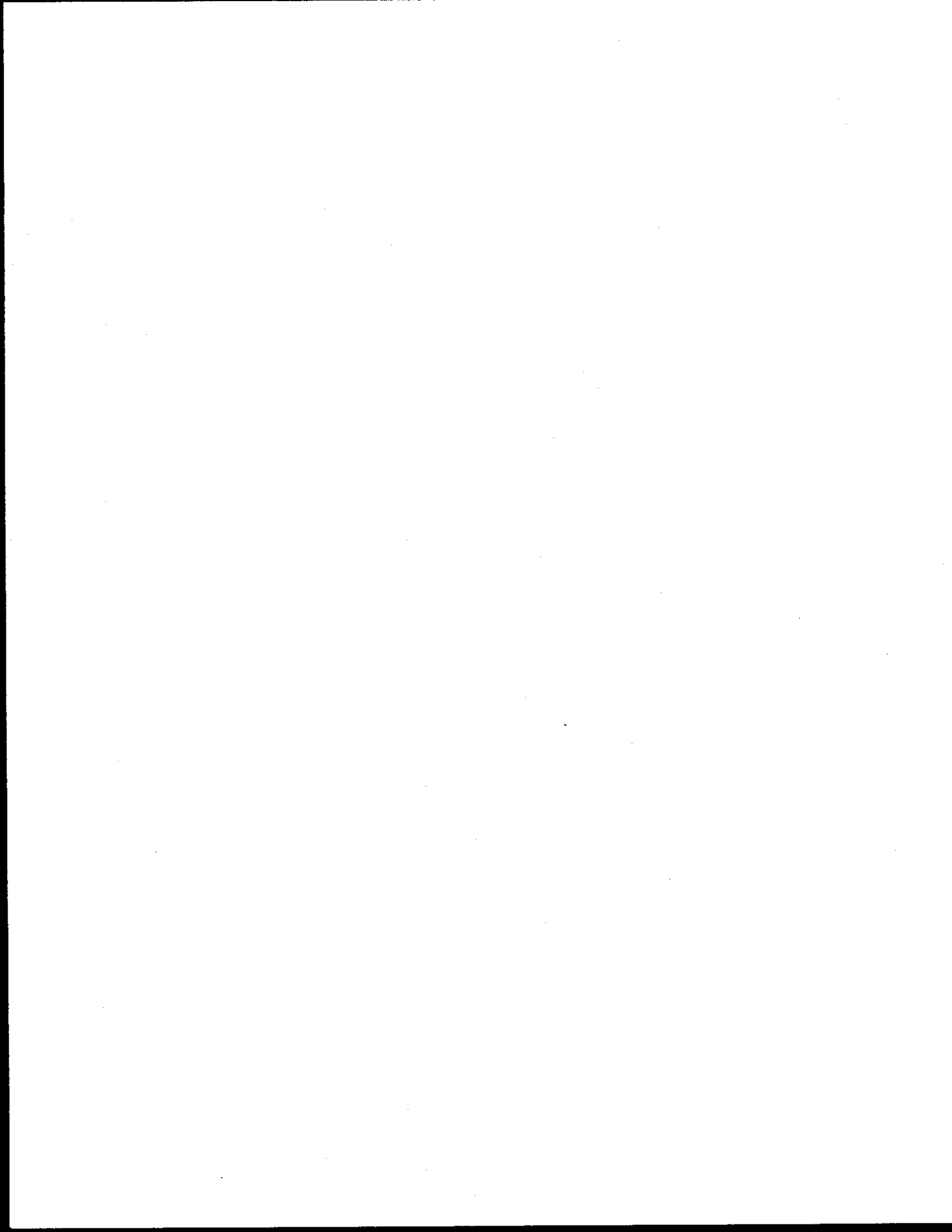


FIGURE 40 - Side Impact Responses with Velocity Sensitive and Fixed Force Impacting Frontal Structures

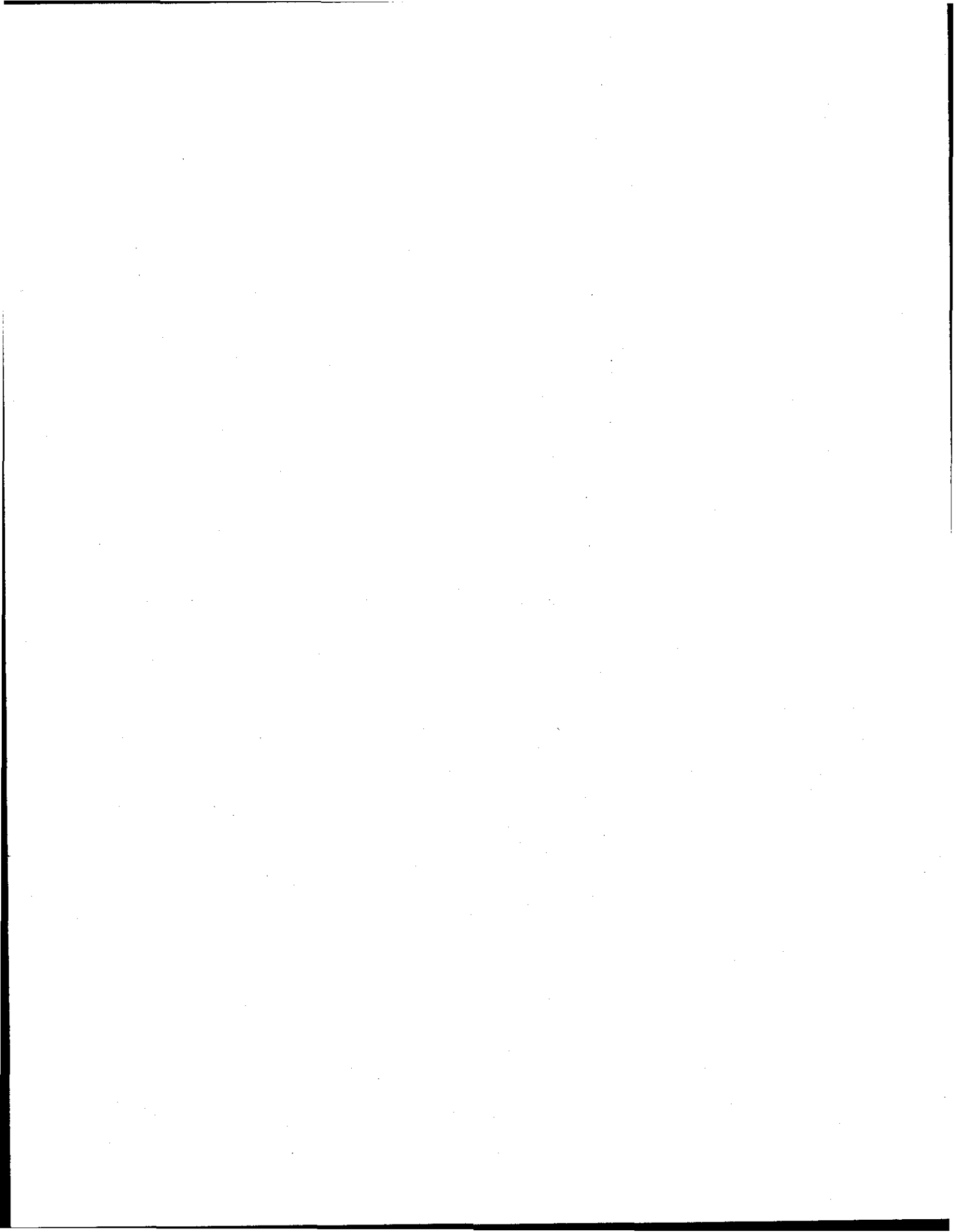


MIXED VEHICLE CRASH COMPATIBILITY

The analyses of mixed vehicle crash compatibility requirements indicates that either velocity sensitive or fixed force structures can be designed to provide reasonable car-to-car crash compatibility for both head-on and side crashes between vehicles of various size. The velocity sensitive structures studied show some advantages in reduced penetration of the struck vehicle in side impacts, and the fixed force structures studied tend to require less frontal crush distance in most crash conditions. In either case, reasonable design compromises that provide adequate protection for the occupant compartment within acceptable crash acceleration limits appear to be feasible.

In summary, automobile structures must generally be strengthened within acceptable crash acceleration

limits to prevent collapse of the occupant compartment in a 50 mph barrier crash. Further, an adequate structural interface between the vehicle and the colliding object must be provided to assure proper structural response during the crash, and the crash energy management characteristic of automobiles of different sizes and weights must be designed to assure intervehicular crash compatibility. Design solutions for full-size automobiles have been developed and tested to establish feasibility. Theoretical analyses of smaller automobiles indicate that solutions exist, and experimental work is underway. Although optimal solutions are not yet at hand, the feasibility of acceptable structural response in 50 mph barrier equivalent crashes is clear. Specific design solutions will be decided primarily on the basis of economic considerations.



Restraint System

Restraint system designs must consider three major areas; (1) human survival limits of force, acceleration, pressures, etc. for the loading characteristics of the chosen restraint system; (2) compartment response or motion characteristics, and (3) the available distance in the compartment. Since the compartment response and distance characteristics vary according to vehicle class, this section has been subdivided into two sections, dealing with requirements for the full size vehicle and the subcompact vehicle.

RESTRAINT SYSTEM REQUIREMENTS FOR THE STANDARD-SIZE VEHICLE

The deceleration vs displacement characteristic of the vehicle forestructure, assumed for the purposes of this investigation, is shown in Figure 41. Figure 42 presents a family of curves showing how a vehicle with such a structural response will decelerate from various speeds in frontal barrier impacts. In Figure

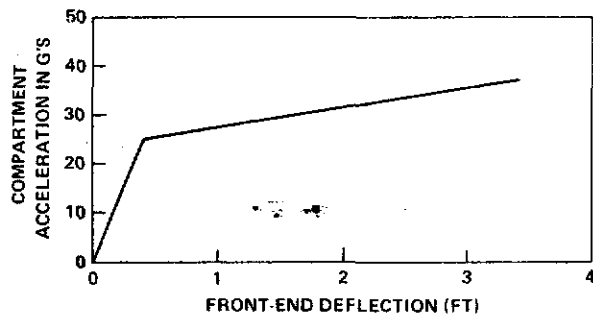


FIGURE 41 — Compartment Deceleration as a Function of Front-End Deflection for the Modified Standard-Size Vehicle

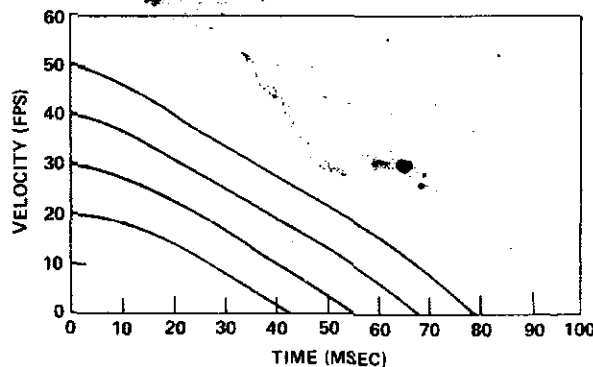


FIGURE 42 — Velocity Histories for the Modified Standard-Size Vehicle at 20, 30, 40, and 50 MPH Barrier Impacts

43, the velocity-time history representing a 30 mile-per-hour barrier impact with this structure is shown together with the velocity-time history of a conventional vehicle in the same severity crash. Also shown on this Figure is the velocity-time history of a point on an occupant restrained by a hypothetical, deploying restraint system. The area between the occupant velocity curve and the vehicle velocity curve is, of course, the interior distance traversed by the occupant. In considering only one occupant curve, it is assumed that the restraint system activates in the same time for both vehicles and that the deceleration pulse applied to the occupant by the restraint system is the same in both cases. In practice this will not be the case. These assumptions, however, were made solely for the purpose of establishing two points. First, if the two restraint systems activate in the same time, the occupant of the modified vehicle will move unrestrained through a greater distance inside the compartment than the occupant of the conventional vehicle by an amount equal to the crosshatched area of Figure 43. Secondly, if the two restraint systems apply the same decelerations to the occupant, the stiffer structure will require additional internal distance relative to the conventional vehicle by an amount equal to the shaded area of Figure 43. Thus a restraint system for the modified vehicle will have to impart higher average accelerations to the occupants to safely bring them to rest within the interior space available (without exceeding injury limits) in the same severity crash.

The geometry of the standard-size vehicle compartment assumed for the purposes of this study is

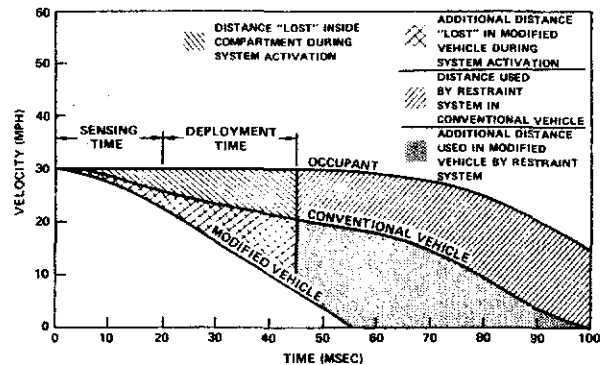
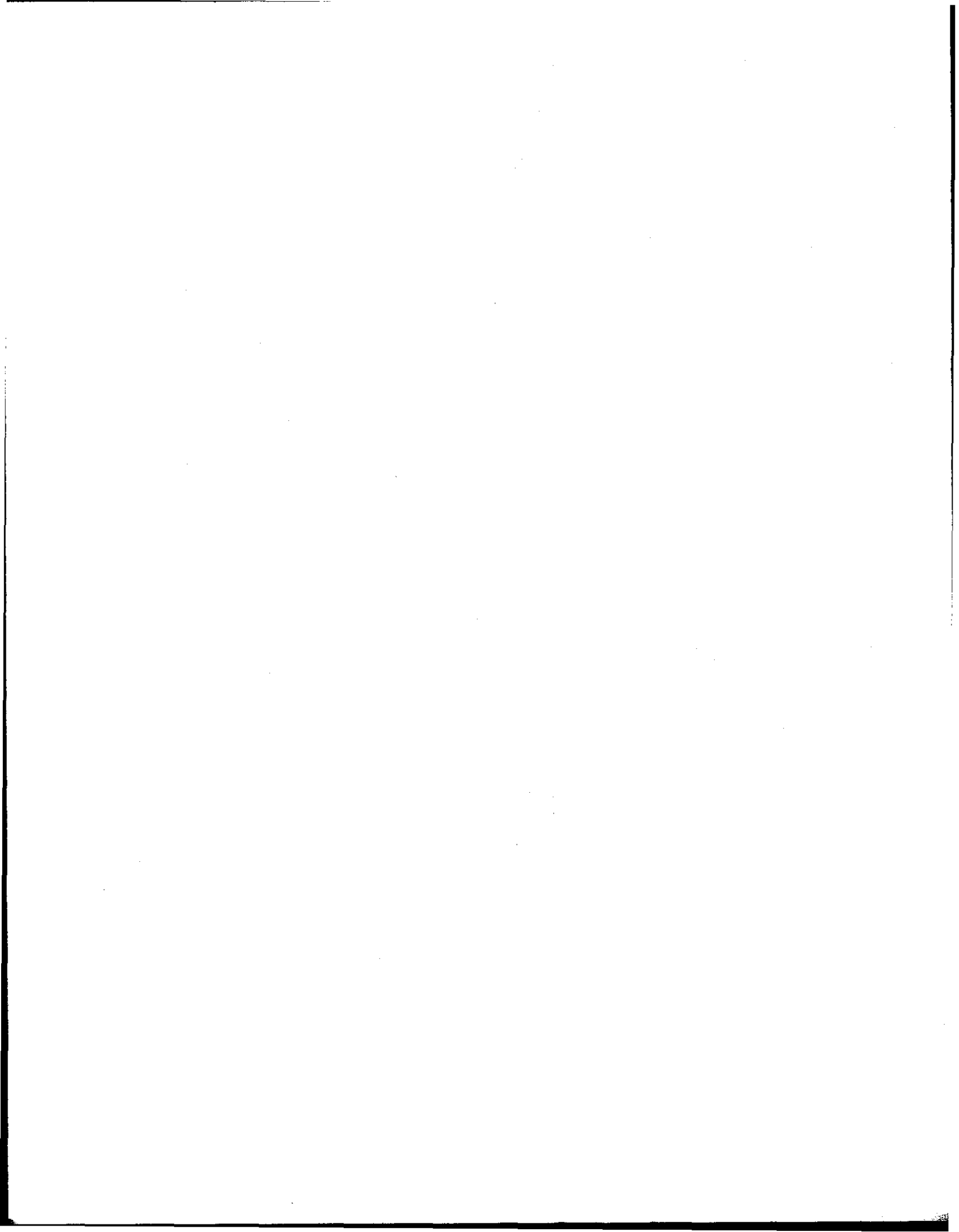


FIGURE 43 — A Comparison of the Velocity Histories of a Conventional Standard-Size Vehicle with the Modified Standard-Size Vehicle in a 30 MPH Barrier Impact



shown in Figure 44. These dimensions are considered to be representative of a late-model full-size vehicle. Figure 44a shows a 95th-percentile man seated in the front seat with the seat in its rearmost position. Figure 44b is the corresponding geometry with a 50th-percentile man with the seat in its midposition, and Figure 44c shows a 5th-percentile female with the seat in the forwardmost position. It is noted that 34 to 37 inches of interior space is available from the chest of the occupants to the vehicle firewall.

The description of the vehicle environment embodied in Figures 41 and 43 will be used to predict

restraint performances in the following portions of this section of the paper.

An important part of the restraint system is the knee restraint. Shown in Figure 44 is the position of a knee restraining lower dash panel. This panel has been positioned to be two inches from the knee of the 50th-percentile male occupant when the seat is in the midposition. The assumed force-deflection properties of this knee restraint are given in Figure 45. They have been selected to limit femur loads to around 1,000 pounds per knee and to efficiently absorb energy. In practice, this can be accomplished in a

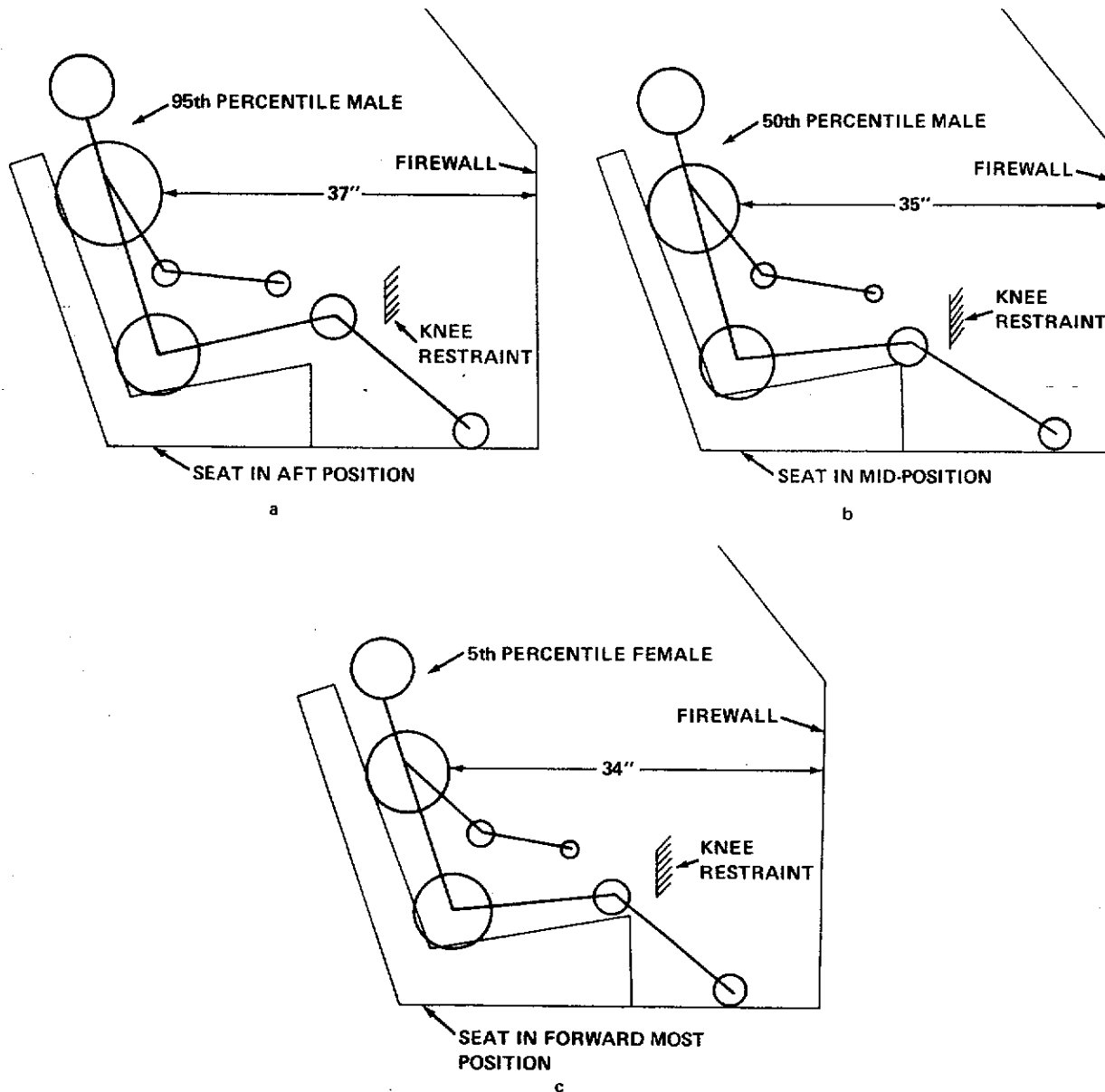
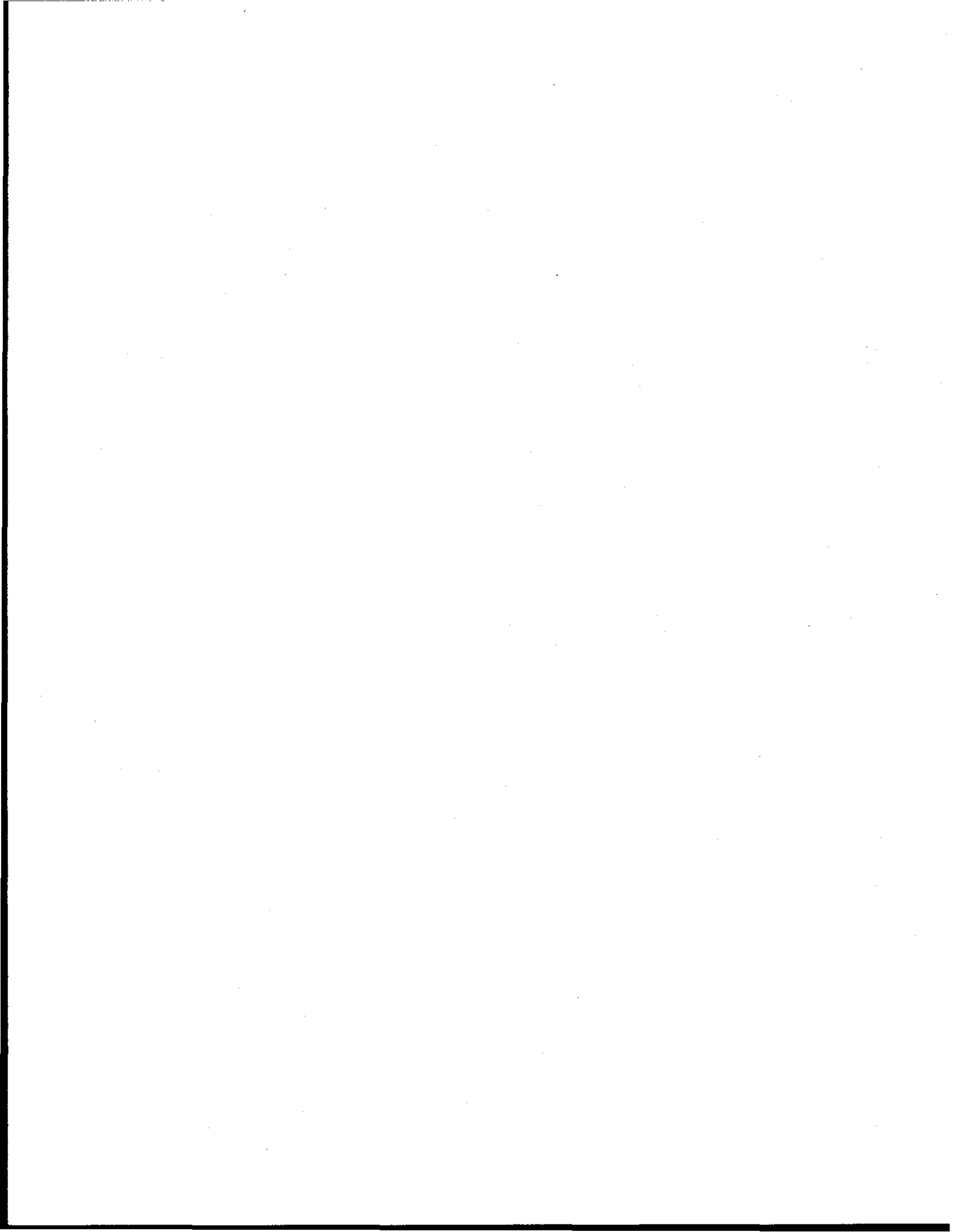


FIGURE 44 - The Assumed Interior Geometry of the Modified Standard-Size Vehicle



number of ways. Aluminum honeycomb has been employed in a number of instances and performs quite well, even in oblique impacts.

The upper torso restraint is assumed to be an inflatable system. Two interdependent factors exist which together determine the adequacy of a deploying restraint system. The first of these factors is the total time from the initiation of the impact (bumper contact) until significant restraining forces are applied to the occupants. For the purposes of this report, this

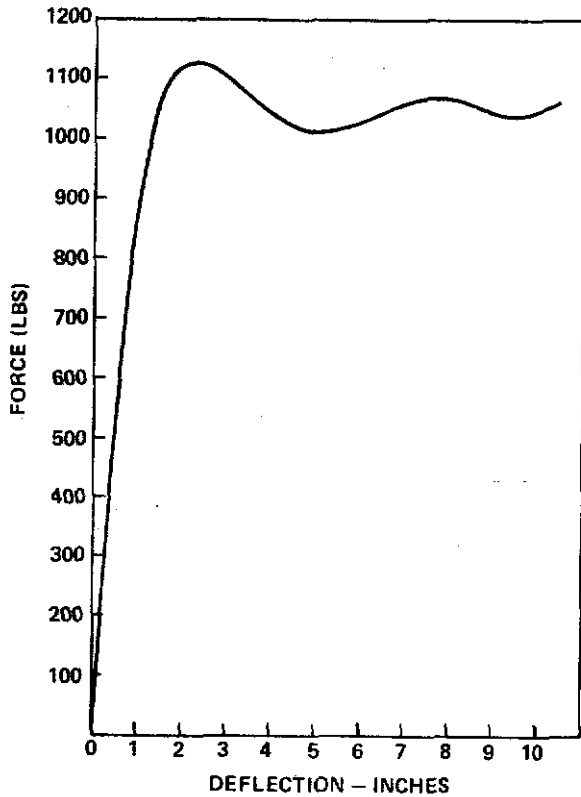


FIGURE 45 - The Assumed Force-Deflection Characteristics of the Knee Restraint

parameter is termed *system actuation time*. System actuation time is composed of *sensing time* and *system deployment time*.

The second of these factors is the load characteristic of the restraint system from the time restraining forces are applied to the occupants until they are brought to rest. As a description of this load characteristic, the term *load efficiency* will be used. Load efficiency (e) is defined as the ratio of the average deceleration applied to the chest of the occupant during his arrest (\bar{g}) to that value of acceleration which could cause significant injury (g^*). In this study, peak acceleration is limited to 60g.

Figure 46 shows the relationship between the required efficiency of a restraint system and the

system actuation time for the case of a 50 mile-per-hour barrier impact with the modified structural response. Plotted on this same Figure is the corresponding relationship for a 30 mile-per-hour barrier impact with a conventional standard-size vehicle.

Current sensors designed for a 30 mile-per-hour barrier impact typically activate in about 20 to 25 milliseconds. Current air bags typically deploy in about 35 to 40 milliseconds in the case of a passenger system and in about 20 to 25 milliseconds for the smaller driver systems. Thus, in a 30 mile-per-hour barrier impact, typical system activation times for the driver and passenger restraint systems are about 45 milliseconds and 60 milliseconds, respectively.

It can be seen from Figure 46 that the driver and passenger systems need only apply average decelerations in the order of 20 to 30 percent of the injury level or 12 to 20g's in order to function satisfactorily for 30 mph unmodified vehicle impacts.

System activation time for the modified standard-size vehicle impacting the barrier at 50 miles per hour will be less than that for the conventional vehicle impacting at 30 miles per hour due to a reduction in sensing time. With a stiff and dependable structure, front-end deflection becomes a reliable indicator of a

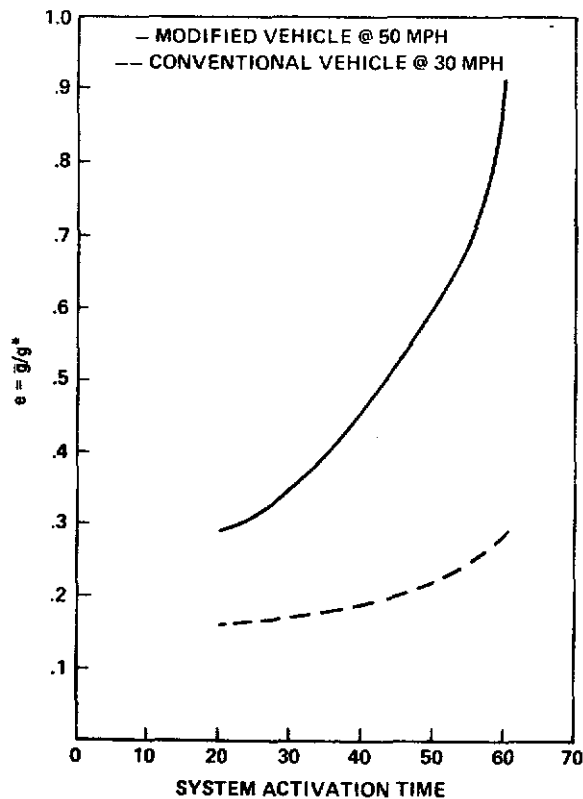
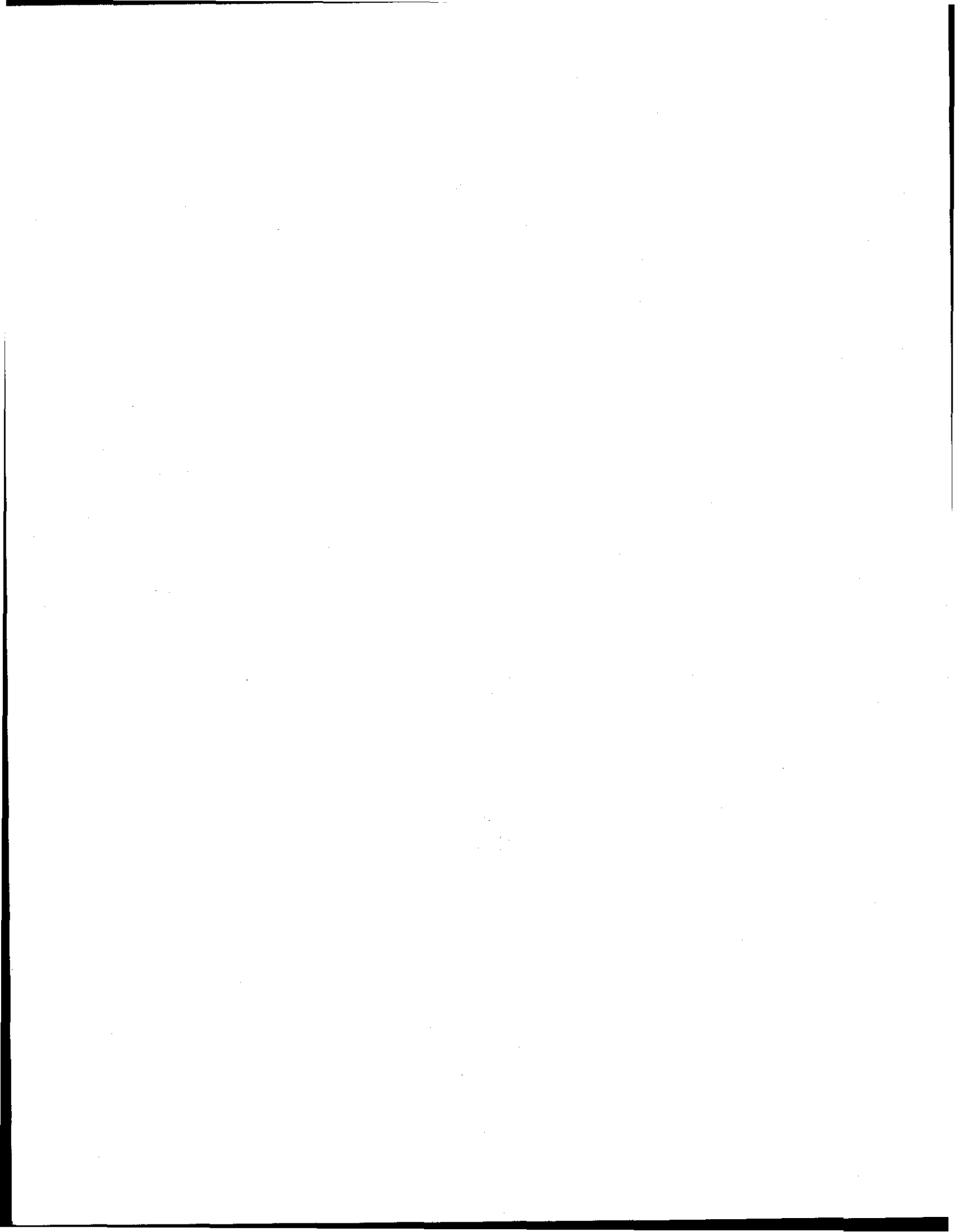


FIGURE 46 - Load Efficiency Versus System Activation Time for the Standard-Size Vehicle



potentially injurious crash. If it is assumed that permanent energy absorbing padding of interior surfaces is capable of providing protection at barrier impact speeds of up to 10 miles per hour, then a deflection sensor can be designed to actuate at front-end deflections greater than that realized in the 10 mile-per-hour impact. For modified vehicle response assumed, a front-end deflection greater than 4 inches indicates a barrier impact velocity greater than 10 miles per hour. Figure 47 is a plot of the sensing time for the deflection sensor as a function of barrier impact velocity. At 50 miles per hour, sensing time is about 4.5 milliseconds.

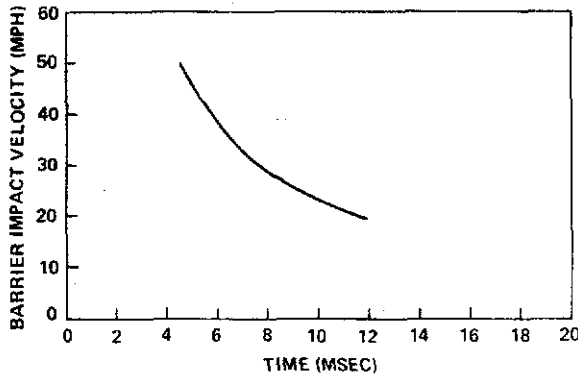


FIGURE 47 - Sensing Time as a Function of Barrier Impact Speed for the Modified Standard-Size Vehicle

Assuming no reduction in system deployment time, the system activation times for the driver and passenger systems would then be on the order of 25 to 30 milliseconds and 40 to 45 milliseconds, respectively, for the 50 mile-per-hour case. Referring again to Figure 46 it is seen that the driver system would require a load efficiency of about 35 percent and a passenger system about 50 percent. The passenger and driver restraint systems will be discussed separately in the following sub-sections.

PASSENGER RESTRAINT SYSTEM

A comparison between an inflatable restraint system capable of providing standard-size vehicle front seat passengers with protection in a 50 mph barrier impact and a system capable of 30 mph protection, was constructed by use of a modification of a computerized simulation model.¹⁵

Briefly, the model assumes the air bag to be inflated to a prescribed pressure and shape (Figure 48). Impact of the flat-faced torso mass is produced in the modified version of the simulation by accelerating the bag and reaction plate toward the torso in the same manner as an acceleration sled would impact

a sled occupant. Vents are specified to open at a predetermined bag internal pressure. Fabric stress reacts the internal pressure in the inflated state. As the torso penetrates the bag, pressure is transferred from the fabric to the contact area of the torso. In addition, fabric tension produces an additional force on the torso.

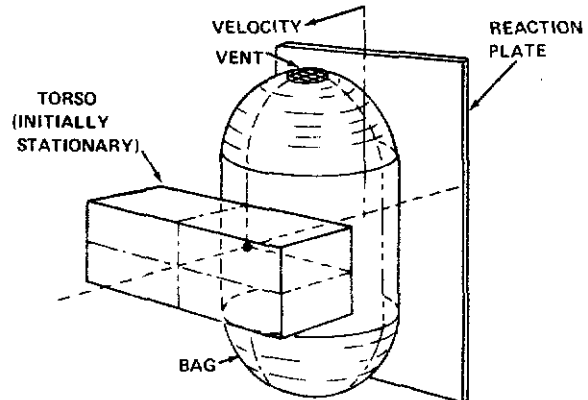


FIGURE 48 - Air Bag Model Configuration

The model was exercised, using torso masses and widths representing a 95th percentile and a 50th percentile male and a 5th percentile female. The total weight of these three occupant sizes was assumed to be 215 lbs., 164 lbs., and 105 lbs., respectively. Torso masses were taken as 70 percent of these values. This percentage was based on data showing pelvic acceleration versus femur force for a series of air bag tests with anthropometric devices¹⁶ as shown in Figure 49. From this Figure, it has been estimated that about 30 percent of an occupant's weight will effectively be restrained through the knees.

The model was first exercised for a conventional, standard-size vehicle, acceleration-time history in a 30 mph (nominal) barrier impact. The vehicle response was taken from test 7B¹⁶. The bag, about 10 cubic feet in volume (17760 in³), was allowed to contact the torso mass 60 milliseconds into the event. The

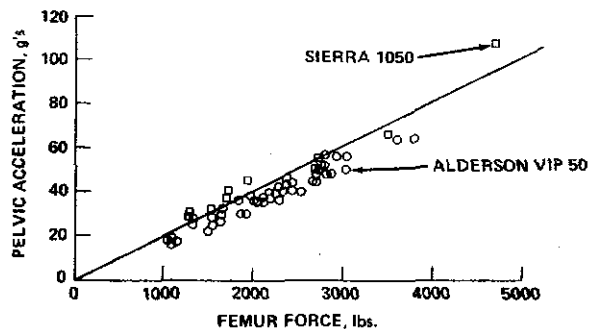


FIGURE 49 - Femur Force Versus Pelvis X-Component Acceleration for Sierra and Alderson Dummies



bag pressure at contact was assumed to be 1 psig. The vents, 50 square inches in area, were opened at 2psig. These bag parameters were chosen to be representative of a current system.

The deceleration history resulting from this simulated 30 mph barrier impact with a 50th percentile male torso is shown in Figure 50. This deceleration pattern is not unlike that obtained in 30 mph barrier impacts with anthropometric devices.

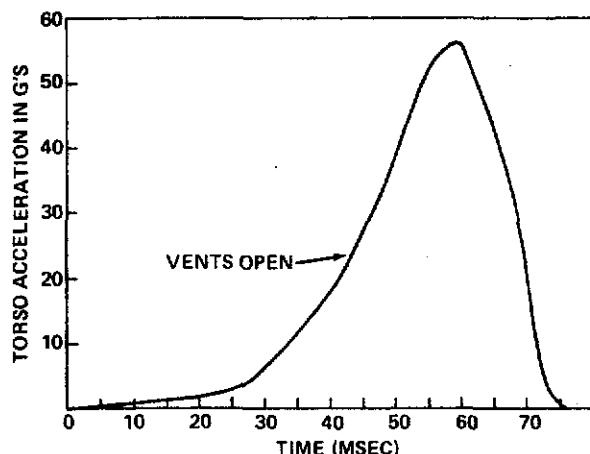


FIGURE 50 - Torso Acceleration History for a Simulated 30 MPH Impact with a Conventional Standard-Size Vehicle

The model was next exercised for a vehicle deceleration history resulting from a 50 mph barrier impact, with the structural response of Figure 41. In these simulations, the bag, still about 10 ft³ in volume, was assumed to contact the torso at 25 milliseconds into the event. Remembering that sensing time is about 4.5 msec with the modified structure at this speed, the deployment time assumed is then slightly over 20 milliseconds. Venting area and initial pressure were varied, keeping the venting pressure 2 psig above the initial pressure, until acceptable "rides" were obtained with all three torso configurations. Figure 51 is the deceleration history resulting from this simulated 50 mph barrier impact with a 50th percentile male torso with the derived bag parameters. With the 5th percentile female, decelerations were higher and bag penetration less, while with the 95th percentile male, the opposite was true. The derived bag parameters were as follows:

Pressure at full inflation	8 psig
Vents open at	10 psig
Weight of gas in the bag	1.1684 lb.

A comparison of the above with the 30 mph case, where weight of gas derived was .8033 lbs., shows that about 50 percent more gas must be supplied to

the bag in about 50 percent of the time (20 msec versus about 40 msec). Thus, the average mass flow rate into the bag during inflation will be about 4 times what is required for a 30 mph system.

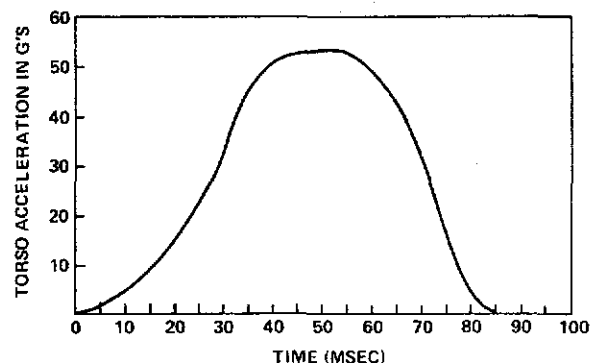


FIGURE 51 - Torso Acceleration as a Function of Torso Penetration for a Simulated 50 MPH Impact with a Modified Standard-Size Vehicle

The above comparative analysis was based on the assumptions that:

- (1) bag configuration would not change, and
- (2) significant reductions in deployment time could be achieved, discussed below.

Bag Configuration - The bag geometry assumed for the 50 mph system was the same as that assumed for current systems; namely, a single compartment significantly wider than the occupant. Figure 52 is a replot of Figure 51, showing torso acceleration as a function of bag penetration. Note how far the block penetrated the bag before restraining forces became significant. During the initial stages of bag-torso interaction neither the bag pressure nor the fabric tension can exert significant forces on the torso because of the assumed initial shape of the bag. The force due to bag pressure building up slowly with torso penetration because of the slow buildup of contact area. The forces due to fabric tension build

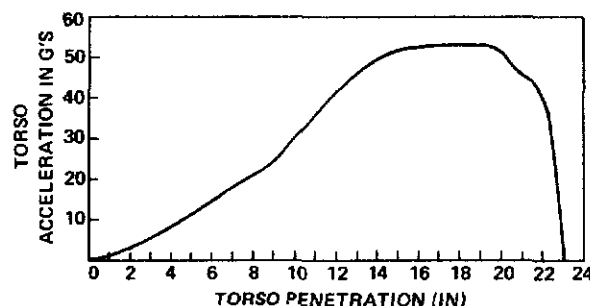
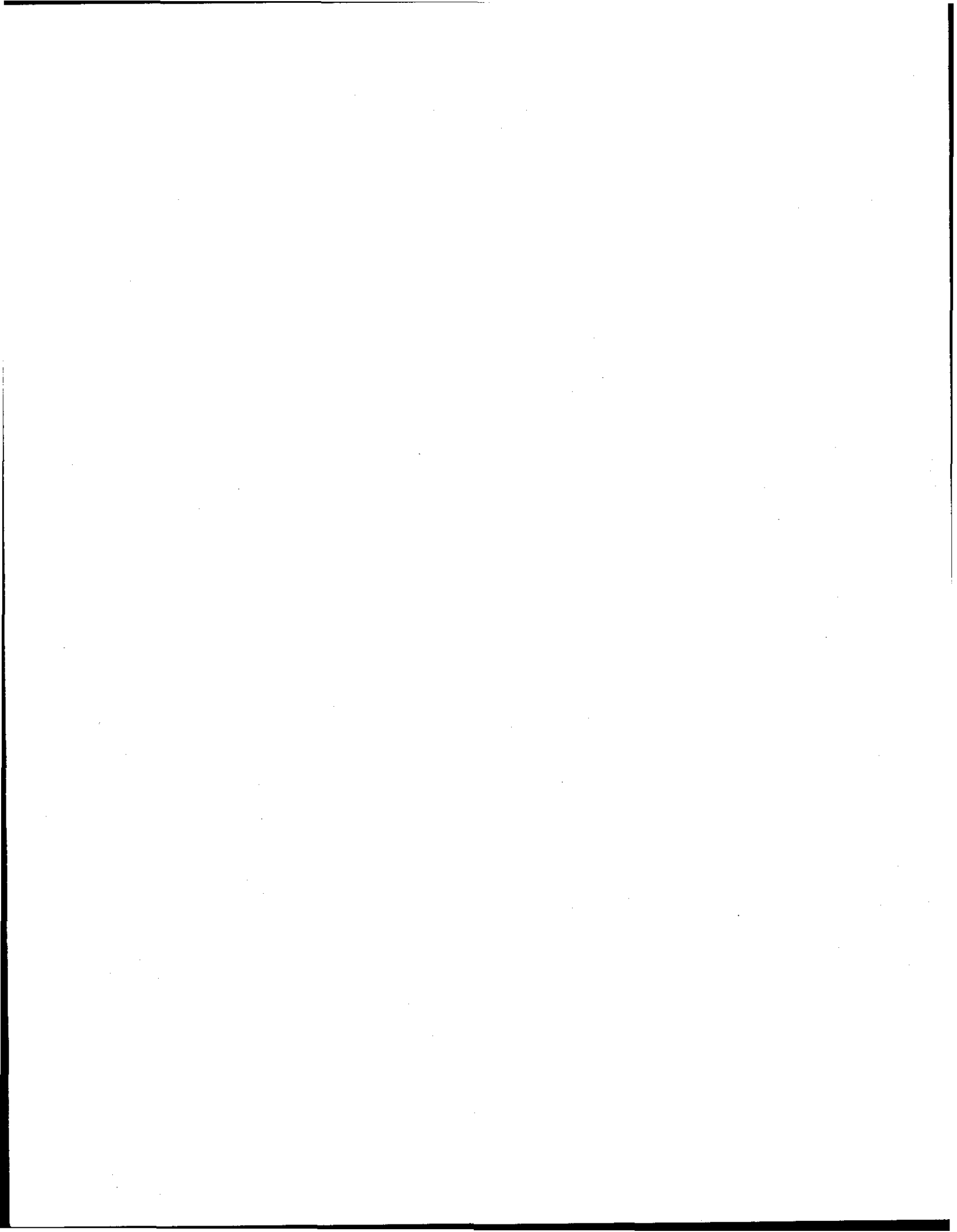


FIGURE 52 - Torso Acceleration as a Function of Torso Penetration for a Simulated 50 MPH Impact with a Modified Standard-Size Vehicle



up slowly because the torso must significantly penetrate the bag to produce sizeable longitudinal components of these vectors (the so-called "wraparound" effect).

The buildup of both the "pressure force" and the fabric tension force with occupant penetration can be increased by shaping the leading surface of the bag (1) to more closely complement the torso geometry and (2) to produce an initial "wraparound". Such a bag shape would, of course, have to be achieved by providing the interior of the bag with shaping struts or partitions.

The major benefit of achieving a faster buildup of restraining forces from the bag would be the reduction in the required initial pressures from the 8 psig range indicated previously for an unshaped bag.

Deployment time — The deployment time assumed for the 50 mph system was half that of current systems. If present methods are employed to deploy and pressurize the restraint system, then it is quite conceivable that in the process of achieving faster inflation times, the deployment noise levels and the severity of motions imparted to out-of-position occupants will reach unacceptable levels. One possible method of achieving deployment time reduction while abating these factors is to use compartment air to augment the air supplied to inflate the bag by means of aspirator inflation systems.

One practical method of using compartment air has been demonstrated by a leading company dealing in propellant-inflated air bag systems. In this system, the primary flow of gases into the bag, supplied by the burning of a matrix of small propellant motors, entrains compartment air entering the inflator through check valves located behind the rocket motors (see Figure 53). Since the amount of gas supplied to the bag from the primary source is less than would be required for a nonaspirated system, lower noise levels would be expected. The noise is further reduced in this system by virtue of the use of a number of small jets in place of fewer but larger motors. Motions imparted to out-of-position occu-

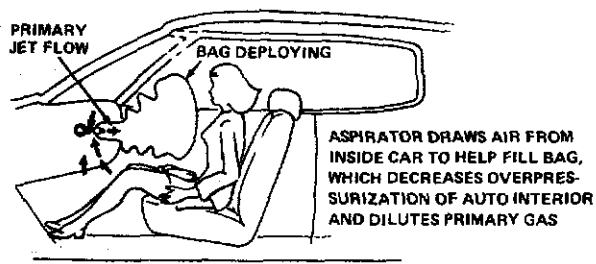


FIGURE 53¹ — Aspirator Deployment During Inflation

pants should also be less with an aspirated system since, in the initial stages of deployment, the buildup of pressure in the bag due to the proximity of the occupant will tend to "stall" the system (i.e., the entrained air flow will be closed off by the reaction of the check valves to back pressure). In such an instance, occupants will tend to "ride down" the vehicle.

Driver Restraint System

The major energy absorber in the driver restraint system is the steering column. Based on the assumed geometry of the full size vehicle, a steering wheel can be placed in a reasonable location in the vehicle compartment (see Figure 54) resulting in its displacement from the firewall being 24½ inches.

With the air bag distributing loads evenly over a large area of the torso, a significant increase in the column collapse loads over those currently realized could be justified with the beneficial result of greater energy absorbing capability. Since the air bag system will not deploy in fixed object frontal collisions at less than 10 miles per hour, however, sufficient column stroke at lower force levels must be retained to avoid producing injuries at low speeds.

A one-dimensional model of steering assembly-chest impact was employed to determine how much collapse of a conventional steering column occurs at barrier equivalent impact speeds of 10 miles per hour. This model is shown schematically in Figure 55.

Estimates were made of the mass, force-deflection, and damping properties of existing steering assemblies, in an effort to generate reasonable values of the model parameters that would describe them. The model was then verified by matching experimentally-derived force-time histories obtained in "blak-tuffy" tests.*

Figure 56 shows a comparison between a 15 mph blak-tuffy impact test¹⁷ and a simulation using the following parameter values:

Column/Wheel Weight	20 lbs.
Column/Wheel Damping	35 lb. - sec/ft.
Column Force-Deflection Characteristic	
	$F = 2400 X (0 < X \leq 1/2 \text{ inch})$ lbs.
	$F = 1200 (X > 1/2 \text{ inch})$ lbs.
Blak-Tuffy Weight	75 lbs.

*In these tests, a blak tuffy (a torso block constructed of wood and rubber) is swung into the steering wheel assembly following SAE recommended practice.



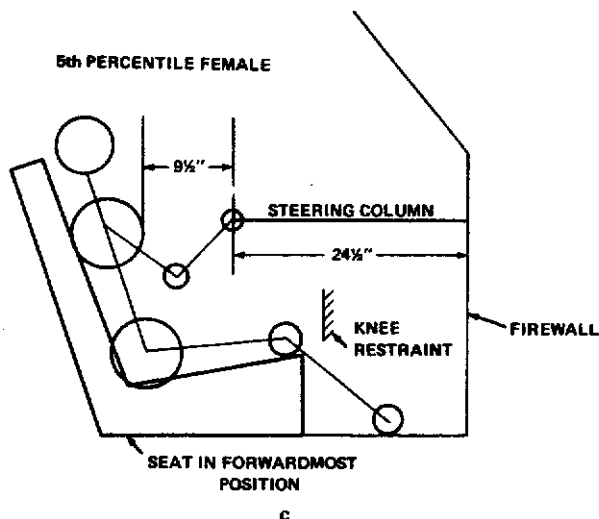
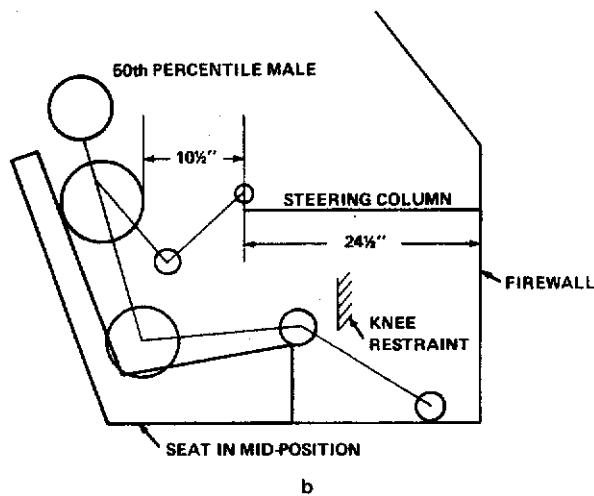
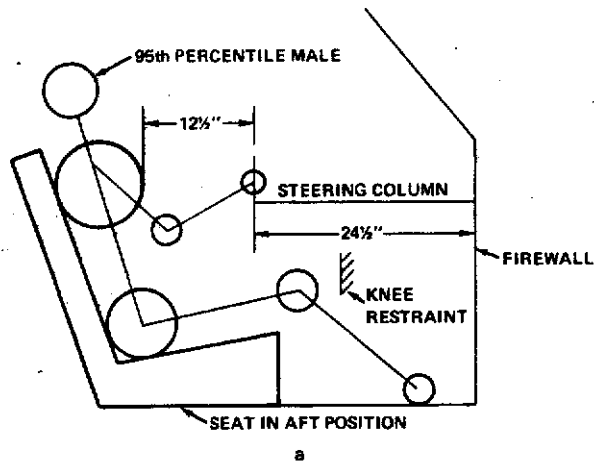


FIGURE 54 - The Assumed Interior Geometry of the Driver Position of the Modified Standard-Size Vehicle

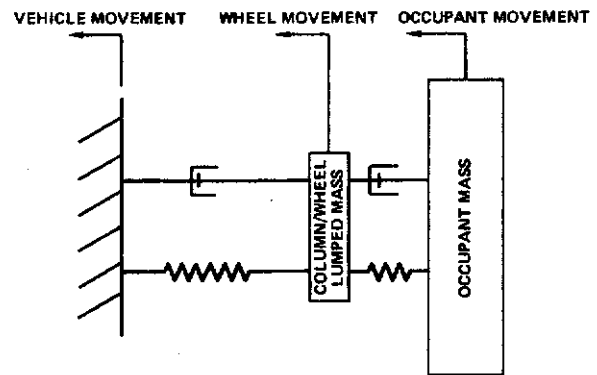


FIGURE 55 - Steering Column Model

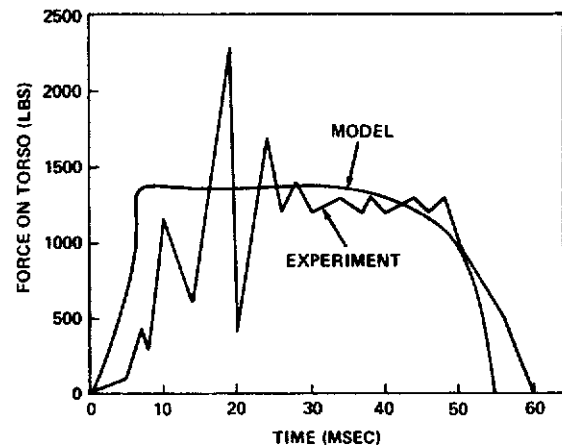


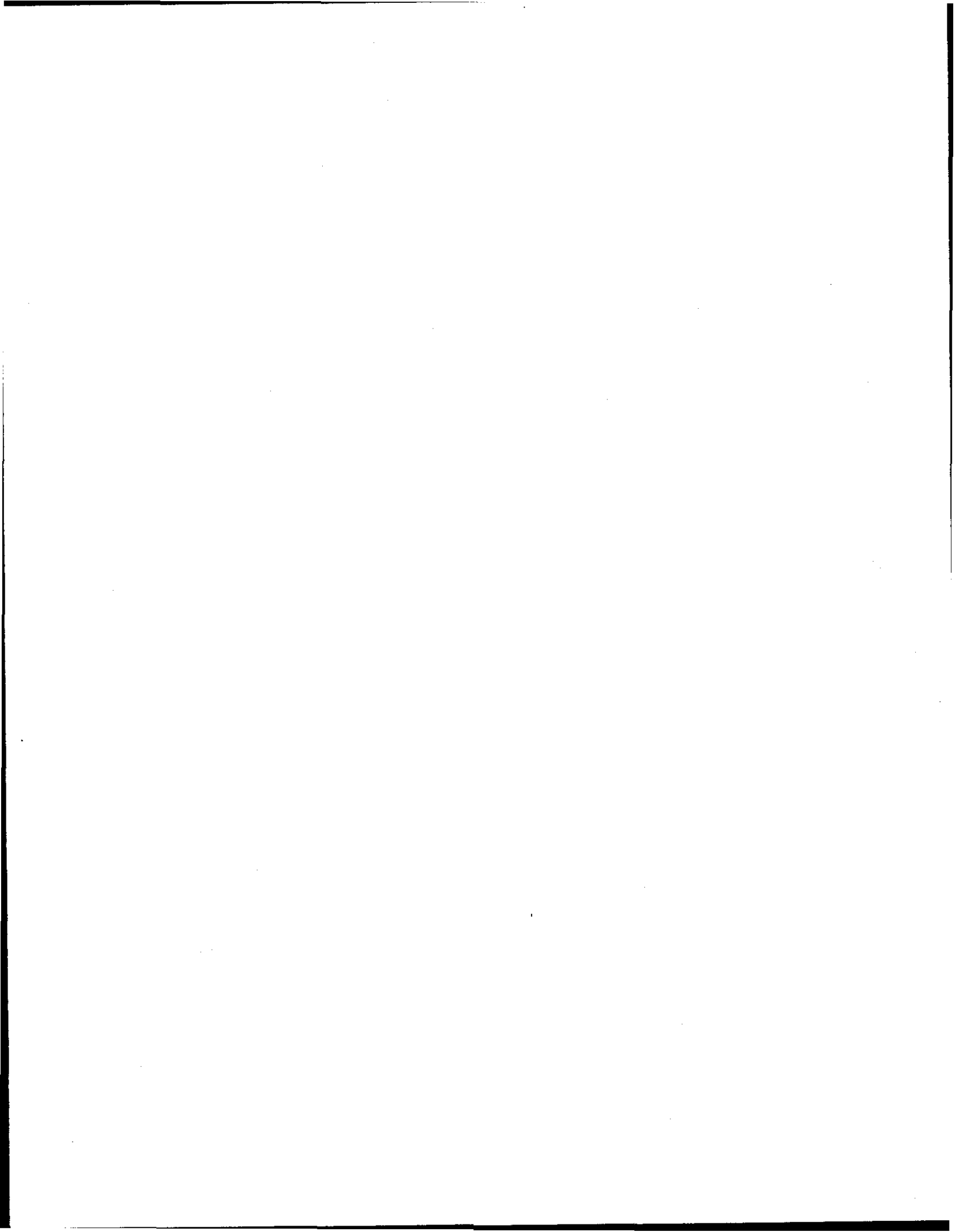
FIGURE 56 - A Comparison of Steering Column Model Results with Experimental Data

Blak-Tuffly Damping 50 lbs. - sec/ft.
Tuffly Force-Deflection
Characteristic $F = 33X(0 < X \leq 3)$ lbs.
 $F = 12 \times 10^6(X - 3)$ ($X > 3$ inches) lbs.

From Figure 56 it was concluded that the above values for the steering assembly model reasonably represented a conventional steering assembly. It was assumed that the addition of a steering wheel air bag unit would be compensated by reducing the weight of the other elements of the steering assembly to the extent that the net change in steering assembly weight would not be significant.

The force deflection properties of the human thorax in contact with a wheel were assumed to be that shown in Figure 57.¹⁷ The value of damping was assumed to be 50 lb. - sec/ft. The mass of the occupant in the model exercises was taken to be 70 percent of the total mass of the occupant.

The results of 10 mph simulated impacts are shown in Figure 58, giving the velocity and decelera-



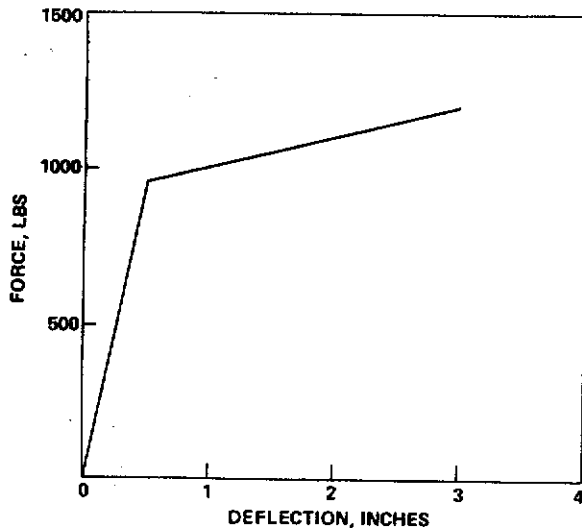


FIGURE 57 - The Assumed Force-Deflection Characteristics of the Human Thorax

tion histories of the occupants as well as the maximum chest and steering column deflection. The worst case in terms of the column and chest deflections occurs with the 95th percentile male occupant. Column deflection in this case was 2.39 inches. On the basis of these modeled impacts, it was concluded that two inches of column designed to collapse at 1,200 lbs. (plus 1/2 inch ramp from 0 to

1200 lbs.) was required to protect occupants in low-speed collisions.

The remainder of the column was designed to collapse at about 3,200 lbs. This safely arrests the 95th percentile male, and avoids excessive acceleration of the 5th percentile female. Thus, the steering column force deflection characteristics assumed were as shown in Figure 59.

The HSRI two-dimensional crash victim simulator program¹⁸ was employed to simulate head-on, fixed-object collisions of the modified standard size vehicle. In these simulations it was assumed that the driver air bag would deploy in 20 milliseconds from sensor

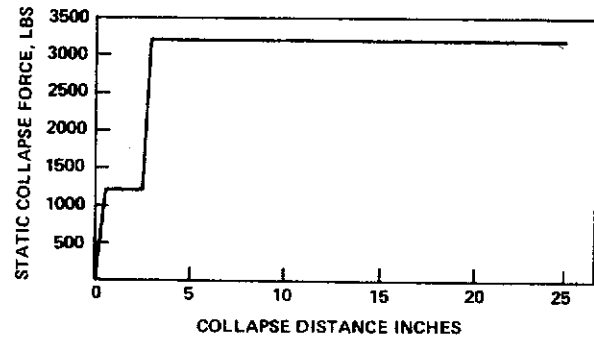


FIGURE 59 - Static Force-Deflection Characteristic of the Assumed Steering Column for the Modified Standard-Size Vehicle

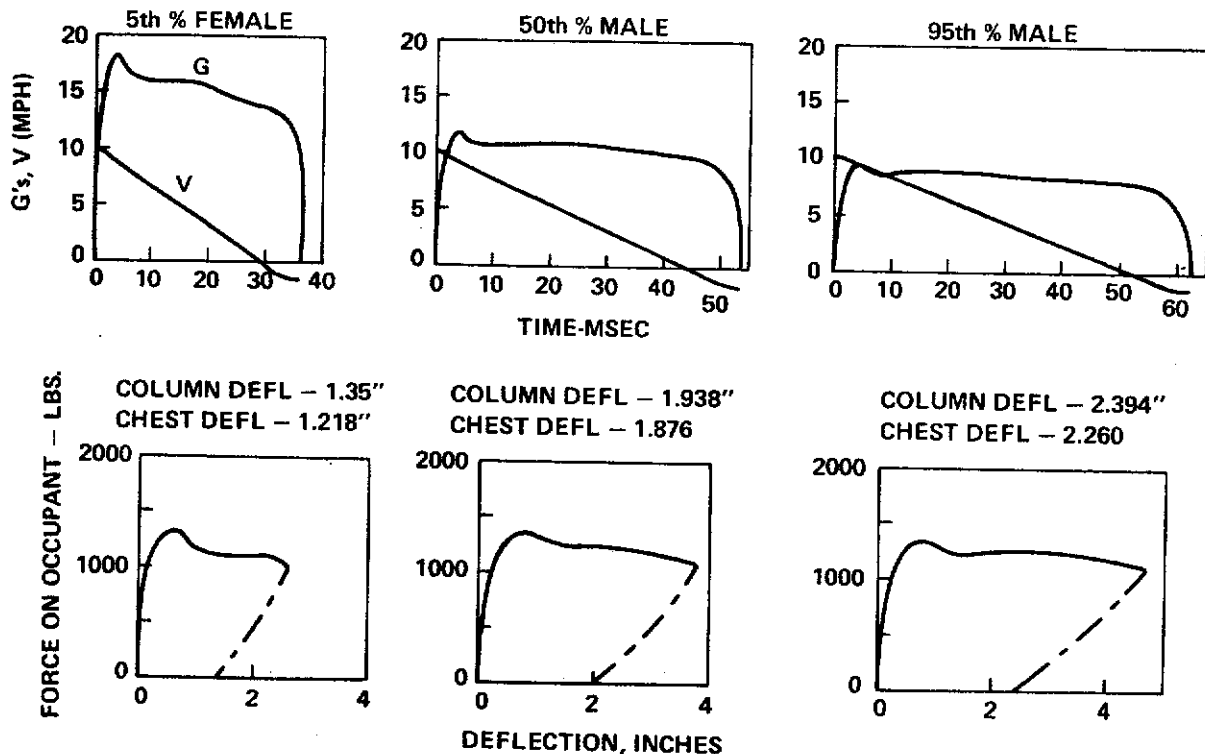
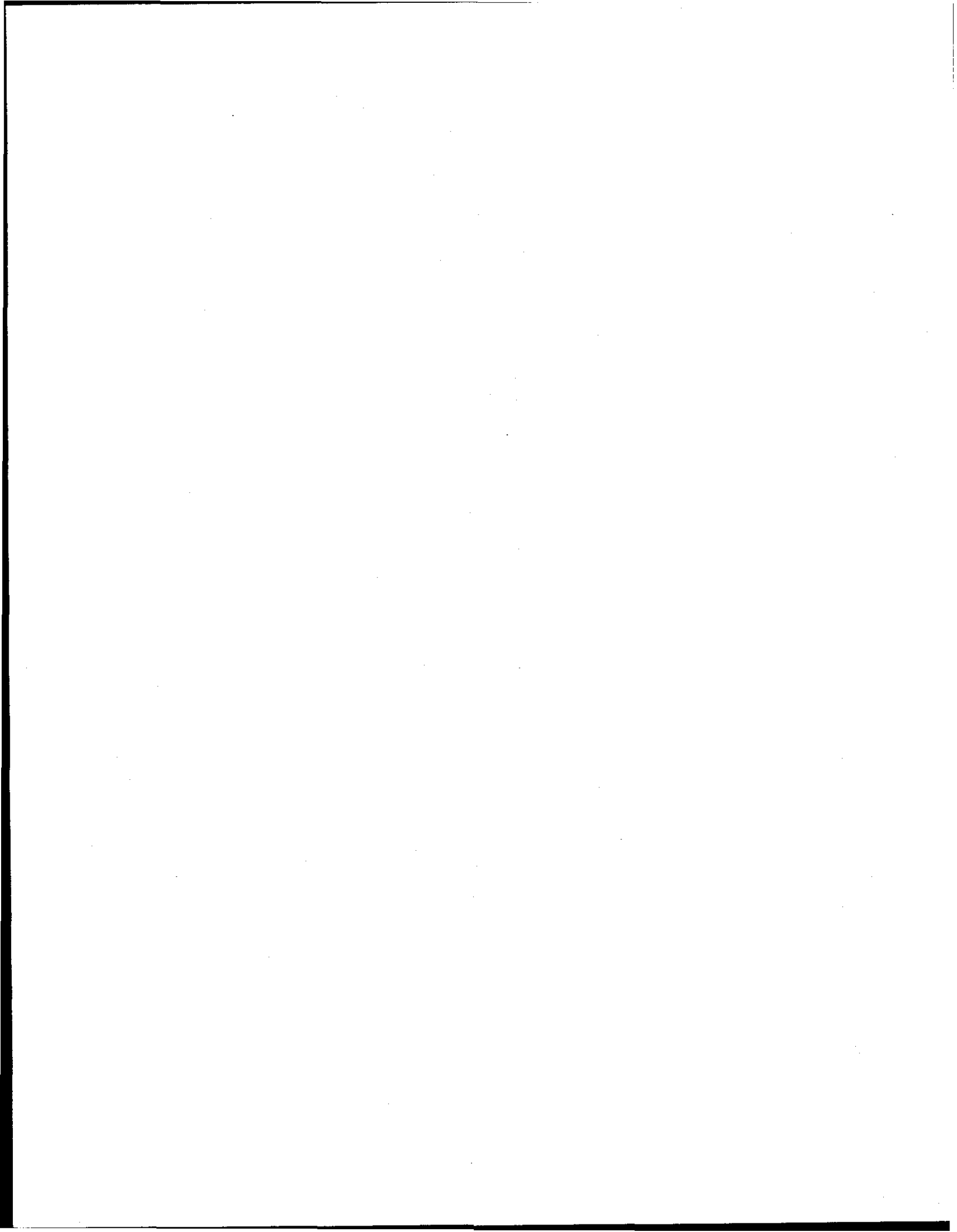


FIGURE 58 - The Results of Simulated 10 MPH Impacts with the 50th and 95th Percentile Male and 5th Percentile Female Thorax



firing with a sensing time of about 5 milliseconds, i.e., the system activation time is about 25 milliseconds. The driver bag was hypothesized to extend six inches from the wheel when fully deployed. This extension just puts the bag in contact with the torso of the 5th percentile female driver at 25 milliseconds into the 50 mile per hour fixed object frontal collision. In the case of the other two occupant sizes, the bag will be fully deployed for a few milliseconds before contact is made. Based on previous observations it was felt that a force deflection characteristic of the form $F = ax^2$ was a reasonable approximation of the bag loading curve expected. The constant was chosen so that about 2½ inches of bag deflection would produce a force great enough to collapse the initial stage of the column and a bag deflection of about four inches would produce a force great enough to collapse the second stage. Calculations based on the adiabatic compression of an unvented bag of circular cross section, indicated that an initial bag pressure of about 5 psig was required. The air bag and steering column combination would then have the force deflection characteristics shown in Figure 60.

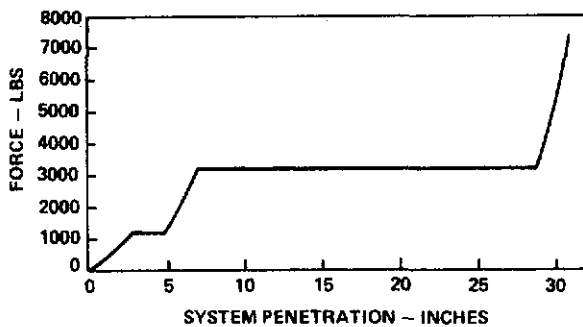


FIGURE 60 - Static Force-Deflection Characteristic of the Assumed Bag and Steering Column Combination for the Modified Standard-Size Vehicle

The HSRI model does not have provisions for assigning mass to contact surfaces. Thus, the effect of the steering assembly mass either had to be corrected for or ignored. Two simulations were run on the one-dimensional steering wheel impact model to investigate the effect of the mass. The first run was a simulation of a 50 mile per hour barrier impact, 50th percentile male occupant, with the bag and column configuration of Figure 60 and a 20 pound steering assembly. The second run was identical to the first except no mass was given the steering assembly. Based on the results of these two simulations, it was concluded that with the air bag in use, neglecting the mass of the steering assembly would not introduce serious errors in the two-dimensional simulations.

The results of the two dimensional simulation for the 50th percentile male driver are shown in Figure

61 which shows the initial and final positions of the driver and the trajectories of the chest, hip, and knee. Note that about 13½ inches of steering column and about 12½ inches of knee target collapse were required. Figure 62 shows plots of the head and chest accelerations for this occupant. The 5th percentile female simulation shows reduced travel and slightly higher accelerations while the reverse is true for the 95th percentile male. On the basis of these simulations, it is estimated that this system will prevent serious injury to practically all of the female anthropometric range and about 80 percent of the male anthropometric range at a barrier impact speed of 50 mph. At an estimated barrier impact speed in the range of 40-45 mph practically all of the male population would be protected.

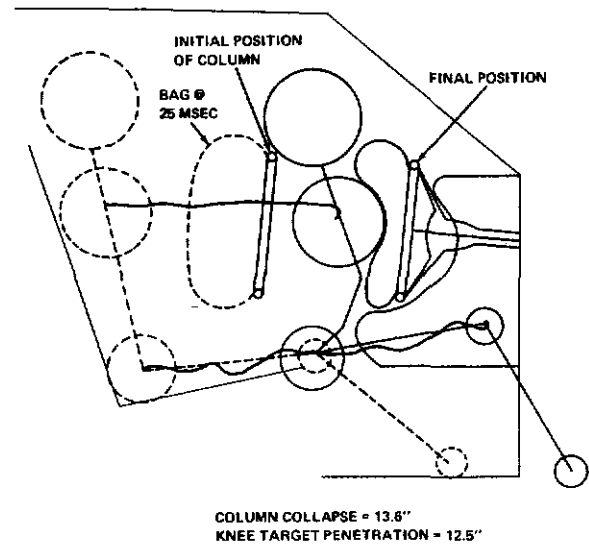


FIGURE 61, - The Resulting Kinematics of a 50th Percentile Male Driver from a Two-Dimensional Simulation of a 50 MPH Barrier Impact with a Modified Standard-Size Vehicle

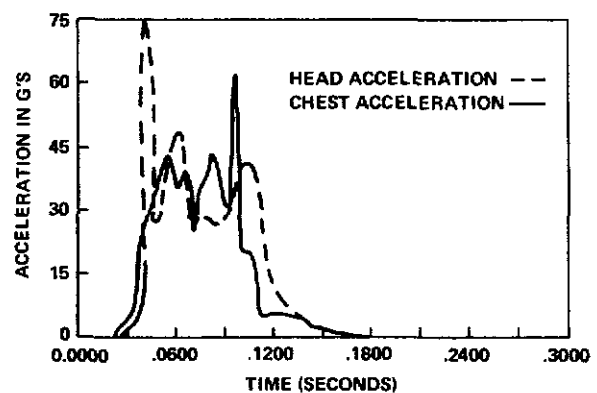
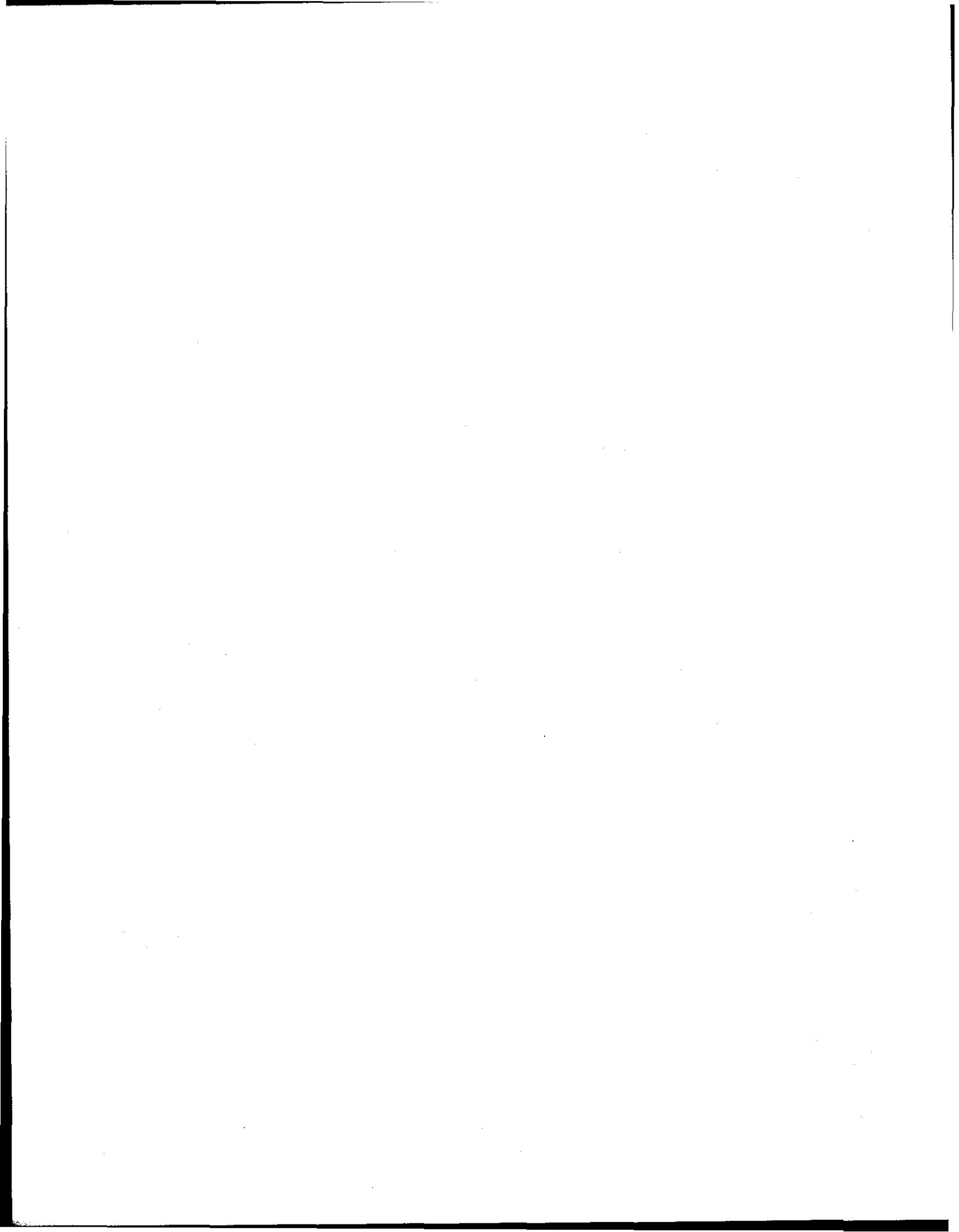


FIGURE 62 - The Calculated Head and Chest Resultant Accelerations of a 50th-Percentile Male Driver in a 50 MPH Barrier Impact with a Modified Standard-Size Vehicle - Two-Dimensional Simulation



It should be noted that these estimates are based on the assumed column characteristic shown in Figures 59 and 60. These characteristics were chosen to demonstrate one feasible means of providing driver protection. Optimization of the overall driver restraint design will require consideration of other column characteristics. For example, an alternative design for the steering column has recently evolved which offers advantages over that presented above. This design, shown in Figure 63, significantly reduces column collapse for large occupants while permitting increased column collapse for small occupants. Potentially, 95 percent of the male population could be protected by such a design.

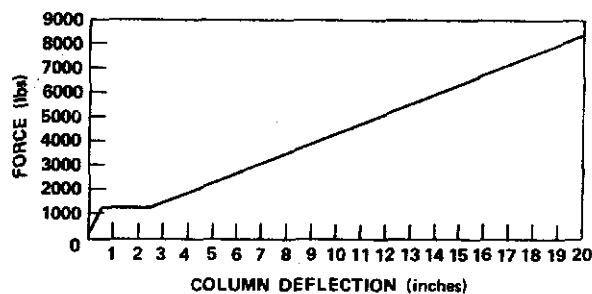


FIGURE 63 - Force-Deflection Characteristics of an Alternate Steering Column Design for 50 MPH Protection

In summary it is concluded that providing protection for the driver and front seat passenger in a frontal impact equivalent to a 50 mph barrier impact is an achievable goal for the standard-size vehicle.

RESTRAINT SYSTEM REQUIREMENTS FOR THE SUBCOMPACT VEHICLE

The deceleration versus displacement characteristic of the subcompact vehicle forestructure is shown in Figure 64. This characteristic was selected to assure acceptable values of vehicle crush in 50 miles per hour barrier impacts and to allow reasonable time for restraint system actuation. The buildup of compartment accelerations with crush distance (termed

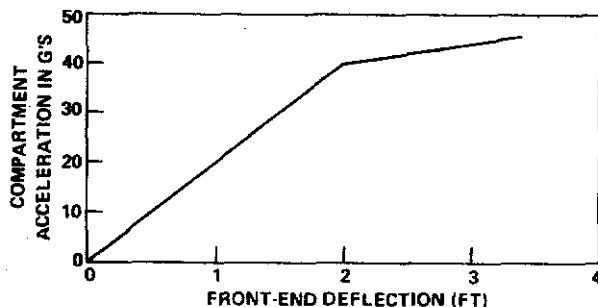


FIGURE 64 - Compartment Deceleration as a Function of Front-End Deflection for the Modified Sub-Compact Vehicle

"ramp angle") is a critical parameter. Increasing the ramp angle reduces the time available for restraint system activation. On the other hand, decreasing the ramp angle will increase collapse of the vehicle forestructure, limiting protection from compartment intrusion. Although the selected structural response characteristic is not necessarily an optimal solution, it represents an acceptable design for this feasibility investigation. Figure 65 is a family of curves showing how this subcompact vehicle will decelerate from various speeds in frontal barrier impacts.

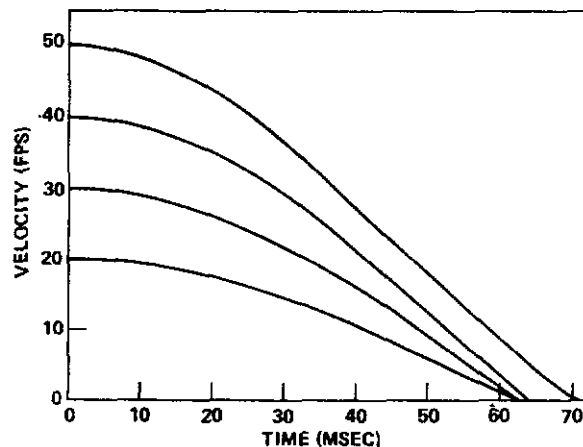
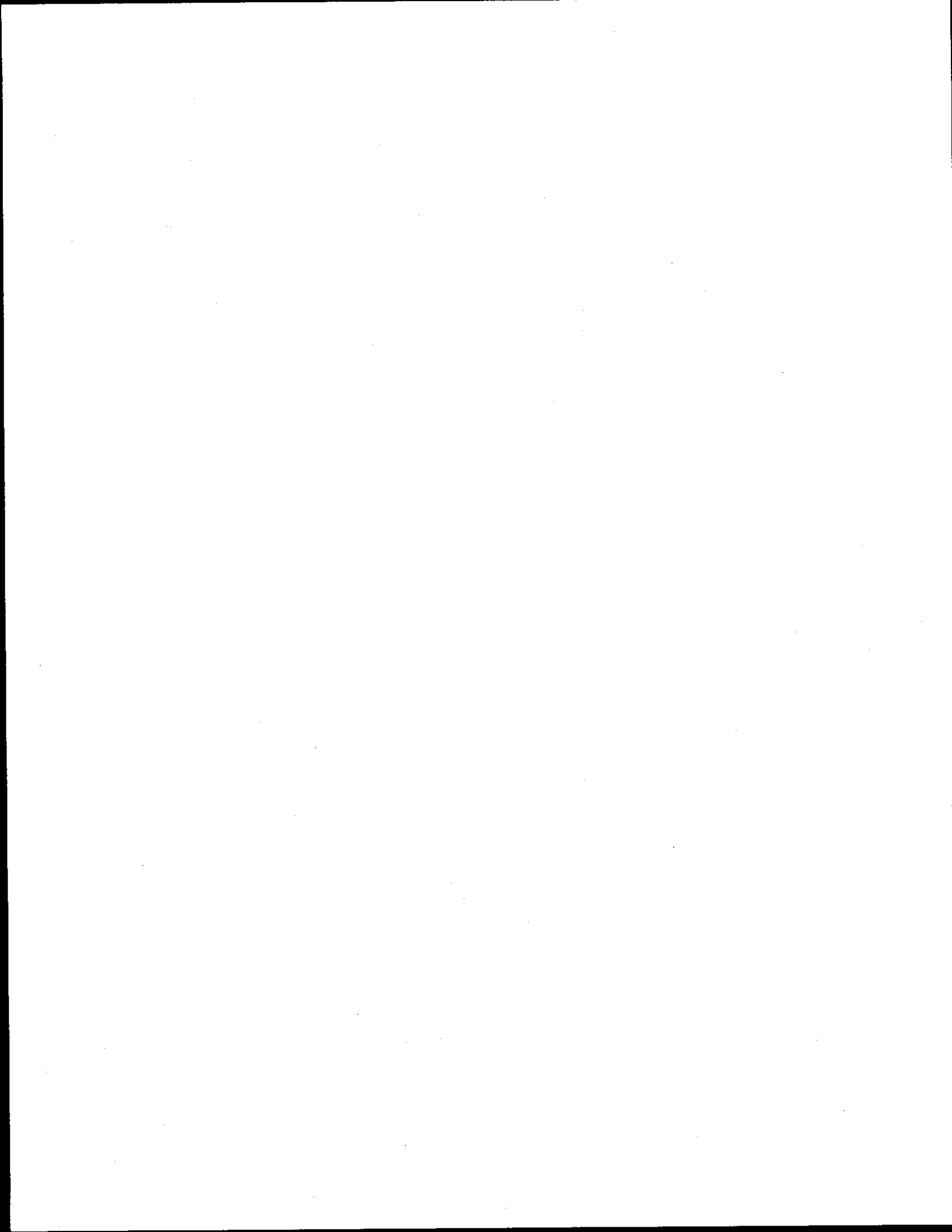


FIGURE 65 - Velocity Histories for the Modified Sub-Compact Vehicle in 20, 30, 40, and 50 MPH Barrier Impacts

The subcompact size vehicle compartment dimensions assumed for the purposes of this report are shown in Figure 66. These dimensions are considered to be representative of a late model subcompact vehicle in the Pinto/Vega class. Figures 66a, b and c show a 95th percentile male, a 50th percentile male and a 5th percentile female seated in the front seat with the seat adjusted as indicated on these figures. Note that 30 to 33½" of interior space is available from the chest of the occupants to the vehicle firewall. Also shown in these figures is the position of a knee restraining lower dash panel. As in the full size vehicle, this panel has been positioned to be 2 inches from the knee of the 50th percentile male occupant when the seat is in the mid position. The assumed force deflection characteristics are the same as in the case of the standard-size vehicle, see Figure 45.

Figure 67 shows the relationship between the required load efficiency of a restraint system for the subcompact and the system actuation time for the case of a 50 mile per hour barrier impact with the structural response of Figure 64. Plotted on this same figure is the corresponding relationship for a 30 mph barrier impact with a conventionally constructed subcompact.



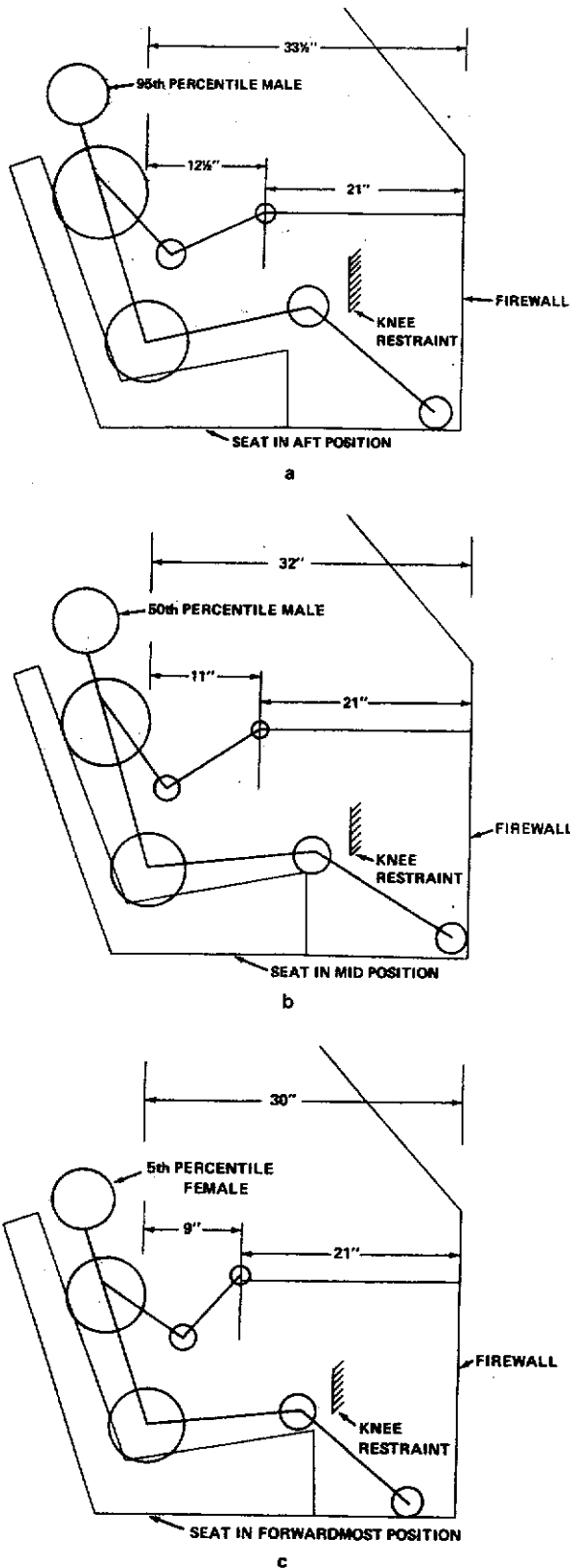


FIGURE 66 - The Assumed Interior Geometry of the Modified Sub-Compact Vehicle

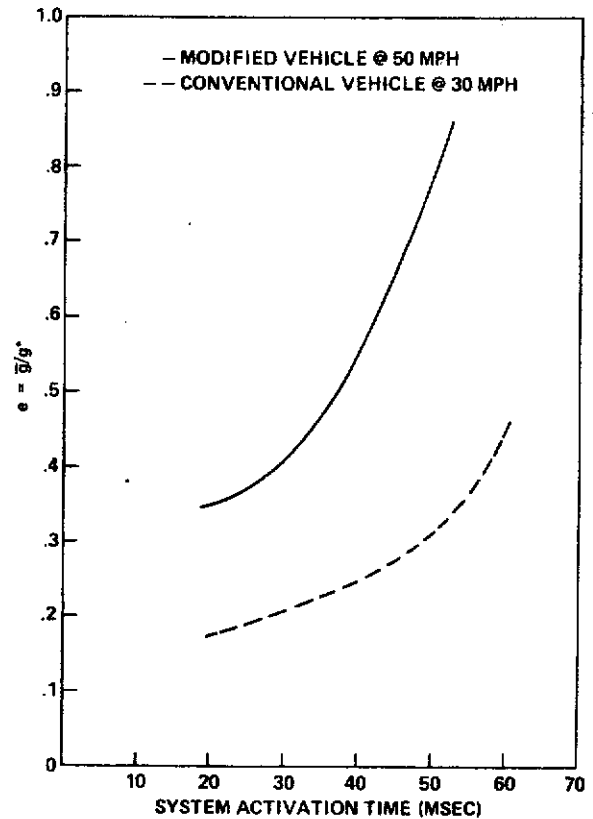


FIGURE 67 - Load Efficiency Versus System Activation Time for the Sub-Compact Vehicle

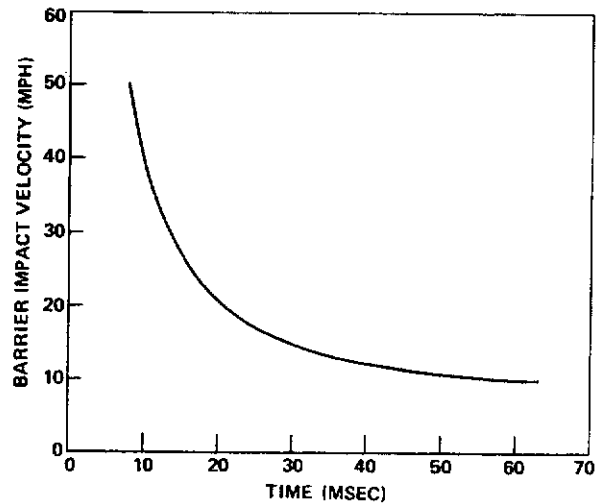
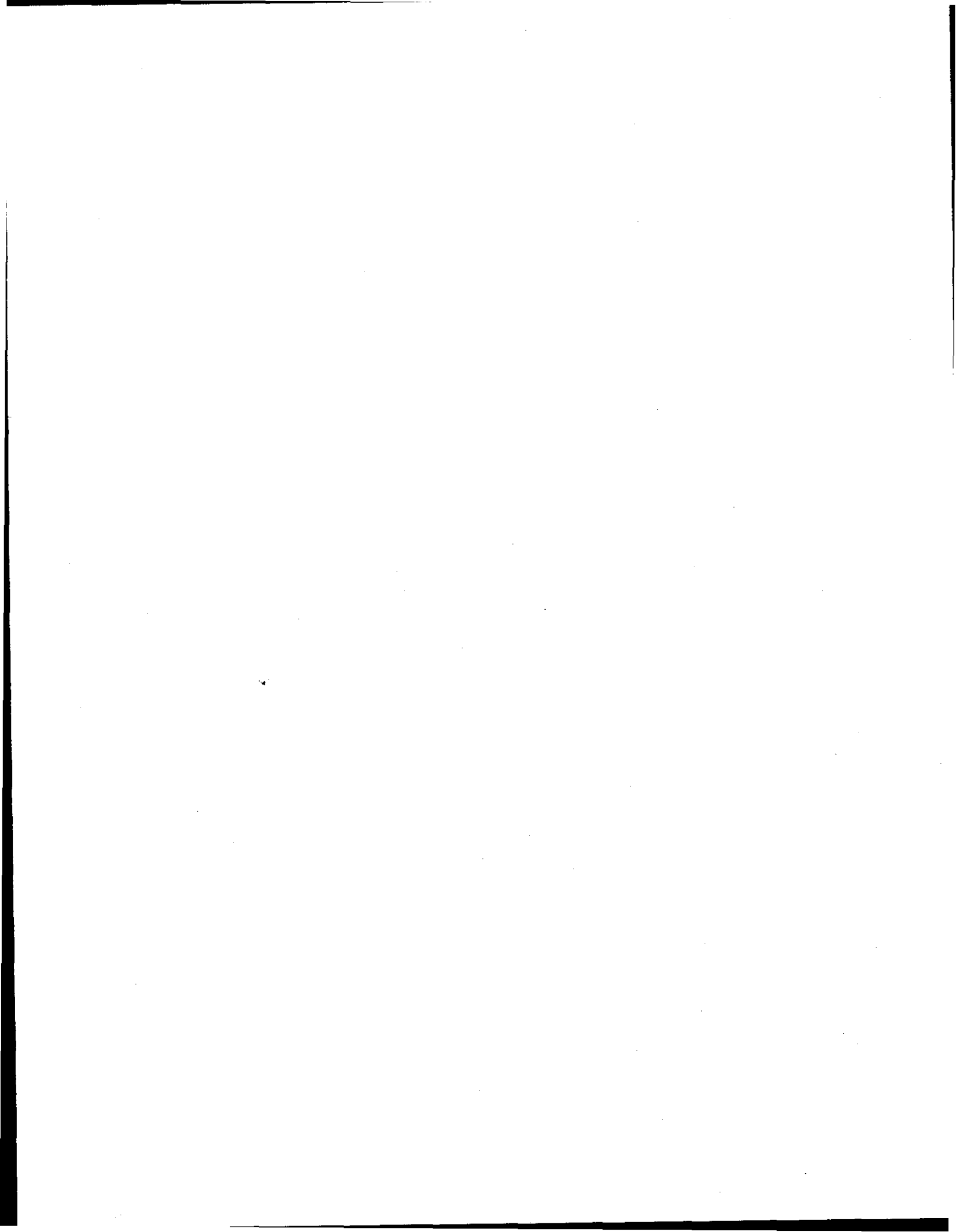


FIGURE 68 - Sensing Time as a Function of Barrier Impact Speed for the Modified Sub-Compact Vehicle

As in the case of the standard-sized vehicle, it is assumed that permanent energy absorbing padding of interior surfaces is capable of providing protection at barrier impact speeds of up to 10 mph. A deflection sensor is again hypothesized which triggers upon a front end crush of an amount greater than that achieved in the 10 mph collision. Figure 68 is a plot



of the sensing time for such a deflection sensor as a function of barrier impact velocity. At 50 mph, sensing time is about 8 milliseconds.

Assuming typical inflation times of about 20 milliseconds for the driver bag and about 30 milliseconds for the front passenger bag results in system activation times of 28 and 38 milliseconds for each system. Figure 67, indicates that a driver system must have a load efficiency of about 39 percent and a passenger system, an efficiency of about 52 percent.

PASSENGER RESTRAINT SYSTEM

Unfortunately, the air bag simulation model employed in a previous section of this report to compare 50 mph and 30 mph systems for the standard-size vehicle could not be employed in the corresponding comparison study for the subcompact due to a constraint in the model dealing with the width of the bag relative to the width of the occupant. Because of this constraint, the passenger bag could not be reduced in volume to correspond to a reasonably-sized subcompact passenger bag (volume = 7 ft.³) without giving either the occupant or the bag unrealistic dimensions.

The computer results for the standard-size vehicle passenger bag indicate that load efficiencies of slightly over 30% are achievable for that situation with conventionally constructed bags. Figure 67 indicates that, given a 20 msec deployment time, a load efficiency of 40% would be required. With a small volume bag, a higher load efficiency should be attainable, quite likely up to that required. If not, contouring of the bag may be required.

The same comments concerning the advantages of an aspirated system as advanced in the earlier section on standard-size vehicles apply to the subcompact vehicle. One additional characteristic of this system bears mentioning in connection with its use in vehicles of this class. The aspirator system, by employing compartment air to fill the bag, will reduce compartment overpressure compared to that produced by a non-aspirated system. This is a distinct advantage when one considers the ratios of total bag volume to compartment volume in subcompact cars.

DRIVER RESTRAINT SYSTEM

The driver restraint system for the subcompact vehicle will be very similar to the driver restraint system for the standard-size vehicle. Based on the assumed geometry of the subcompact, a steering wheel can be placed in a reasonable location in the vehicle compartment (see Figure 66) resulting in its

displacement from the firewall being 21 inches. Since no ride-down benefit exists for either the standard-size car or the subcompact car driver at barrier impact speeds of 10 mph, the design of the initial portion of the column, load-limited to 1200 pounds, will be the same, i.e., about 2 inches will be required. The remainder of the column would be designed to collapse at 3200 lb., i.e. the force deflection characteristics are as shown in Figure 59.

The HSRI Two-Dimensional Crash Victim Simulator Program was again employed, this time to simulate head-on, fixed-object collisions of the modified subcompact vehicle. In these simulations it was assumed that the driver bag would deploy in 20 milliseconds. With a sensing time of 8 milliseconds, the system activation time is about 28 milliseconds. The driver bag was hypothesized to extend six inches from the wheel when fully deployed. This extension just puts the bag in contact with the torso of the 5th percentile female driver at 28 milliseconds into the 50 mph barrier collision. The bag loading characteristic was assumed to be that assumed previously for the standard sized vehicle driver bag.

The results of the two-dimensional simulation for the 50th percentile subcompact driver are shown in Figure 69 which shows the initial and final positions of the driver and the trajectories of the chest, hip, and knee. It is noted that about 13.2 inches of steering column and about ten inches of knee target collapse were required. Figure 70 shows plots of the head and chest accelerations for this occupant size. On the basis of this simulation, and the corresponding

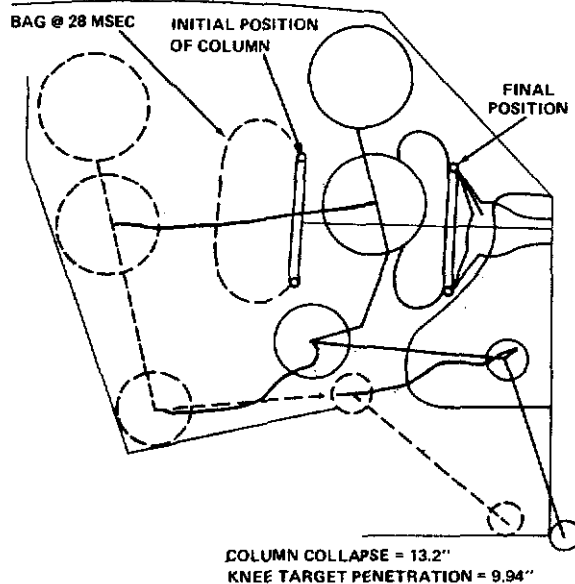
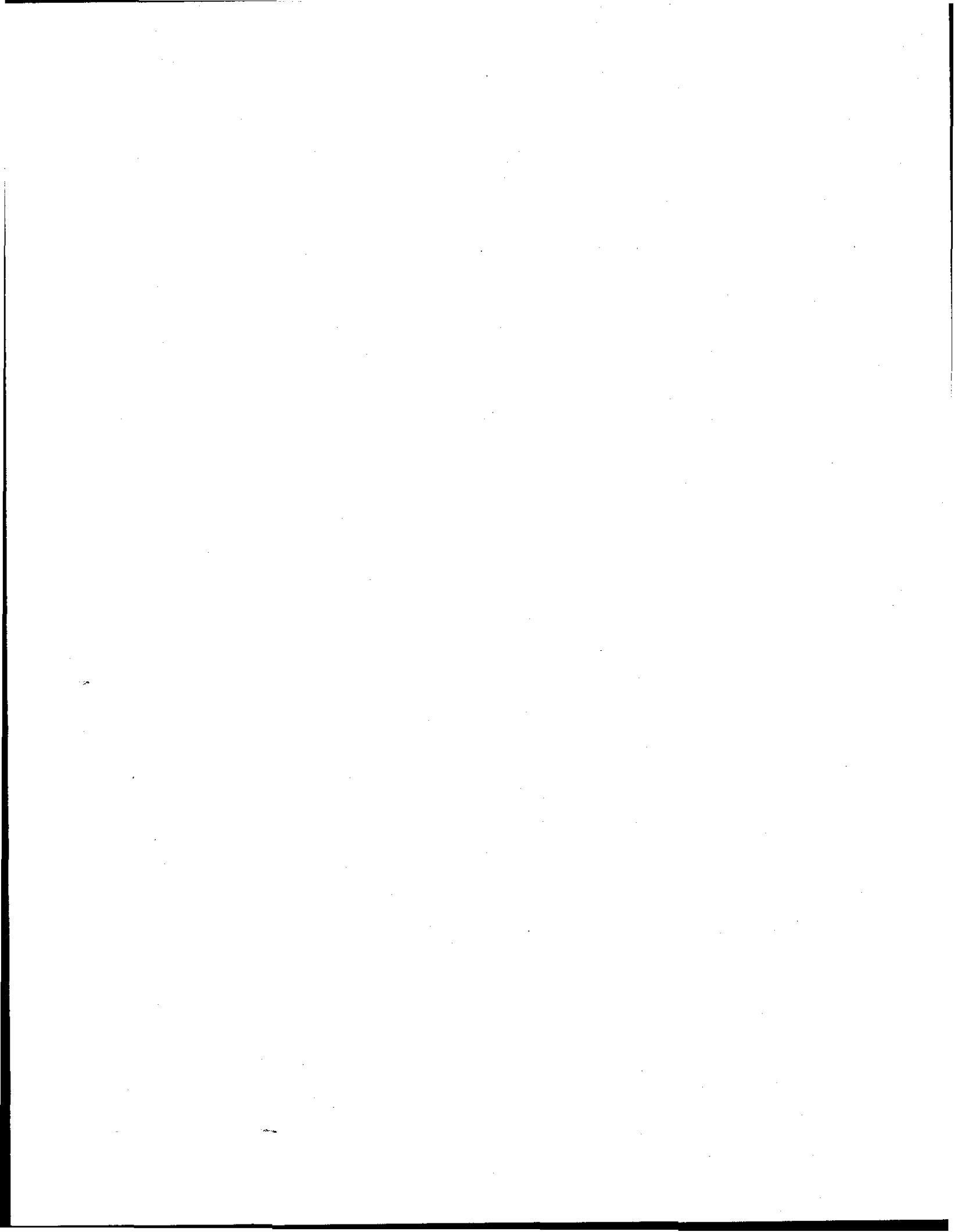


FIGURE 69 - The Resulting Kinematics of a 50th-Percentile Male Driver from a Two-Dimensional Simulation of a 50 MPH Barrier Impact with a Modified Sub-Compact Vehicle



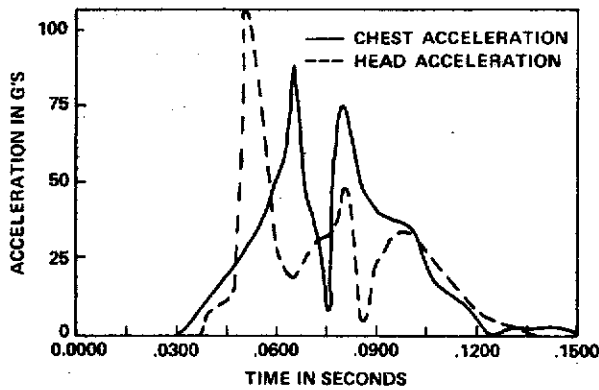
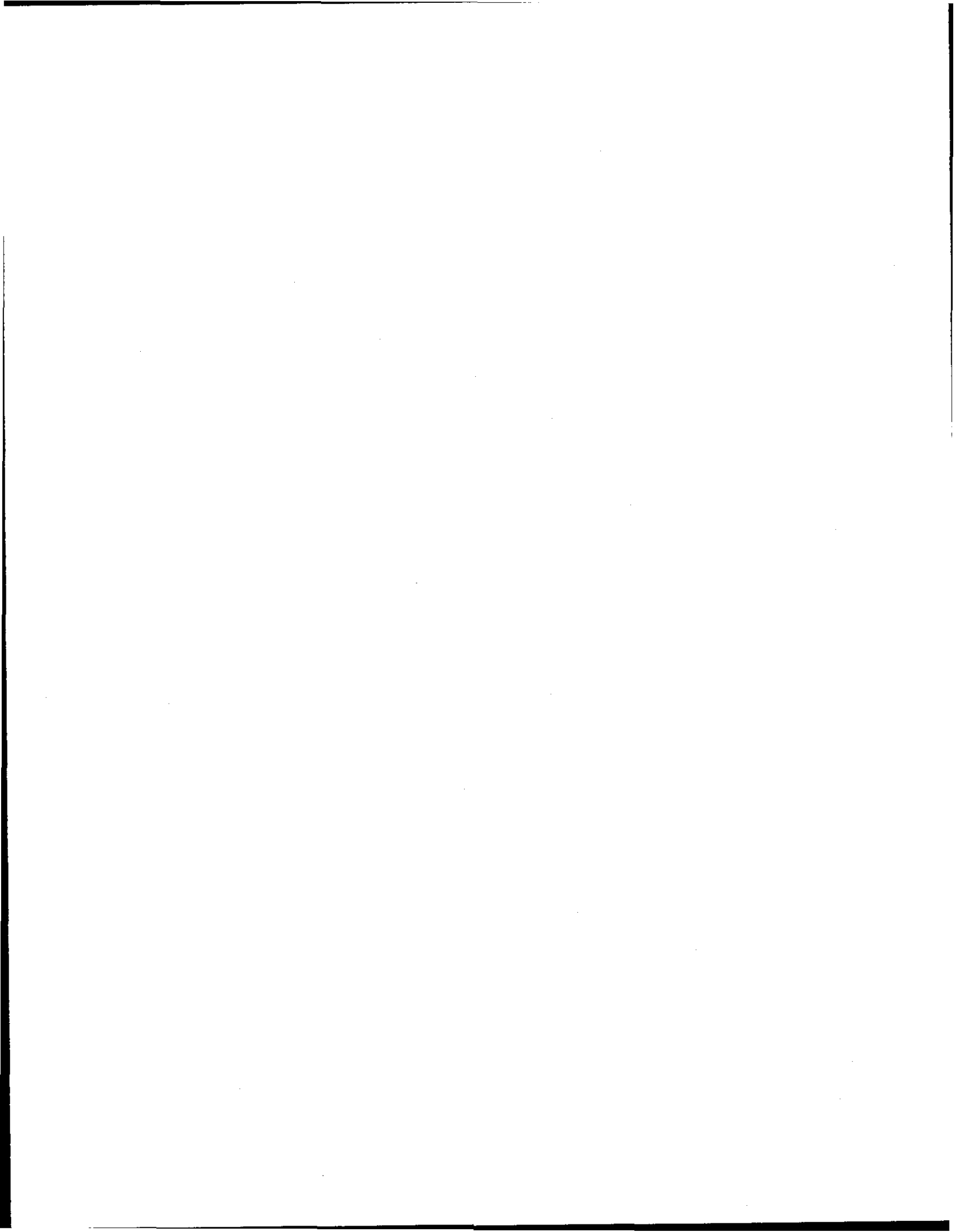


FIGURE 70 - The Calculated Head and Chest Resultant Accelerations of a 50th-Percentile Male Driver in a 50 MPH Barrier Impact with a Modified Sub-Compact Vehicle - Two-Dimensional Simulation

simulations for the 5th percentile female, and the 95th percentile male, it is estimated that this system will provide protection from serious injury to practically all of the female anthropometric population and to about 60 percent of the male population at a barrier impact speed of 50 mph. At an estimated barrier impact speed of about 40 mph, practically all of the male anthropometric range would be protected.

As pointed out in the section dealing with the driver of the standard size vehicle, optimization of the restraint design can be expected to improve performance. It is estimated that a driver restraint incorporating the characteristics of Figure 63 will give protection to over 85 percent of male drivers of subcompact vehicles.



Economic Impact of 50 mph Passive System

Vehicle design changes for safety or other purposes must be evaluated in terms of the resulting performance improvement and cost to the consumer. The cost clearly must be justified. One of the yardsticks used by the NHTSA for the determination of the reasonableness of possible safety requirements is that the benefits be equal to or exceed the estimated cost of the improvement to the consumer. The projected benefits and costs for 50 mph protection have been determined using the current vehicle population as a base line.

VEHICLE COSTS

Figure 71 summarizes estimates of consumer costs which would result from the installation of energy

management improvements and a passive restraint system in a contemporary 4,000 lb. vehicle to give 50 mph frontal protection. Vehicle weight changes are also shown in Figure 71.

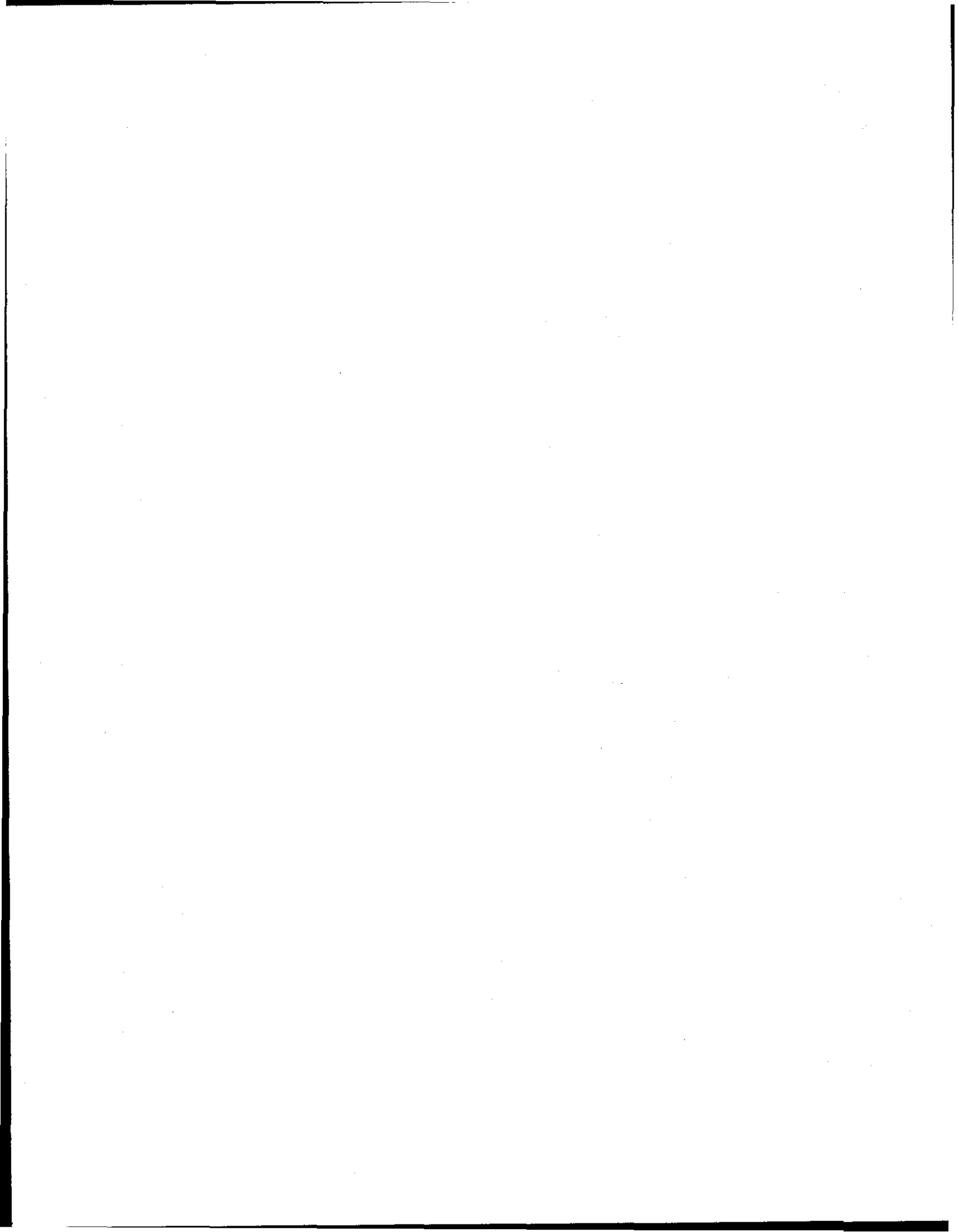
The total incremental cost of structural modifications for 50 mph protection is estimated to be \$172. The structural weight increase of 205 lbs. was based on the development work carried out by Cornell Aeronautical Laboratory, Inc., to provide a frontal structure capable of providing protection in 60 mph barrier impacts.

The inflatable restraint system cost was estimated to be \$100 more than the current belt system. This represents a \$30 increase over the cost estimated for a 30 mph air bag system.

CHANGES*	WEIGHT (LB)	PRICE (\$)
Add 50 MPH Air Bag System	75	\$163
Add Structure Modifications		
4130 Steel	138	152
Low Carbon Steel	141	68
Foamed Urethane	6	6
Steering & Chassis	19	11
Tires & Rims	17	12
Assembly Time (60 min)		25
Cyclical Redesign		32
Total Additions	396 Lbs.	\$469
ADJUSTMENTS		
Deduct 5 MPH Bumper (Included in Structure Mod.)	(80)	(54)
Deduct Belt System (Standard No. 208, 1-1-72)	(10)	(63)
Total Adjustments	(90) Lbs.	(\$117)
NET WEIGHT AND COST	306 Lbs.	\$352

FIGURE 71 - Estimates of Possible Consumer Costs Resulting from Installation of Energy Management Improvements and a Passive Restraint System

*Relative to Contemporary 4000 Lb, Passenger Car Base



An additional cost of \$80 was included to account for (1) the increased cost of steering, chassis, tire, and tire rims necessitated by the total increase in vehicle weight and (2) the additional assembly and fixed costs.

Since the prevention of damage to safety-related components required by FMVSS No. 215,¹⁹ Exterior Protection, is inherent in the structural modifications needed for 50 mph passive protection, the cost of FMVSS No. 215 compliance in current vehicles has been subtracted from the 50 mph system cost to arrive at a net incremental cost. Thus, the additional initial cost to the consumer for 50 mph protection was estimated to be \$352 per vehicle. This cost was assumed to be an average value for the total vehicle population. The annual initial cost for the 50 mph protection was determined on the basis of an annual production of 10 million vehicles to be \$3.52 billion.

Vehicle operating cost penalties of 0.14 cents per mile have been added to the initial cost to arrive at a total consumer cost estimate. Assuming each vehicle travels 10,000 miles per year, the additional operating cost amounts to \$1.4 billion during the service lives of the 10 million passenger cars produced annually. This operating cost has been added to the annual initial cost of \$3.52 billion to arrive at a total additional consumer cost of \$4.92 billion for 50 mph (equivalent barrier speed) passive protection in passenger cars of one model year.

SAFETY BENEFITS

The net safety benefits for the 50 mph passive systems discussed in this study include the prevention of 13,300 fatalities and 586,000 injuries annually. Expressed in terms of overall effectiveness, this translates into saving 75% of all frontal crash occupant fatalities and 59% of all frontal crash injuries occurring below 50 mph. Assuming societal costs of fatalities and injuries as \$200,000 and \$7,200 respectively, the safety benefits to society amount to \$6.9 billion annually.

BENEFITS VS COST

Figure 72 graphically illustrates the benefits and costs for 50 mph protection. The benefits outweigh the costs by a factor of 1.4.

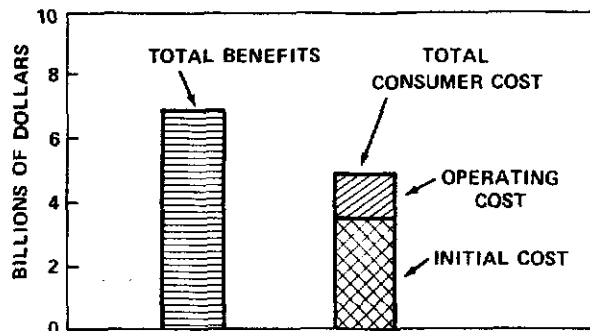
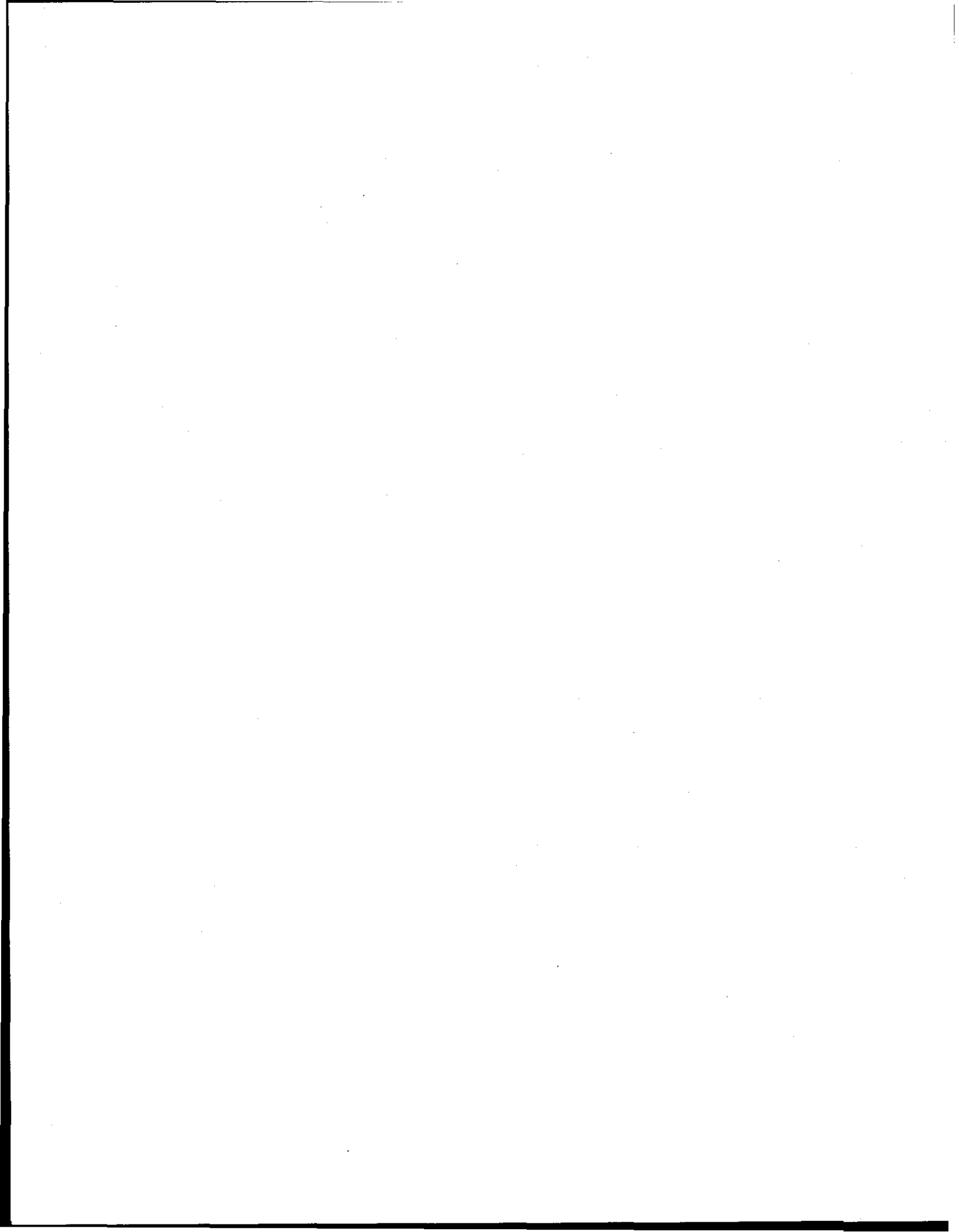
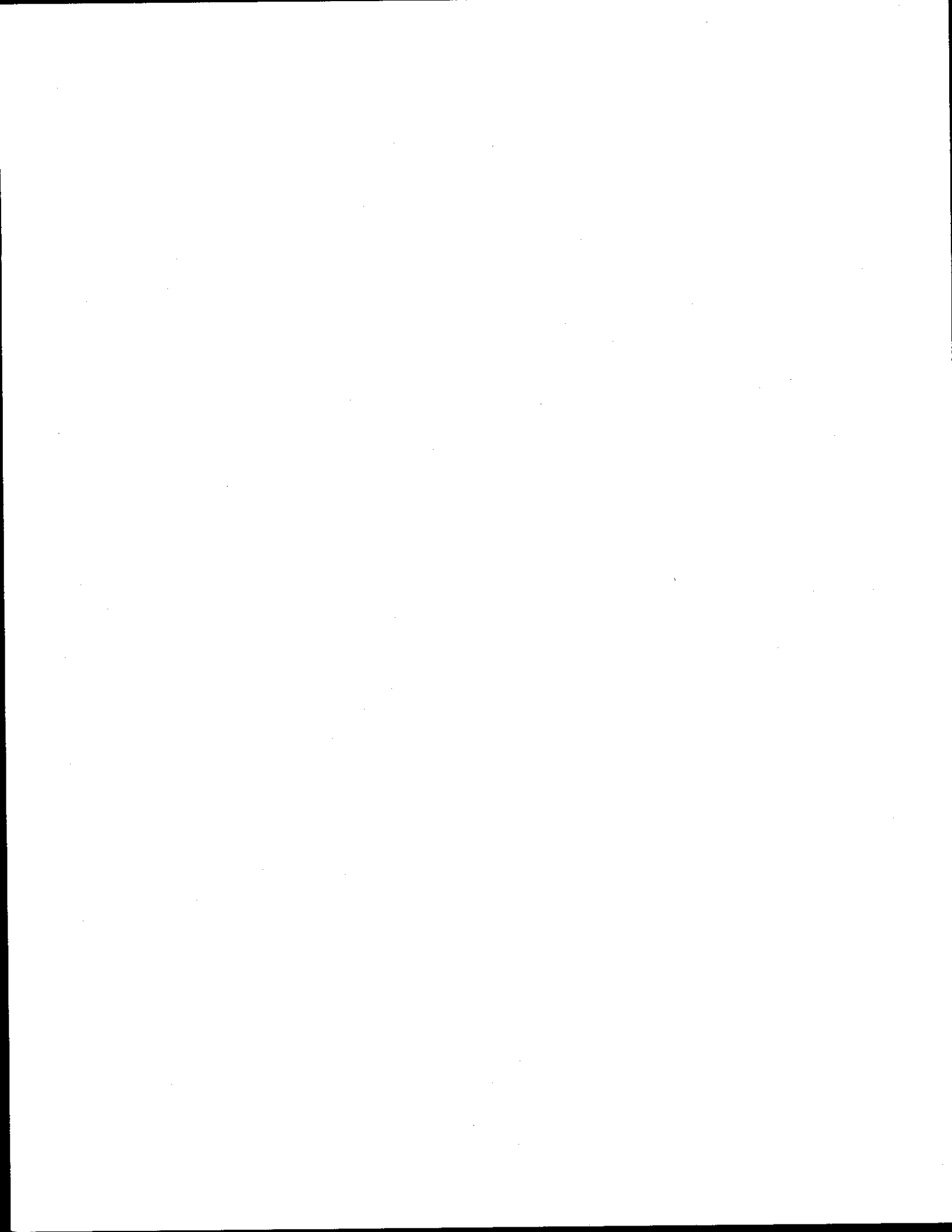


FIGURE 72 - Comparison of Annual Estimated Benefits with Consumer Cost for 50 MPH Passive Protection



Conclusions

1. Inflatable restraint systems and vehicle forestructure can be designed to protect occupants in passenger car frontal collisions of 50 mph, barrier equivalent speed. Results show probable savings of more than 75% of all fatalities and 60% of all injuries now occurring in frontal passenger car collisions below 50 mph.
 2. The benefits of providing 50 mph frontal impact protection outweigh the costs by a factor of 1.4.
 3. Structural modifications required for 50 mph barrier crash survivability are not inconsistent with those needed for compatibility in car-to-car crashes.
 4. The performance of present inflatable restraint systems will have to be improved for 50 mph protection. It is estimated that, for systems which deploy no faster than current 30 mph systems, load efficiencies as high as 52% may be required.
 5. Providing vehicle forestructure capable of 50 mph frontal impact protection can be accomplished with either velocity sensitive or fixed force structure, the choice being primarily dictated by economics.
-



References

1. NHTSA Report "Safety Benefits of Occupant Crash Protection" Standard Docket 69-7.
2. General Motors Corporation, 51 fatalities in frontal collisions vs. Estimated Equivalent Barrier Speed, 1968, 1969 and 1970 Files. (NHTSA Docket 69-7-51).
3. Ford Motor Company Report S-71-40 p. 37, "Percentage Distribution of Impact Speeds --" as Adjusted for C.G. & Accident Location.
4. Spencer, Paul R., *Energy Considerations In Vehicle Barrier Impact Testing*. Published in Proceedings of Institute of Environmental Sciences, 1971 Annual Technical Meeting, Los Angeles, Calif., 1971.
5. Miller, Patrick M., & Major, Richard P., *Basic Research in Automobile Crashworthiness - Summary Report*, Cornell Aeronautical Laboratories, Inc., CAL No. YB-2684-V-6, November, 1969.
6. Miller, Patrick W., and Nabb, Kenneth N., *Basic Research in Automobile Crashworthiness - Testing and Evaluation of Forward Structure Modification Concept*; Cornell Aeronautical Laboratories, Inc., CAL No. YB-2684-V-1, September, 1969.
7. Miller, Patrick M. and Greene, James E., *Basic Research in Automobile Crashworthiness - Additional Evaluation of the Engine Deflection Concept - Volume VII*; Cornell Aeronautical Laboratories, Inc., Report No. DOT-HS-800-548, March, 1971.
8. NHTSA Contract FH-11-7317, Cornell Aeronautical Laboratories, Inc., Attachment No. 1 to 16th Monthly Progress Report, Period of October 1 to November 1, 1970.
9. NHTSA Contract FH-11-7622, Cornell Aeronautical Laboratories, Inc., Attachment No. 1 to Fifth Progress Report, Period of November 1, to November 30, 1970.
10. NHTSA Contract FH-11-6799, Vehicle Safety Design Surveillance System, 1968, New York State.
11. NHTSA Contract FH-11-7317, Cornell Aeronautical Laboratories, Inc., Attachment No. 2 to the 16th Monthly Progress Report, Period of October to November 1, 1970.
12. NHTSA Contract FH-11-7317, Cornell Aeronautical Laboratory, Inc., Attachment No. 1 to the 19th Monthly Progress Report, Period of January 1 to February 1, 1971.
13. NHTSA Contract FH-11-7201, Battelle Memorial Institute, "The Evaluation of Phase I Reports on Experimental Safety Vehicles Program," February, 1970.
14. Mayor, Richard P., and Naab, Kenneth N., *Basic Research in Automobile Crashworthiness - Testing and Evaluation of Modifications for Side Impacts*; Cornell Aeronautical Laboratories, Inc., CAL No. YB-2684-V-3, November, 1969.
15. Dufort, R. H., "Computer Program for an Air Bag Restraint System," Cornell Aeronautical Laboratories Report No. YB-2985-V-2, September, 1971.
16. Martin, J. F., and Romeo, D. J., "Preliminary Vehicle Tests - Inflatable Occupant Restraint Systems," Cornell Aeronautical Laboratories Report YB-2990-K-2, March, 1971.
17. Kroell, C. K., Schneider, D. C., and Nahum, A. M., "Impact Tolerance and Response of the Human Thorax," Paper No. 710851, presented at the 15th Stapp Car Crash Conference, November 17-19, 1971.
18. Robbins, D. H., and Roberts, V. L., "Development of Two- and Three-Dimensional Crash Victim Simulators," Highway Safety Research Report No. BioM 70-3, July, 1970.
19. FEDERAL REGISTER, Vol. 36, No. 222, December 2, 1971.

